ENGINEERING CHIMERIC ANTIGEN RECEPTOR (CAR) T CELLS TO ELICIT AN ENDOGENOUS ANTITUMOR IMMUNE RESPONSE

by

Nicholas Frederik Kuhn

A Dissertation

Presented to the Faculty of the Louis V. Gerstner Jr.

Graduate School of Biomedical Sciences,

Memorial Sloan Kettering Cancer Center

in Partial Fulfillment of the Requirements for the Degree of

Doctor of Philosophy

New York, NY

September, 2019

Renier J. Brentjens, MD, PhD
Dissertation Mentor

Date

To my family, Christel, Claudius, Leonie, and Rainer.

“The unexamined life is not worth living.”

Socrates

“Dogs are forever in the push-up position.”

Mitch Hedberg

ABSTRACT

Chimeric antigen receptor (CAR) T cells provide great efficacy in B cell malignancies. However, improved CAR T cell therapies are still needed to increase patient responses and broaden the application of CAR T cell therapy beyond B cell malignancies. Here, we engineered tumor-targeted CAR T cells to constitutively express the immunestimulatory molecule CD40 ligand (CD40L) and explored efficacy in different mouse leukemia/lymphoma models. CD40L binds to its cognate receptor CD40 expressed predominantly on antigen-presenting cells (APCs) and stimulates their maturation and licensing. We observed that $CD40L^+$ CAR T cells circumvent tumor immune escape via antigen loss through CD40/CD40L-mediated cytotoxicity and induction of a sustained, endogenous immune response. After adoptive cell transfer, the $CD40L^+$ anti-CD19 CAR T cells displayed superior antitumor efficacy compared to anti-CD19 CAR T cells alone. $CD40L^+$ CAR T cells licensed antigen-presenting cells, enhanced recruitment of immune effectors, and mobilized endogenous tumor-recognizing T cells. These effects were absent in *Cd40*$^{-/-}$ mice, highlighting the importance of CD40/CD40L interactions in the host animal.

Furthermore, $CD40L^+$ CAR T cell treatment induced accumulation of conventional dendritic cell type 1 (cDC1) populations at the tumor site. Subsequently, lymphoma-bearing *Batf3*$^{-/-}$ mice lacking cDC1s had an impaired antitumor response and reduced survival after $CD40L^+$ CAR T cell transfer compared to wild-type mice. This suggested an involvement of cDC1s in the improved antitumor response of $CD40L^+$ CAR T cell treatment. cDC1s are responsible for cross-presenting tumor antigen to cytotoxic $CD8^+$ T cells, thereby stimulating a T cell-mediated antitumor response. Priming of endogenous non-CAR $CD8^+$ T cells to recognize CAR-antigen negative tumor cells via their TCR was increased when mice received $CD40L^+$ CAR T cells, demonstrating the ability of $CD40L^+$ CAR T cells to stimulate an endogenous antitumor response. Elevated priming of endogenous $CD8^+$ T cells was abrogated in *Batf3*$^{-/-}$ mice, indicating that $CD40L^+$ CAR T cells prime non-CAR $CD8^+$ T cells via cross-presenting cDC1s. Finally, re-challenge experiments with CD19-negative tumor

cells in cured mice showed that CD40L$^+$ CAR T cells can induce a sustained antitumor memory response protecting mice from CAR-antigen negative tumor outgrowth that is dependent on endogenous non-CAR CD8$^+$ T cells. Collectively, these results provide a rationale for CD40L$^+$ CAR T cells in cancer treatment.

BIOGRAPHICAL SKETCH

Nicholas (Nick) F. Kuhn was born to German parents Christel and Rainer Kuhn on July 26th 1989 in Summit, NJ, USA. At the age of four, Nick and his family moved to Schallbach, Germany, where he attended elementary school. He then attended middle/high school at the Hans-Thoma-Gymnasium in Lörrach. After graduating from high school in 2008, Nick went to Würzburg to study Biomedicine at the Julius Maximilian University where he completed his Bachelor of Science degree under the mentorship of Michael Sendtner working on unsuccessfully identifying neurotrophic factor receptors in the developing mouse brain. Following his stay in Würzburg, Nick enrolled in the Molecular Medicine Master's program at the Charité in Berlin in 2011. There, he completed his Master's degree under the guidance and mentorship of Julia Polansky-Biskup and Alf Hamann at the Deutsche Rheuma-Forschungszentrum (DRFZ) in Berlin and developed his interest in immune cell interactions by semi-successfully investigating epigenetic regulators of memory T cell responses.

In 2013, after reading about genetically engineered T cells targeting cancer cells in patients, Nick thought that was pretty, pretty, pretty good and applied to different graduate schools in the USA. The following year, he joined the Louis V. Gerstner Jr. Graduate School of Biomedical Sciences at Memorial Sloan Kettering Cancer Center in New York, NY, with the aim of pursuing his PhD in an immunotherapy lab. Nick joined the laboratory of Renier Brentjens in the summer of 2015 and started to work on genetically engineering T cells and their application in cancer treatment.

ACKNOWLEDGEMENTS

First, I want to thank my mentor, Dr. Renier Brentjens, for his continued support throughout my PhD, for trusting me to fail on my own and to learn from those mistakes, and for providing me with the necessary freedom to take ownership of and responsibility for my project.

I want to thank all the Brentjens lab members who I've crossed paths with in the past four years for their day-to-day willingness to readily share reagents, lab tricks, and, if needed, their time and help when a mountain of samples had to be processed. I am especially grateful for everyone's flexibility in sharing hood, procedure room, Gallios, Attune, and 1-hr-spinoculation times. Working in different labs over time, one inevitably comes across a person who is a stickler for no one interfering with their time and space, despite the inherent unpredictability of certain aspects of lab work. I want to thank everyone for not being that person (which makes you think - maybe it was me...). Thank you to all current lab members: Christina Bebernitz, Tony Daniyan, Dylan Drakes, Ruby Freeman, Chris Hackett, Janneke Jaspers, Jonathan Khan, Abdul Khan, Carol Li, Andrea Lopez, Terence Purdon, Eric Smith, Mette Staehr, Dharmarao Thapi, Dayenne van Leeuwen, Dinali Wijewarnasuriya, and Sarah Yoo. I want to thank Analisa Wills for never failing to track down people, available seminar rooms, or other miscellaneous stuff that we high-maintenance lab people cannot get done. I also want to thank her for being incapable of being in a bad mood. And thank you to former Brentjens lab members who I have crossed paths with: Mauro Avanzi, Kevin Curran, Hollie Jackson, Reed Masakayan, Manjusha Namuduri, Sarwish Rafiq, and Oladapo Yeku.

I want to especially thank Tony Daniyan for his tireless curiosity about not only his own work, but also about other people's challenges and his willingness to offer advice and thoughts on how to tackle them. I am grateful for him always being available to mentally throw ideas around, literally any time of the day, no matter how inconvenient the time might be for him.

Also, I want to express my gratitude to the members of my PhD committee, Dr. Andrea Schietinger and Dr. Michel Sadelain, for their excellent critical advice throughout my PhD. Thank you to all members of both labs for providing reagents at times of need, as well as technical advice.

Thank you to my classmates Steve Albanese, Jake Boyer, Chris Hulton, Nayan Jain, Xiaoyi Li, Michelle Riegman, Ben Tischler, and Yuchen Xie. Especially sharing the first couple of years of graduate school together enriched my experience at GSK tremendously.

I also want to extend my thank you to current and past members of the GSK graduate school who have been essential in creating an atmosphere that allowed me to focus on my lab work full-time and kept other distractions to a minimum: Ken Marians, Linda Burnley, Iwona Abramek, Maria Torres, Ivan Gerena, Michael Overholtzer, and David McDonagh.

The following funding sources need to be acknowledged, because without them this work would have not been possible: National Institute of Health and National Cancer Institute (5F31CA213668-02), The Annual Terry Fox Run for Cancer Research in New York, NY, Kate's Team, The Cabot Family Charitable Trust, The Leukemia and Lymphoma Society, The William Lawrence and Blanche Hughes Foundatoin, and The Emerald Foundation.

Thank you to all my old friends on the old continent and beyond.

Finally, I want to express my deep gratitude to my parents, Christel and Rainer, for their unconditional support and unfiltered advice throughout my life. And I want to thank my sister Leonie and brother Claudius for putting things into perspective.

LIST OF TABLES

LIST OF FIGURES

LIST OF ABBREVIATIONS

ACT: adoptive cell therapy

ADCC: antibody-dependent cellular cytotoxicity

ALL: acute lymphocytic leukemia

ALT: alanine transaminase

AML: acute myeloid leukemia

AST: aspartate transaminase

BBB: blood-brain barrier

BCG: Bacillus Calmette-Guérine

BiTE: bispecific T cell engager

CAIX: carbonic anhydrase IX

CAR: chimeric antigen receptor

CD: cluster of differentiation

CD40L: CD40 ligand

cDC: conventional dendritic cell

CDC: complement-dependent cytotoxicity

CLL: chronic lymphocytic leukemia

CML: chronic myeloid leukemia

CMV: cytomegalovirus

CRS: cytokine release syndrome

Cy: cyclophosphamide

DAG: diacylglycerol

DC: dendritic cell

DLI: donor leukocyte infusion

EBV: Epstein-Barr virus

EGFR: epidermal growth factor receptor

FDA: food and drug association

FLT3L: Flt3 ligand

GM-CSF: granulocyte-macrophage colony-stimulating factor

HLA: human leukocyte antigen

i.p.: intraperitoneal

i.v.: intravenous

Ig: immunoglobulin

IL: interleukin

IRES: internal ribosome entry site

KO: knockout

mAb: monoclonal antibody

MAC: macrophage

NK cell: natural killer cell

NSCLC: non-small cell lung cancer

pDC: plasmacytoid dendritic cell

PMA: phorbol 12-myristate 13-acetate

pMHC: peptide-major histocompatibility complex

scFv: small chain variable fragment

SFU: spot forming unit

TCR: T cell receptor

tdLN: tumor-draining lymph node

TIL: tumor-infiltrating lymphocyte

TLR: toll-like receptor

VST: virus-specific T cell

WT: wild-type

CHAPTER 1

INTRODUCTION

Over the past 40 years, cancer has consistently attributed to 20% of all causes of death in the United States, only trailing heart disease as the main cause (Noone et al., 2018). Overall, the lifetime risk of an average US American to be diagnosed with cancer is between 35 and 40%, regardless of race, ethnicity, or sex (Noone et al., 2018). Understanding the pathology of this cancer and development of treatment strategies is and has been a major focus of modern medicine. This has lead to a deep appreciation for the complexity of cancer as a genetic disease (Vogelstein et al., 2013). Cancer cells arise through malignant transformation of healthy cells and can originate from all main tissue types in the human body: epithelial tissue (carcinoma), connective tissue (sarcoma), bone marrow (leukemia and myeloma), and lymphatic tissue (lymphoma). Further complexity is provided by the cell of cancer origin within the tissue, interindividual genetic differences between cancer patients, as well as intraindividual differences within the heterogenous pool of cells constituting the tumor mass (Vogelstein et al., 2013). Despite this immense complexity, several hallmarks of cancer have been defined to help understand the biological characteristics and processes of neoplastic diseases (Hanahan and Weinberg, 2011). These ten hallmarks are: (1) the ability of cancer cells to sustain proliferative signaling and growth; (2) evasion of growth suppression; (3) resisting cell death; (4) replicative immortality; (5) inducing angiogenesis; (6) activating invasion and metastasis; (7) avoiding immune destruction; (8) deregulated cellular metabolism; (9) tumor-promoting inflammation; and (10) genome instability. Understanding the concept of these hallmarks serves as the foundation for the main cancer treatment modalities of chemotherapy, radiation therapy, surgery, and immunotherapy.

Immunotherapy

Immune system

The immune system is a host defense system that protects a multicellular organism from foreign pathogens and molecules. The basis of the immune system can be summarized by the general concept of distinguishing “self” from “non-self”. An immune response is initiated upon the detection of non-self. This immune response can be divided into an innate and an adaptive response. Innate immunity is a fast-acting response against microbes, which typically responds in the same way to repeated infections. The main components are physical epithelial barriers, antimicrobial biochemical barriers, phagocytic cells, and a diverse array of blood proteins, such as members of the complement system and soluble pro-inflammatory mediators. Adaptive immunity develops over a longer time frame and is defined by its ability to remember previous infections by the same pathogen. This allows specific and faster immune responses upon every subsequent infection. Adaptive immunity is only found in vertebrates and its main components are lymphocytes and lymphocyte-secreted proteins called antibodies.

A Brief History of Immunotherapy

In 1891, a bone surgeon called William B. Coley reported on his observations of soft tissue sarcoma patients and the treatment of three patients by inoculation of streptococcus bacteria (Coley, 1891). The deliberate infection of sarcoma patients with bacteria was based on the case reports on several cancer patients experiencing cancer regression after developing erysipelas, an acute infection of the skin caused by streptococcus infection. Eventually, heat-killed bacteria were used for treatment to minimize the risk of infection and occasional antitumor responses were induced (Coley, 1893). The underlying mechanism of the antitumor response was not known at the time, but further experimental and clinical evidence in the following century showed that activation of the host immune system can trigger an immune response that targets transformed cancer cells and not just invading pathogens.

Early work in mice recapitulated the findings in humans, wherein growth of different transplantable tumors was inhibited by infecting the mice with Bacillus Culmette-Guérin (BCG), a type of vaccine containing live mycobacteria (Old et al., 1959). The use of a mouse model allowed further analysis of the antitumor response and led to the discovery of tumor necrosis factor (TNF) and the realization that immune mediators can be cytotoxic to cancer cells (Carswell et al., 1975). Further evidence that the immune system can be directed towards an antitumor response was gathered from experiments using a different immune signaling cytokine – interferon (IFN) – to increase survival in tumor-bearing mice after injection of the cytokine (Gresser et al., 1969). These seminal discoveries fostered an appreciation for the involvement of the immune system in eradicating cancer and laid the foundation for the successful development of immunotherapies over the past decades. This culminated in the approval of several immune modulators for the clinical management of cancer by the United States Food and Drug Administration (FDA). These treatment modalities encompass monoclonal antibodies directly targeting cancer cells (rituximab) or inhibiting immune checkpoints (ipilimumab), protective vaccines against cervical cancer (Gardasil) or therapeutic vaccines against prostate cancer (sipuleucel-T), oncolytic viruses (talimogene laherparepvec), and genetically engineered T cells against blood malignancies (tisagenlecleucel) (Galluzzi et al., 2014).

Preclinical & Clinical Immunotherapies

The first approved immunotherapies are based on the effector functions of monoclonal antibodies (mAbs). By binding to a specific target antigen, antibodies can be designed to bind to almost any cell surface molecule. After binding, mAbs can directly block the function of the target molecule, induce immune-mediated killing of the target cell through complement-dependent cytotoxicity (CDC) or antibody-dependent cellular cytotoxicity (ADCC), or carry cytotoxic payload directly to the target cell. All these strategies have been brought to the clinic, with some examples being cetuximab and trastuzumab (blocking of epidermal growth factor receptor (EGFR)-family signaling molecules), rituximab (induction of ADCC by CD20 binding), and gemtuzumab ozogamicin (antibody-drug conjugate

carrying a cytotoxic agent to $CD33^+$ cells) (Scott et al., 2012). Further engineering of antibodies has led to the development of bispecific antibodies that have dual specificity, allowing engagement of cytotoxic T cells with $CD19^+$ leukemia cells by using the CD3/CD19-bispecific T cell engager (BiTE) blinatumomab (Klinger et al., 2012). Other non-antibody single agent immune modulators include (but are not limited to) thalidomide-derivatives, such as lenalidomide, which are used to treat different hematological diseases (Dimopoulos et al., 2007; Singhal et al., 1999), toll-like receptor (TLR) agonists such as BCG for the treatment of bladder cancer and imiquimod for basal cell carcinoma (Hoffman et al., 2005; Morales et al., 1976), and novel agents such as the cGMP-AMP synthase (cGAS)-stimulator of interferon genes (STING) agonists that can induce potent interferon responses and antitumor immunity as demonstrated in preclinical mouse models (Ng et al., 2018).

Additional strategies to unleash the immune system against tumor cells have been inspired by protective active vaccination of humans against infectious pathogens. The therapeutic cancer vaccine sipuleucel-T against castration-resistant prostate cancer is an autologous cell product (Kantoff et al., 2010). It is comprised of dendritic cells (DCs) isolated from the patient and activated with a fusion protein consisting of prostate specific antigen and the DC maturation factor granulocyte-macrophage colony-stimulating factor (GM-CSF). After infusion, sipuleucel-T primes T cells to attack the prostate cancer cells. The use of oncolytic viruses is another way of injecting biological material into patients to counteract tumor growth. Oncolytic virotherapy is based on the use of non-pathogenic viral strains that specifically infect and lyse cancer cells (Russell et al., 2013).

Recent more impressive results in the clinic have been achieved with immunomodulatory antibodies that target immune inhibitory molecules expressed on tumor cells, stromal cells, or on the immune cells themselves (Galluzzi et al., 2018). The most successful immune checkpoint blockade (ICB) antibodies in the clinic target cytotoxic T lymphocyte activator 4 (CTLA-4) and programmed death 1 (PD-1), two molecules expressed on T cells that facilitate T cell inhibition.

Release of this inhibition by ICB antibodies has led to durable responses in a minority of patients and is now standard of care for several solid tumor types (Zappasodi et al., 2018). Fueled by this success, targeting other inhibitory molecules like LAG-3, TIM-3, TIGIT, VISTA, BTLA, and B7-H3 is actively being pursued in clinical trials now (Marin-Acevedo et al., 2018). Contrary to ICB antibodies, immunestimulatory antibodies targeting OX40, 4-1BB, ICOS, or GITR are being clinically developed and present the agonistic counterpart of immunemodulatory antibodies (Melero et al., 2013). Ultimately, the aim of both approaches is to either disinhibit or directly stimulate a T cell-based antitumor response.

The focus on T cells as potent tumor cell killers has led to the development of adoptive cell transfer (ACT) of T cells. Here, T cells are isolated from patients, expanded ex vivo, and then injected back into the patient with the aim of having multiplied the number of T cells that now can eliminate the cancer cells in situ (Rosenberg and Restifo, 2015). The first transfer of cells to treat cancer was done in the form of allogeneic bone marrow transplants after radiation-induced myeloablation in leukemia patients (Mathé et al., 1965). Bone marrow cells were transferred to ensure hematopoiesis after treatment-related bone marrow failure. When comparing leukemia patients receiving syngeneic (from identical twins) to allogeneic (from human leukocyte antigen (HLA)-matched siblings) bone marrow transplants, an antileukemic effect was more often observed in patients developing graft-versus-host disease (GVHD) after receiving an allogeneic transplant (Weiden et al., 1979). The importance of T cells in mediating GVHD and the graft-versus-leukemia (GVL) effect was demonstrated when leukemia patients received T cell-depleted bone marrow transplantations and presented with lower incidence of GVHD, but relapsed with leukemia more frequently due to the absence of the GVL effect ((Apperley et al., 1986).

Further development of ACT in the past decades has led to the isolation of tumor-infiltrating lymphocytes (TILs) directly from the tumor tissue, with the aim of specifically expanding tumor-recognizing T cells before ACT. This work has led to the identification of the specific T cell receptor (TCR) molecules

recognizing tumor-associated antigens, which allowed ex vivo engineering of T cells to express these TCRs to generate an even larger number of tumor-specific T cells (Rosenberg and Restifo, 2015). The use of chimeric antigen receptor (CAR) T cells has further expanded the arsenal of tumor-directed T cells by introducing a synthetic CAR molecule into the T cell that equips the T cell with new target cell specificity and activation signals (Sadelain et al., 2013). These "living drugs" used in ACT exert their antitumor function through cell-mediated cytotoxicity, proliferate in vivo, and can impart the patient with life-long immunity against cancer.

Chimeric Antigen Receptor T Cells

T lymphocytes

T lymphocytes are members of the adaptive immune system that arise in the bone marrow, mature in the thymus, and can be categorized based on the composition of their TCR. αβ T cells express the variable α and β chains of the TCR, which together form a heterodimer and determine the antigen specificity of the T cell. They can be further subdivided into $CD4^+$ helper T cells, $CD8^+$ cytotoxic T cells, and $CD4^+$ regulatory T cells (Tregs). $CD4^+$ T cells provide help in B cell differentiation, antigen-presenting cell (APC) maturation, and $CD8^+$ cytotoxic T cell activation. $CD8^+$ cytotoxic T cells lyse cells infected with viruses or intracellular bacteria. $CD4^+$ Tregs have suppressive function and regulate T cell immune responses through inhibitory pathways. The second class of T cells express the γδ TCR heterodimer and also have helper and cytotoxic effector functions, predominantly in early immune response upon pathogen invasion.

On a molecular level, T cell activation and differentiation is dependent on three different signaling cues. "Signal 1" is provided by antigen recognition through binding of the TCR to its cognate peptide-major histocompatibility complex (pMHC) on APCs. This ensures that T cell activation only gets initiated when the specific antigen recognized by the T cell is locally available and presented on pMHC. "Signal 2" is mediated by costimulators expressed on APCs. The combination of signal 1 and 2 is necessary for full T cell activation and function

(June et al., 1987; Mueller et al., 1989). T cells that only receive signal 1 without costimulation eventually undergo programmed cell-death (apoptosis) or enter a state of unresponsiveness (anergy) (Chen and Flies, 2013). “Signal 3” is provided by soluble factors called cytokines, which instruct the T cell to differentiate towards a specific T cell subtype and induce upregulation of pro-survival factors.

Adoptive cell transfer

After identification of T cells in the 1960s (Miller, 1961, 1962) and the emerging understanding of T cell biology and their role in GVHD and GVL after bone marrow transplantation, the idea arose of directly isolating a patient’s own TILs, expanding them ex vivo, and then injecting them back into the patient. The technology of transferring cells from a donor to a recipient was pioneered by Thomas and colleagues with the aim of transplanting bone marrow cells into patients (Thomas et al., 1975). This approach was adapted for T cell ACT by Rosenberg and colleagues in the 1980s. Initial success of TIL therapy was reported in transplantable tumor mouse models, where TILs together with systemically administered cyclophosphamide (Cy) and interleukin (IL)-2 where able to eradicate cancer cells (Eberlein et al., 1982; Rosenberg et al., 1986). In humans, metastatic melanoma was treated with TIL therapy and objective tumor regression was observed in 9 of 15 patients (Rosenberg et al., 1988). This laid the groundwork for future ACT studies and more evidence that T cells are capable of killing transformed cells was derived from human transplant studies. Patients relapsing with leukemia after receiving a bone marrow transplant received a donor leukocyte infusion (DLI) from the original donor and experienced durable remissions in chronic myeloid leukemia (CML), acute myeloid leukemia (AML), and acute lymphoblastic leukemia (ALL) (Collins et al., 1997; Kolb et al., 1995). Another example of the potency of T cell-dependent antitumor effects is illustrated in patients developing Epstein-Barr virus (EBV)-associated lymphoproliferative disease post allogeneic bone marrow transplant. After receiving a DLI containing EBV-specific cytotoxic T cells, a small number of patients experienced clinical remissions (Papadopoulos et al., 1994).

Additionally, infusion of cytomegalovirus (CMV)-specific T cells (VSTs) into immunecompromised patients after bone marrow transplantation provided patients with protective immunity against CMV (Walter et al., 1995). All these therapies had in common the isolation of existing cancer- or virus-specific T cell populations and their use as a “living” drug to combat abnormal cells. The advent of T cell engineering, developed in the concurrent decades, allowed agnostic design of new T cell specificities independently of pre-existing immunity.

T cell engineering

The technology of T cell engineering is based on introducing a gene-of-interest into a T cell encoding for a protein in *trans* that imparts a desired function to the engineered T cell. These gene modifications can be generally divided into viral and non-viral gene delivery methods. The first viral modifications of primary T cells were based on γ-retroviral transduction of activated T cells (Bunnell et al., 1995; Gallardo et al., 1997; Mavilio et al., 1994; Rosenberg et al., 1990). Together with lentiviral gene delivery, γ-retroviral T cell transduction has been the method of choice in several successful clinical trials utilizing engineered T cells (Brentjens et al., 2011; Kalos et al., 2011; Kochenderfer et al., 2010). Both retroviral gene delivery platforms insert into the genome, allowing stable gene expression post transduction. Stable gene insertion harbors the risk of insertional oncogenesis, as documented in patients receiving gene-edited bone marrow cells (Hacein-Bey-Abina et al., 2003). However, mature T cells seem to be less prone to transformation after retroviral gene transduction (Newrzela et al., 2008; Scholler et al., 2012). Differences between lentiviral and γ-retroviral gene delivery has been observed in terms of their integration sites across the genome, with lentiviral vectors less likely integrating close to promoters and other gene regulatory regions, but more likely to cause aberrant gene transcription due to disruption of splice sites (Mitchell et al., 2004; Suerth et al., 2012). Whereas lentiviruses are capable of infecting non-dividing cells, retroviruses depend on mitotically active cells for successful infection (Suerth et al., 2012).

Non-viral gene delivery methods have also been used in T cell gene engineering. The transposon/transposase system “sleeping beauty” is a two-part

system, consisting of the gene-of-interest (=transposon) and the gene-integrating enzyme (=transposase) (Wang and Rivière, 2015). Both components are introduced into the T cell as DNA plasmids via electroporation, where, after translation the transposase inserts the transgene into TA dinucleotide repeats of the genome. This enables stable transgene expression in modified primary T cells (Kebriaei et al., 2016). Non-viral RNA-delivery methods via electroporation allow transient expression of the transgene if genome integration is not desired (Maus et al., 2013).

Introducing TCR α and β chains with known specificities into T cells allows redirection of T cells to a desired antigen. However, expression of transgenes in T cells is associated with diverse challenges and limitations. The endogenous α and β chains can mispair with the introduced αβ chains, leading to unanticipated TCR specificities and non-functional TCRs (Schumacher, 2002). Also, the introduced TCR has to compete with the endogenous TCR for signaling members of the CD3 TCR complex, potentially limiting surface expression and signaling output (Ochi et al., 2011; Voss et al., 2008). Another limitation of TCR gene transfer is the HLA restriction of the TCR, making this therapy only useful for a specific subset of patients carrying the TCR-specific HLA haplotype. Most clinically used TCRs are restricted to HLA-A*01 and HLA-A*02 haplotypes, thereby only covering a subset of patients (Klebanoff et al., 2016).

The clinical experience of TCR-engineered ACT has highlighted the unfortunate toxicities caused by TCR-crossreactivity. MAGE-A3, a cancer-testes antigen not expressed in normal tissue, was targeted in melanoma and sarcoma patients with an HLA-A*01-restricted MAGE-A3-specific affinity-enhanced TCR (Morgan et al., 2013). Shortly after ACT, two patients suffered fatal cardiotoxicity due to recognition of the unrelated cardiac protein titin by the MAGE-A3-specific TCR (Cameron et al., 2013). These unanticipated toxicities highlight both the therapeutic potential and danger of adoptively transferred T cells engineered to eliminate a specific cell population. Repurposing the potency of T cells independently of pMHC:TCR specificity led to the development of synthetic

receptors that can target a T cell to virtually any surface molecule and instruct the T cell to exert its effector functions upon target molecule encounter.

CAR design

The first synthetic receptors designed for T cell activation were fusion proteins composed of a immunoglobulin (Ig)-derived variable light (VL) or heavy (VH) chain fused to the constant region of the TCR α or β chain (Gross et al., 1989; Kuwana et al., 1987). Both fusion proteins were transfected into a transformed murine T cell line (EL4) and after receptor stimulation cytoplasmic calcium concentrations increased; seving as readout for receptor-specific cell activation (Kuwana et al., 1987). Further work fusing the intracellular chain of the CD3ζ molecule to the extracellular domains of CD4, CD8, or Fc receptors was sufficient to induce activation of transformed T cell lines upon extracellular receptor crosslinking (Irving and Weiss, 1991; Letourneur and Klausner, 1991; Romeo and Seed, 1991). Eshhar and Brocker then designed single chain fusion receptors consisting of an extracellular single chain variable fragment (scFv) plus the intracellular CD3ζ or Fcγ domains (Brocker et al., 1993; Eshhar et al., 1993). This allowed modular engineering of receptors based on the choice of the antibody-derived scFv. These receptors were initially called “T-bodies” and are now more generally known as “first generation CARs”. However, signaling via the CD3ζ chain alone provided only “signal 1” to primary resting T cells and, therefore, was insufficient to fully activate modified T cell (Brocker and Karjalainen, 1995). Only providing costimulation together with CD3ζ chain activation enabled augmented T cell cytokine release, even in primary T cells isolated from cancer patients (Gong et al., 1999). This realization inspired the development of “second-generation CARs” that additionally contain the intracellular domain of the costimulatory molecule CD28 in combination with the scFv and CD3ζ chain in one gene product (Finney et al., 1998). CD28 is constitutively expressed on naïve T cells and upon binding to its ligands CD80 and CD86 on APCs “signal 2” is transmitted to the T cell, which is essential to initiate growth, survival, and memory formation. Besides some cancer cells of hematological origin, most cancer cells do not express CD80 and/or CD86 on

their surface, preventing full T cell activation upon TCR engagement. Thus, incorporating the costimulatory CD28 molecule into the CAR molecule obviates the need for cancer cell CD80/CD86 expression to induce a functional T cell response. Upon antigen-binding, second-generation CARs are capable of secreting high amounts of IL-2 (Hombach et al., 2001), efficiently lyse cells expressing target antigen, and have a superior proliferative response compared to first generation CARs (Maher et al., 2002).

Introduction of different costimulatory domains showed robust activation of second-generation CAR T cells and emphasized the importance of and ability to provide signal 1 and 2 via a synthetic receptor. One of the first alternative costimulatory domains used in second generation CAR T cells instead of CD28 was 4-1BB (Imai et al., 2004), but other stimulatory domains such as ICOS, OX40, DAP12, NKG2D and others have also been successfully implemented (Van Der Stegen et al., 2015). Combining two costimulatory domains with the CD3ζ chain, so-called “third generation CARs”, have also generated functional CAR T cells. There, CD28 was combined with OX40 (Pulè et al., 2005), or with 4-1BB (Wang et al., 2007). A third generation CAR incorporating the 4-1BB plus ICOS costimulatory domains has also been described (Guedan et al., 2018). Whereas third generation CARs displayed similar or even improved tumor cytolysis compared to second generation CARs, clinical data suggests no improved antitumor efficacy (Morgan et al., 2010; Till et al., 2012).

CD19 CAR T cell therapy

CD19 is a 95 kD type I transmembrane protein that spans across the plasma membrane with an extracellular N-terminus and an intracellular C-terminus (Wang et al., 2012). No ligand for CD19 has so far been identified. CD19 is part of a multi-component signaling complex together with CD21, CD81, and CD225 and regulates signaling thresholds important for B cell activation and development (Engel et al., 1995; Tedder et al., 1997). CD19 is specifically expressed on B cells starting at the pro-B cell stage during development and CD19 expression is only lost at terminal plasma cell differentiation (Wang et al., 2012). CD19 is also expressed on most malignant B cells in leukemia and

lymphoma and on follicular DCs. With this restricted expression pattern, CD19 was identified as an ideal surface target antigen to treat B cell malignancies with CD19-targeted CAR T cells. This lead to the first demonstration of eradicating $CD19^+$ human leukemia and lymphoma cells with a single infusion of first generation CD19 (19z) CAR T cells in a xenograft mouse model (Brentjens et al., 2003). Following studies showed that second generation 1928z CAR T cells outperformed first generation 19z CAR T cells in a B cell lymphoma model (Kowolik et al., 2006). Further validation of the superior antitumor effect by second-generation CAR T cells soon followed in additional xenograft studies (Brentjens et al., 2007; Milone et al., 2009). The use of mouse tumor models showed that both first and second generation CAR T cells can also function in a fully syngeneic setting (Cheadle et al., 2010; Davila et al., 2013).

The first clinical case report of using second-generation CD19 CARs described a patient with follicular lymphoma experiencing a partial remission lasting 32 weeks before eventually relapsing with $CD19^+$ disease (Kochenderfer et al., 2010). Additional clinical results were reported for chronic lymphocytic leukemia (CLL) patients. In combining lymphodepletive conditioning with second generation CD19 CARs, two out of three CLL patients showed long-term complete remissions (Kalos et al., 2011). The importance of conditioning prior to ACT was documented in a larger study of 10 patients with refractory B cell leukemias, where none of the patients receiving no pre-conditioning responded to the CAR T cell infusion (Brentjens et al., 2011). Consistent clinical success of CD19 CAR therapy across several treatment centers has been achieved in B cell ALL (B-ALL). Complete responses were reported in both adult and pediatric patients with B-ALL (Brentjens et al., 2013; Davila et al., 2014; Grupp et al., 2013; Lee et al., 2015; Maude et al., 2014; Park et al., 2018). This clinical success eventually led to the approval of CD19 CAR therapy for B-ALL in children and young adults (Maude et al., 2018) and refractory diffuse large B cell lymphoma (Neelapu et al., 2017), making it the first FDA-approved cancer treatment modality based on genetic engineering of cells.

The 15+ years of clinical experience has defined several challenges in CD19 CAR therapy. Whereas response rates range from 50-80% (Park et al., 2018; Schuster et al., 2018), some patients do not respond at all to autologous CAR therapy. Additionally, several centers have reported the outgrowth of antigen-negative or antigen-low tumor cells that escape CAR T cell-mediated tumor killing (Maude et al., 2014; Park et al., 2018; Rizvi et al., 2015; Turtle et al., 2016). This outgrowth causes relapse in patients that cannot be treated with the initial CAR therapy anymore, making alternative treatment strategies targeting different surface antigens necessary (Fry et al., 2018).

CD19 CAR T cell therapy-related adverse events

CD19 CAR T cell treatment-related adverse events have also been described. One commonly experienced short-term toxicity is termed cytokine release syndrome (CRS) and involves an inflammatory host response that manifests itself by high fevers, myalgia, and malaise. Severe cases of CRS have resulted in hypotension, hypoxia, coagulopathy, multiorgan toxicity, and even death (Brudno and Kochenderfer, 2016). Management of CAR therapy-associated CRS has been achieved by glucocorticoid injection and, in severe cases, antibody-mediated IL-6 receptor blockade (tocilizumab) plus supportive therapy in an intensive care unit (Bonifant et al., 2016). Neurological symptoms such as encephalopathy, aphasia, delirium, tremor, seizures, and fatal cerebral edema have also been associated with CAR therapy (Santomasso et al., 2018). These neurological symptoms were correlated with pretreatment disease burden, CAR T cell dose, peak CAR T cell expansion, severity of CRS, and preexisting neurologic comorbidities (Gust et al., 2017; Hay et al., 2017). The breakdown of the blood-brain barrier (BBB) seems to permit accumulation of pro-inflammatory cytokines in the cerebrospinal fluid, leading to cerebral inflammation and onset of symptoms (Gust et al., 2017). Further studies are needed to address management of these neurological toxicities. Besides CRS and neurotoxicity, the third anticipated adverse event caused by CD19 CAR therapy is B cell aplasia. The absence of B cells is a direct functional readout of CD19 CAR T cell efficacy and is reversible upon CD19 CAR T cell removal (Paszkiewicz et al., 2016). B

cell aplasia is managed with intravenous immunoglobulin injection to supplement the deficit in antibody production.

CAR T cells in other malignancies

Following the clinical success of CD19 CAR T cell, other B cell-specific surface markers were targeted to combat B cell malignancies. Anti-CD20 and anti-CD22 CAR T cell trials have demonstrated similar response rates in non-Hodgkin lymphoma and B-ALL, respectively, compared to anti-CD19 CAR T cell therapy (Fry et al., 2018; Zhang et al., 2016). Additional hematological diseases are under investigation and being targeted with genetically engineered CAR T cells. Multiple myeloma has successfully been targeted with BCMA- and GPRC5D-specific CAR T cells in clinical and preclinical studies (Raje et al., 2019; Smith et al., 2019). In developing CAR T cells to treat AML, several potential targets have been identified. However, current preclinical and clinical investigation is warranted to validate a safe target in AML CAR therapy (June and Sadelain, 2018).

The translation of CAR therapy into solid tumor malignancies has been most challenging. Finding a target cell-specific antigen is highly imperative, as any off-tumor/on-target activity – akin to B cell aplasia in CD19 CAR therapy – in the setting of solid tumors could be lethal. This is documented by two unfortunate clinical case reports of using CAR T cells to treat metastatic renal cell carcinoma or colon cancer. Patients with metastatic kidney cancer were injected with CAR T cells specific for carbonic anhydrase IX (CAIX), an enzyme expressed by certain kidney cancers (Lamers et al., 2006). After CAR T cell administration, patients developed liver toxicities and cholangitis due to CAIX expression and recognition on healthy epithelial cells in the bile duct (Lamers et al., 2006). One patient with metastatic colon cancer was injected with ERBB2-specific CAR T cells and suffered lethal lung toxicities due to low levels of ERBB2 expression on healthy lung epithelium (Morgan et al., 2010). Another case of on-target/off-tumor CAR toxicity in the lung was reported in patients with $CAECAM5^{+}$ malignancies (Thistlethwaite et al., 2017). Together, this highlights the potency of CAR T cells in lysing antigen-positive cells and the importance of carefully considering targets

for safe patient treatment. So far, some safe targets in solid malignancies have been identified, but CAR T cell treatment in those cases has at best resulted in stable disease (Knochelmann et al., 2018). This emphasizes the need to develop safer and more potent CAR T cell treatment strategies in order to make this technology useful for treatment in a wider array of cancer malignancies.

Emerging CAR T cell strategies

Current efforts are focused on additional engineering of T cells besides only introducing a CAR molecule. The ability to fuse intracellular signaling domains of choice directly to extracellular domains of choice allows the design of any desired synthetic receptor. The use of chimeric costimulatory receptors (CCRs) was demonstrated early on in TCR-stimulated cells that expressed a CCR combining an antigen-specific scFv and the intracellular CD28 signaling domain (Krause et al., 1998). Upon TCR and antigen stimulation, T cells expanded and secreted IL-2, which then inspired the generation of a second-generation CAR that incorporated both the CD3ζ chain from the TCR and the CD28 costimulatory domain (Maher et al., 2002). CCRs also laid the foundation for dominant-negative receptors (DNRs) and switch receptors. DNRs are engineered proteins that contain the extracellular domain of a T cell inhibitory receptor but lack the cytoplasmic inhibitory signaling domains (Knochelmann et al., 2018). Overexpression of DNRs containing only the extracellular and transmembrane domain of PD-1, TGF-β receptor, or Fas in T cells has been shown to resist PD-L1, TGF-β, or Fas ligand-mediated T cell suppression, respectively, augmenting CAR T cell function and proliferation (Cherkassky et al., 2016; Kloss et al., 2018; Yamamoto et al., 2019). Switch receptors are artificial proteins that combine an extracellular recognition domain from “protein A” with a cytoplasmic signaling domain of “protein B”. Fusion of PD-1 with CD28 resulted in a PD1:CD28 switch receptor that, when expressed in $CD8^+$ cytotoxic T cells and exposed to PD-L1, resulted in T cell activation rather than anergy (Prosser et al., 2012). A different strategy was based on connecting the IL-4 receptor ectodomain to the IL-7 receptor endodomain (Leen et al., 2014). This chimeric cytokine receptor instructed T cells to maintain a Th1 effector phenotype in the context of inhibitory

IL-4 cytokine stimulation and improved the in vivo antitumor function of the engineered T cells.

Different strategies have been employed to control CAR expression and increase CAR therapy safety. Expression of an inhibitory CAR (iCAR), that contains a PD-1 or CTLA-4 cytoplasmic domain instead of a costimulatory domain, in combination with a conventional CAR in the same T cell allows control of cell activation dependent of antigen presence (Fedorov et al., 2013). If the iCAR recognizes “antigen A” and the CAR recognizes “antigen B”, T cell activation is inhibited when antigen A alone or A and B together are rexpressed on the target cell. This allows more restrictive antigen-dependent CAR activation and potentially limits on-target/off-tumor toxicities in healthy tissue expressing antigen A. The concept of splitting the two stimulatory domains into two different CAR molecules recognizing two different antigens allows controlled T cell activation only in the presence of both antigens (Kloss et al., 2013; Wilkie et al., 2012). These dual-targeted” CAR T cells also have a more restrictive activation threshold, but there often is still significant activation of the CAR T cell even if only one antigen is present. The generation of synthetic Notch (synNotch) receptors allows expression of a specific CAR only after priming with a separate activation signal (Lim and June, 2017). The activation signal is chosen to bind to the synNtch receptor on the surface of the engineered cell, leading to transcriptional activation and expression of a gene of interest (Morsut et al., 2016). The combinatorial strategy applied to CAR T cells limits CAR expression and effector function only in the context of both the synNotch activation signal and the CAR antigen (Roybal et al., 2016). These different CAR activation modalities of NOT- and AND-gated CAR activation provide ways to explore more safe CAR T cell therapy design for targeting solid tumor tissue.

Recent efforts have demonstrated improved cytotoxic function of the CAR T cells by modulating the components of the CAR and introducing novel costimulatory domains (Feucht et al., 2019; Kagoya et al., 2018), by controlling CAR expression at a physiological level through targeted genomic integration of the CAR transgene (Eyquem et al., 2017), by engineering the CAR T cell to

secrete a therapeutically active anti-PD-1 scFv (Rafiq et al., 2018), or by over-expressing a second transgene, such as immunestimulatory cytokines or ligands, in addition to the CAR in the T cell to enhance the antitumor efficacy of the CAR T cell (Hu et al., 2017; Pegram et al., 2012; Zhao et al., 2015). Several different cytokines that are naturally not secreted by T cells have been introduced into CAR T cells, such as IL-12, which is canonically secreted by licensed DCs (Macatonia et al., 1995) and in the context of CAR T cell therapy was shown to improve the antitumor response by affecting “bystander” cells present in the tumor microenvironment. Immune-inhibitory macrophages and myeloid-derived suppressor cells (MDSCs) lost their suppressive capacities when being exposed to IL-12-secreting CARs (Chmielewski et al., 2011; Kerkar et al., 2011; Yeku et al., 2017). IL-18 secretion by CAR T cells was shown to enhance CAR T cell proliferation and antitumor efficacy, as well as to recruit non-CAR T cells to the antitumor response (Avanzi et al., 2018; Hu et al., 2017). Engineering CD19 CAR T cells to express IL-15, another cytokine naturally not produced by lymphocytes, also improved anti-tumor CAR function in murine xenograft leukemia models (Hoyos et al., 2010; Hurton et al., 2016). As an alternative to secretable cytokines, forced expression of the membrane-bound molecule 4-1BB ligand (4-1BBL) enhanced CAR T cell treatment in preclinical models by increasing T cell persistence and decreasing T cell exhaustion (Stephan et al., 2007; Zhao et al., 2015). Our lab has recently published the use of a different membrane-bound ligand, CD40 ligand (CD40L, CD154), in concert with CAR T cells to enhance the antitumor effect (Curran et al., 2015; Kuhn et al., 2019).

CD40/CD40 Ligand Biology

CD40/CD40L in the immune system

CD40L is a type II transmembrane protein that belongs to the tumor necrosis factor gene superfamily and is mainly expressed on activated T cells and platelets. On T cells that have been stimulated through their T cell receptor (TCR) and costimulatory ligands such as CD28, pre-formed CD40L is upregulated within minutes on the cell surface, reaches peak levels after 6 hours,

and then its surface expression declines over the next 24 hours (Casamayor-Palleja et al., 1995; Castle et al., 1993; Jaiswal et al., 1996). CD40L binds to CD40, which is expressed on several immune cells including B cells, dendritic cells (DCs), and macrophages, as well as on hematopoietic and solid tumor cells (Elgueta et al., 2009). DCs belong to the innate immune system and have important established functions in antitumor response, wherein they can prime antitumor T cell responses through their TCR by presenting antigenic peptides on their cell surface via MHC-I and MHC-II (Banchereau and Steinman, 1998). The CD40-CD40L interaction leads to activation of DCs, wherein they are matured and primed to secrete the pro-inflammatory cytokine IL-12 and support $CD4^+$ T cell helper responses (Cella et al., 1996; Heufler et al., 1996). Further, CD40-mediated activation of DCs improves T cell function through priming of $CD8^+$ cytotoxic T cells (Bennett et al., 1998; Ridge et al., 1998; Schoenberger et al., 1998). Pharmacological activation of DCs via agonistic anti-CD40 or checkpoint blockade in combination with chemotherapy was shown to drive T cell-mediated immunity against cancer in syngeneic in vivo mouse models (Byrne and Vonderheide, 2016; de Mingo Pulido et al., 2018; Salmon et al., 2016).

CD40 on tumor cells

CD40 is expressed on many cancer cells of hematological origin, such as CLL, ALL, lymphoma, multiple myeloma, and AML, but also on many non-hematological cancer cells (Elgueta et al., 2009). Melanoma, lung, prostate, bladder, cervical, and ovarian cancer have all been reported to also express CD40 protein (Elgueta et al., 2009). The function and effect of CD40 signaling in these different cancer types is only partly understood and warrants further investigation. Low level of CD40L expression on non-Hodgkin's lymphoma, Burkitt's lymphoma, and CLL cell has been reported and attributed to constitutive CD40 signaling in these cells promoting upregulation of anti-apoptotic, pro-survival proteins such as Bcl-xL (Choi et al., 1995). A similar effect was documented in human CD40-positive breast cancer cells (Baxendale et al., 2005), showing that low-level CD40/CD40L signaling can promote malignant cell survival across different tumor types.

The mode of CD40 activation on transformed cells seems to be important in determining the signaling outcome. Contrary to chronic low-level activation stimulating survival, transient CD40 stimulation via cross-linking antibodies or high levels of soluble CD40L has a strong anti-proliferative and pro-apoptotic effect on lymphoma cells (Funakoshi et al., 1994). The same enhanced susceptibility to apoptosis after receiving a strong CD40 stimulus was also observed in different carcinoma cells (Hess and Engelmann, 1996; Wingett et al., 1998). The molecular events determining CD40-induced apoptosis in transformed cells remain elusive. Tumor growth inhibition of $CD40^+$ lymphoma and breast cancer cells in SCID mice via an agonistic CD40 antibody or soluble CD40L suggest that the inhibitory effect of CD40/CD40L signaling in tumor cells is independent of functional T and B cells (Funakoshi et al., 1994; Hirano et al., 1999; Tong et al., 2001). Furthermore, many in vitro experiments demonstrating direct proliferative and apoptotic effects in cancer cells upon CD40 stimulation indicate a cell-intrinsic mechanism of tumor cell response (Elgueta et al., 2009).

Aims

Given the known CD40/CD40L biology and the conveyed T cell cytotoxicity through CARs, T cells are genetically engineered to overexpress both CD40L and a CD19-targeted CAR to generate CD40L-modified CAR T cells. The overall aim of the thesis is to interrogate if, in the context of tumor treatment, CD40L-modified CAR T cells are capable of licensing APCs in vivo and if this licensing event can prime endogenous immune effectors to aid in the antitumor response. Ultimately, we hypothesize that CD40L-modified CAR T cells enhance the antitumor response compared to CAR-only T cells. The aims are addressed in chapters 3, 4, and 5.

Genetic engineering of T cells to express CAR and CD40L transgenes

The aim in chapter 3 is to engineer T cells to constitutively express CD40L in combination with a CD19-targeted second generation CAR. The effect of constitutive CD40L expression on CAR T cells will be investigated with regard to their proliferation, viability, differentiation, and their capability to specifically lyse

CAR-targeted tumor cells. Also, chapter 3 will assess the ability of overexpressed CD40L to exert its biological function of stimulating cells through CD40/CD40L interactions. Further, it will serve to determine any differences in antitumor efficacy between CAR-only T cells and CD40L-modified CAR T cells. Importantly, this question will be addressed in a fully immune-competent syngeneic mouse tumor model in vivo. The experiments establish a model that allows investigation of the interactions between the adoptively transferred CAR T cells, tumor cells, and the endogenous host immune system in the following chapters.

In vivo licensing of APCs via CAR T cells

Chapter 4 will focus on in vivo licensing of $CD40^+$ APCs by CD40L-modified CAR T cells and how this event changes the immune cell composition in the host on a molecular and cellular level. The aim is to assess if CD40L-modified CAR T cells provide a pro-inflammatory environment specifically through CD40/CD40L interactions in the host leading to tumor rejection.

Priming and recruitment of $CD8^+$ cytotoxic T cells to aid in antitumor response

Chapter 5 is dedicated to the analysis of endogenous non-CAR T cell populations and their priming after CD40L-modified CAR T cell treatment. The working hypothesis states that CD40/CD40L-licensed APCs upregulate costimulatory molecules and cross-present antigen to $CD8^+$ cytotoxic T cells, thereby priming an endogenous T cell population to recognize and lyse tumor cells. This would provide the host with a sustained endogenous antitumor response initiated by CD40L-modified CAR T cell treatment.

CHAPTER 2

MATERIALS AND METHODS

Animal Models

Mice were bred and housed under SPF conditions in the animal facility of Memorial Sloan Kettering Cancer Center. All experiments were performed in accordance with the MSKCC Institutional Animal Care and Use Committee (IACUC) approved protocol guidelines (MSKCC #00-05-065). Wild-type BALB/c mice were purchased from Charles River. Wild-type C57BL/6, BALB/c Thy1.1^{+} (CBy.PL(B6)-*Thy1*^{a}/ScrJ), and BALB/c CD45.1 (CByJ.SJL(B6)-*Ptprc*^{a}/J) mice were purchased from Jackson laboratories. BALB/c *Cd40*$^{-/-}$ (CNCr.129P2-*Cd40*^{tm1Kik}/J) were kindly provided by Dr. Anna Valujskikh and bred in-house. BALB/c *Batf3*$^{-/-}$ (C.129S-*Batf3*^{tm1Kmm}/J) were kindly provided by Dr. Barney Graham and bred in-house. 8-12 week old gender-matched mice challenged with firefly luciferase-expressing tumor were imaged via bioluminescence to confirm equal tumor load and randomized to different treatment groups one day before treatment. Mice were euthanized when tumor growth led to a weight gain of 20% due to a distended abdomen or when mice suffered from hind limb paralysis. The investigator was blinded when assessing the outcome.

Cell Lines

A20 cells (catalog number TIB-208) and Phoenix-ECO packaging cells (catalog number CRL-3214) were purchased from ATCC. The Eμ-ALL01 cell line was a kind gift from Michel Sadelain (Davila et al., 2013). The ID8.*VegfA-Defb29* cell line was a kind gift from Jose R. Conejo-Garcia. All cell lines were maintained in RPMI-1640 supplemented with 10% heat-inactivated FBS, nonessential amino acids, 1 mM sodium pyruvate, 10 mM HEPES, 2 mM L-glutamine, 1% penicillin/streptomycin, 11 mM glucose, and 2 μM 2-mercaptoethanol. Cell lines were routinely tested for potential mycoplasma contamination.

Generation of retroviral constructs

Plasmids encoding the CAR construct in the SFG γ-retroviral vector (Riviere et al., 1995) were used to transfect gpg29 fibroblasts (H29) with the ProFection Mammalian Transfection System (Promega) according to the manufacturer's instructions in order to generate vesicular stomatitis virus G-glycoprotein-pseudotyped retroviral supernatants. These retroviral supernatants were used to construct stable Moloney murine leukemia virus-pseudotyped retroviral particle-producing Phoenix-ECO cell lines. The SFG-m1928z-CD40L vector was constructed by stepwise Gibson Assembly (New England BioLabs) using the cDNA of previously described anti-mouse CD19 scFv (Davila et al., 2013), Myc-tag sequence (EQKLISEEDL), murine CD28 transmembrane and intracellular domain, murine CD3ζ intracellular domain without the stop codon, P2A self-cleaving peptide, and the murine CD40L protein.

Mouse T cell isolation and retroviral transduction

Mice were euthanized and their spleens were harvested. Following tissue dissociation and red blood cell lysis, $CD3^+$, $CD4^+$, or $CD8^+$ T cells were enriched via negative selection using the EasySep Mouse T Cell Isolation Kit (StemCell). Cells were then expanded *in vitro* by culturing in RPMI-1640 supplemented with 10% heat-inactivated FBS, nonessential amino acids, 1 mM sodium pyruvate, 10 mM HEPES, 2 mM L-glutamine, 1% penicillin/streptomycin, 11 mM glucose, 2 μM 2-mercaptoethanol, 100 IU of recombinant human IL-2 (rhIL-2) (Prometheus Therapeutics & Diagnostics), and anti-CD3/28 Dynabeads (Life Technologies) at a bead:cell ratio of 1:2. 24 h and 48 h after initial expansion, T cells were spinoculated on retronection (Takara)-coated plates with viral supernatant collected from Phoenix-ECO cells as described previously (Lee et al., 2009). After the second spinoculation, cells were rested for one day and then used in adoptive transfer studies.

Human T cell isolation and retroviral transduction

Human T cells were isolated from fresh blood-derived leukocyte concentrate (Leukopack) purchased from the New York Blood Center. Mononuclear cells were separated using density gradient centrifugation with Accu-prep (axis-Shield PoC, AS, Oslo, Norway). Post cell separation, the mononuclear cell mixture was resuspended in RPMI-1640 supplemented with 10% heat-inactivated FBS, 100 U/ml penicillin and streptomycin, 2 mM L-glutamine, and 100 IU/ml rhIL-2. Cells were activated with 10 ug/ml PHA (Sigma Aldrich) and 48 hr later activated T cells were enumerated and retrovirally transduced by spinoculation. T cells were spinoculated with supernatant from HEK293.GalV-9 retroviral producer cells on retronectin-coated plates as described before (Brentjens et al., 2003). After the second spinoculation, new media and rhIL-2 (100 IU/ml) was added and cells were rested for 24 hr and then assessed for transgene expression by flow cytometry.

Human T cell co-culture experiment

Human anti-CD19 CAR T cells were co-cultured with antigen-negative murine NIH/3T3 fibroblast cells or CD19-expressing NIH/3T3 cells (3T3.hCD19) at a 1:1 ratio at $1x10^5$ cells each per well in a 12-well tissue culture plate. After 4, 24, and 48 hr of co-culture, cells were collected and CD40L expression on CAR T cells was assessed by flow cytometry.

Cytotoxicity assays

Short-term quantitative cytotoxicity assay

The short-term cytotoxicity of CAR^+ T cells was determined by a standard luciferase-based killing assay. $1x10^5$ target tumor cells expressing firefly luciferase were co-cultured with effector CAR^+ T cells at different effector-to-target ratios in triplicates in white-walled 96-well plates (Corning) in a total volume of 200 ul of cell media. Target cells alone were plated at the same cell density to determine the maximal luciferase expression as a reference (“max signal”). 16 hr later, 75 ng of D-Luciferin (Gold Biotechnology) dissolved in 50 ul of PBS was added to each well. Emitted luminescence of each sample (“sample

signal") was detected in a Spark plate reader (Tecan) and quantified using the SparkControl software (Tecan). Percent lysis was determined as (1 – ("sample signal" / "max signal")) x 100.

Long-term cytotoxicity assay

$5x10^5$ GFP^+ A20 or A20.CD40-KO were co-cultured with $5x10^5$ CAR^+ T cells at a 1:1 ratio in 1 ml of complete media in a 5 ml round-bottom tube in sterile conditions. Twice a week, half of the media was removed and an equivalent amount of new media was added. At day 0, 7, 14, and 21 an aliquot of each sample was taken for flow cytometric analysis of GFP and surface CD19 expression.

Ex vivo cytotoxicity assay

$CD45.2^+$ wild-type A20 tumor-bearing mice were treated with $3x10^6$ $CD45.1^+$ CAR T cells via i.v. injection on day 7 after tumor challenge. On day 7 after CAR T cell treatment, endogenous $CD45.2^+$ T cells were sorted from spleens by FACS and cultured with luciferase-expressing A20.CD19-KO target cells as described above, except that $1x10^4$ instead of $1x10^5$ target tumor cells were used per well. After 24 hr, tumor cell numbers and percent lysis was determined as described above.

Adoptive transfer of CAR T cells

For tumor studies, mice were injected i.v. with 1 x 10^6 firefly luciferase-expressing tumor cells on day 0. On day 6, bioluminescence imaging using the Xenogen IVIS Imaging System (Xenogen) with Living Image software (Xenogen) for acquisition of imaging datasets was done to guarantee equal tumor burden of mice at time of treatment. Mice were then randomized into different treatment cohorts and on day 7, mice were treated with 1-3 x 10^6 CAR^+ T cells intravenously. In B cell aplasia studies, one cohort of mice received 200 mg/kg cyclophosphamide (Sigma) intraperitoneally on day -1, whereas the other cohort was left untreated. On day 0, both groups received 3 x 10^6 CAR^+ T cells intravenously. Tumor burden over time was monitored by bioluminescent imaging

and quantified over the whole animal body as photons/second/cm^2/steradian (p/s/cm^2/sr).

Tumor challenges with CAR antigen-negative tumor cells

Long-term surviving BALB/c or C57BL/6 mice (99+ after initial tumor challenge with $CD19^+$ tumor cells) were injected i.v. with $1x10^5$ A20.CD19-KO cells (BALB/c) or $1x10^6$ Eμ-ALL01.CD19-KO (C57BL/6). Naïve age-matched mice served as controls. Survival was monitored over time.

Depletion of $CD4^+$ or $CD8^+$ cell populations

To deplete $CD4^+$ T cells in tumor-bearing mice, 200 μg of anti-CD4 depletion antibody (GK1.5) or IgG control antibody (LTF-2) were injected i.p. 2x per week for 4 weeks starting one week prior to CAR T cell treatment. To deplete $CD8^+$ T cells in mice for re-challenge experiments with CD19-negative tumor cells, 200 μg of anti-CD8 depletion antibody (2.43) or IgG control antibody (LTF-2) were injected i.p. on days -3, 0, 7, 14, and 21 relative to tumor cell challenge. Depletion of $CD4^+$ and $CD8^+$ T cells was confirmed in the peripheral blood of treated mice by different antibody clones (RM4-5 for CD4 and 53-6.7 for CD8 staining).

Cell isolation for subsequent analyses

Spleens were mechanically disrupted with the back of a 5-ml syringe, filtered through a 40 μM strainer, washed with PBS, and red blood cell lysis was achieved with an ACK (Ammonium-Chloride-Potassium) Lysing Buffer (Lonza). Cells were washed with PBS, counted, and then used for subsequent analyses. Liver tissue was mechanically disrupted using a 150 μM metal mesh and glass pestle in 3% FCS/HBSS and passed through a 100 μM cell strainer. The liver homogenate was spun down at 400 g for 5 min at 4 °C to pellet the cells, which were then resuspended in 15 ml 3% FCS/HBSS, 500 ul (500 U) heparin, and 8 ml Percoll (GE), mixed by inversion, and spun at 500 g for 10 min at 4 °C. Red blood cell lyisis of the pelleted cells was done with an ACK Lysis buffer. Cells were then washed, counted, and used for subsequent analyses.

In vitro cytokine secretion analysis

For *in vitro* cytokine CAR T cell production, $1x10^5$ CAR^+ T cells and $1x10^5$ A20 tumor cells were co-cultured in a 96-well round-bottom plate in 200 ul of media. For *in vitro* IL-12p70 production of bone marrow-derived dendritic cells (BMDCs), $1x10^6$ BMDCs were co-cultured with $3x10^6$ CAR^+ T cells in 12-well plates in 2 ml of media. After 24 h the supernatant was collected and analyzed using the MILLIPLEX MAP Mouse Cytokine/Chemokine, Premixed 13 Plex kit (Millipore) and the FLEXMAP 3D system (Luminex).

Serum cytokine analysis

Whole blood was collected from mice and serum was prepared by allowing the blood to clot by centrifuging at 20,000 g for 15 min at 4 °C. Cytokine detection was done using the MILLIPLEX MAP Mouse Cytokine/Chemokine, Premixed 13 Plex kit (Millipore) and the FLEXMAP 3D system (Luminex).

Cytokine Array

A20 lymphoma-bearing mice were treated with $3x10^6$ m1928z or m1928z-CD40L CAR T cells on day 7. On day 14, mouse spleens were harvested and homogenized in 1 ml of PBS with cOmplete Protease Inhibitor Cocktail (Roche) on ice. An equal amount of tissue lysate was used to probe cytokines/chemokines using the Proteome Profiler Mouse Cytokine Array Kit, Panel A (R&D Systems, ARY006) according to the manufacturer's instructions. Quantification of the spot intensity on the blot membranes was done after background subtraction with ImageJ.

In vitro T cell stimulation

To assess CD40 surface expression on T cells, purified $CD3^+$ T cells as described above were seeded at $1x10^5$ cells per well in a round-bottom 96-well plate in 200 ul of media and stimulated with or without rhIL-2 (100 IU/ml) and CD3/28 dynabeads (1-to-2 bead-to-T cell ratio). At indicated time points, cells were collected, washed, fixed and stored in 1% paraformaldehyde (Sigma). After all time points were collected, cells were surface stained and analyzed by flow cytometry.

In vitro T cell culture

$1x10^5$ CAR T cells were seeded in 200 ul of media in a 96-well round bottom plate without any supportive cytokines or stimulation. Triplicate wells were seeded for every time point. Cells were collected at indicated time points and quantified using 123count eBeads Counting Beads (Thermo Fisher). Dead cells were excluded by gating on $DAPI^-$ cells.

Bone marrow-derived dendritic cell solation and co-culture with CAR T cells

BMDCs were generated as previously described (Helft et al., 2015). Briefly, $1x10^7$ bone marrow cells per well were cultured in tissue-culture-treated 6-well plates in 4 ml of RPMI-1640 supplemented with 10% heat-inactivated FBS, nonessential amino acids, 1 mM sodium pyruvate, 10 mM HEPES, 2 mM L-glutamine, 1% penicillin/streptomycin, 11 mM glucose, 2 µM 2-mercaptoethanol, and 20 ng/ml GM-CSF (Peprotech). Half of the medium was removed at day 2 and new medium supplemented with GM-CSF (2x, 40 ng/ml) was added. The culture medium was entirely discarded at day 3 and replaced by fresh medium with GM-CSF (20 ng/ml). On day 6 of culture, non-adherent cells in the culture supernatant were used in the co-culture experiments. Cells were co-cultured in 96-well flat bottom culture by co-incubating $1x10^5$ BMDCs and $1x10^5$ CAR^+ T cells per 100 ul for 24 to 48 h. Plates were briefly spun down and culture supernatants were collected and assayed for IL-12p70 secretion via Luminex Mouse TH17 Assay (Millipore) or $ELISA^{PRO}$ kit Mouse IL-12 (p70) (Mabtech) according to the manufacturer's instructions. Cells were used for flow cytometric analysis.

CRISPR/Cas9-mediated knockout in tumor cells

A20 and Eµ-ALL01 cells were transfected by electrotransfer of modified Cas9 mRNA (Trilink) and gRNA using an AgilePulse MAX system (Harvard Apparatus). $2x10^5$ cells were mixed with 5 µg of Cas9 mRNA and 10 µg of gRNA into a 2 mm gap cuvette. For MHC-II knockout, two gRNAs were added simultaneously. Following electroporation, cells were transferred into media and

incubated at 37 °C, 5% CO_2. 48 h later, knockout efficiency was detected by surface staining of target molecule. Single cell clones were generated via serial dilution and expanded to generate a homogenous knockout line. gRNA was generated by *in vitro* transcription using the MEGAshortscript T7 Transcription Kit (Thermo Fisher) and subsequently purified using the MEGAclear Transcription Clean-Up Kit (Thermo Fisher) according to the manufacturer's instructions; or chemically modified gRNA (2'-O-methyl analogs at the first three 5' RNA residues and 3' phosphorothioate internucleotide linkages at the last three 3' RNA residues) was purchased from Synthego.

Flow cytometry and FACS sorting

Flow cytometric analyses were performed using a Beckman Coulter Gallios or a Thermo Fisher Attune NxT flow cytometer. Data were analyzed using FlowJo (Tree Star). DAPI (0.5 mg/ml, Sigma-Aldrich) or a LIVE/DEAD fixable violet dead cell stain kit (Thermo Fisher) were used to exclude dead cells in all experiments, and anti-CD16/CD32 antibody (93) was used to block non-specific binding of antibodies via Fc receptors. The following anti-mouse antibodies were used for flow cytometry: anti-CD3ε (clone 145-2C11), anti-CD4 (GK1.5), anti-CD8α (53-6.7), anti-CD11b (M1/70), anti-CD11c (N418), anti-CD19 (eBio1D3), anti-CD40 (3/23), anti-CD40L (MR1), anti-CD44 (IM7), anti-CD45 (30-F11), anti-CD45.1 (A20), anti-CD45.2 (104), anti-CD62L (MEL14) anti-CD80 (16-10A1), anti-CD86 (GL1), anti-CD103 (2E7), anti-CXCL9 (MIG-2F5.5), anti-F4/80 (BM8), anti-Foxp3 (FJK-16s), anti-IFNγ (XMG1.2), anti-IL-2 (JES6-5H4), anti-IL-4 (11B11), anti-IL-12p40 (C17.8), anti-IL-17A (eBio17B7), anti-Ly-6G/Ly-6C (Gr-1) (RB6-8C5), anti-MHC class I (MHC-I) H-2Kd (SF1-1.1.1), anti–MHC class II (MHC II) I-A/I-E (M5/114.15.2), anti-Myc-tag (9B11), anti-Thy1.1 (HIS51), anti-Thy1.2 (30-H12), and anti-TNFα (MP6-XT22). Quantification of total cell numbers by flow cytometry was done using 123count eBeads Counting Beads (Thermo Fisher). For intracellular staining of IFNγ, TNFα, IL-2, IL-4, and IL-17, a single cell suspension of liver or spleen tissue was generated (for IFNγ and TNFα stain) or in vitro cultured CAR T cells were collected (for IL-2, IL-4, and IL-17 stain) and cells were stimulated with 1x Cell Stimulation Cocktail (phorbol 12-myristate 13-

acetate (PMA), ionomycin, brefeldin A, and monensin) from Thermo Fisher for 5 h. Cells were then processed with the Cytofix/Cytoperm Plus kit (BD Biosciences) per the manufacturer's instructions. For intracellular staining of IL-12p40 and CXCL9 *ex vivo*, the same staining protocol was used without prior stimulation. Staining of Foxp3 was done using the Foxp3/Transcription factor staining buffer set from eBioscience. All antibodies were purchased from Biolegend, BD Biosciences, Cell Signaling, eBioscience, or Thermo Fisher. Sorting of splenocytes after tissue processing was done using a BD FACSAria under sterile conditions. Purity of cell populations was determined by reanalysis of an aliquot of sorted cell samples.

ELISpot assay

Splenocytes from tumor-challenged non-treated or treated mice were harvested on day 14 after tumor inoculation. Single cell suspensions were prepared and sorted by FACS as described above. $1x10^5$ T cells ($CD4^+$ $Thy1.2^+$ or $CD8^+$ $Thy1.2^+$ or $CD8^+$ $CD45.2^+$) cells were assayed per well. Cells were either left unstimulated or stimulated with $1x10^5$ tumor cells (A20.GFPluc, A20.MHCII-KO or A20.B2M-KO) or concanavalin A (4 ug/ml) as a positive control. After a 24 hr culture period, detection of INFγ-producing T cells was performed according to manufacturer's instructions using Millipore ELISpot plates (Mabtech).

Immunofluorescent Microscopy

Mouse lymph nodes or spleens were snap frozen in OCT Compound (Tissue-Tek) and stored at -80 °C. 10 µm sections of frozen tissue were dried for 1-2 h at room temperature and then fixed in 100% acetone for 20 min at -20 °C, dried for 5-10 min at room temperature, and blocked for 90 min with 10% rat serum and TruStain FcX (anti-mouse CD16/32) antibody (1:100) in PBS. After washing the tissue sections in PBS for three times at room temperature, the samples were incubated with rat anti-mouse CD3-A488 (Biolegend), rat anti-mouse/human B220-A549 (Biolegend), and mouse Myc-Tag-A647 (Cell Signaling) antibodies overnight at 4 °C in the dark. The sections were then washed again three times in PBS at room temperature and counterstained with 1 µg/ml DAPI in PBS for 10

min at room temperature in the dark. Samples were mounted with Fluoromount-G (Thermo Fisher) and scanned using Pannoramic Flash (Perkin Elmer) with a 20x/0.8NA objective. Images were processed using CaseViewer (3D Histech) and ImageJ (NIH).

Necropsy and Histopathology

Mice were euthanized with CO2. Following gross examination all organs were fixed in 10% neutral buffered formalin, followed by decalcification of bone in a formic acid solution (Surgipath Decalcifier I, Leica Bioosystems). Tissues were then processed in ethanol and xylene and embedded in paraffin in a Leica ASP6025 tissue processor. Paraffin blocks were sectioned at 5 microns, stained with hematoxylin and eosin (H&E), and examined by a board-certified veterinary pathologist. The following tissues were processed and examined: heart, thymus, lungs, liver, gallbladder, kidneys, pancreas, stomach, duodenum, jejunum, ileum, cecum, colon, lymph nodes (submandibular, mesenteric), salivary glands, skin (trunk and head), urinary bladder, uterus, cervix, vagina, ovaries, oviducts, adrenal glands, spleen, thyroid gland, esophagus, trachea, spinal cord, vertebrae, sternum, femur, tibia, stifle join, skeletal muscle, nerves, skull, nasal cavity, oral cavity, teeth, ears, eyes, pituitary gland, brain.

Hematology and Serum Chemistry

For hematology, blood was collected into tubes containing EDTA. Automated analysis was performed on an IDEXX Procyte DX hematology analyzer and platelet count was determined. For serum chemistry, blood was collected into tubes containing a serum separator, the tubed were centrifuged and the serum was obtained for analysis. Serum chemistry was performed on a Beckman Coulter AU680 analyzer and the concentration of the following analytes was determined: alanine aminotransferase (ALT) and aspartate aminotransferase (AST).

Quantification and Statistical Analysis

All statistical analyses were performed using GraphPad Prism software (GraphPad). Data points represent biological replicates and are shown as the

mean ± SEM or mean ± SD as indicated in the figure legends. Statistical significance was determined using an unpaired two-tailed Student's t-test. The log-rank (Mantel-Cox) test was used to determine statistical significance for overall survival in mouse survival experiments. Significance was assumed with *$p < 0.05$; **$p < 0.01$; ***$p < 0.001$; ****$p < 0.0001$.

Table 2.1 Reagents and other Resources

REAGENT or RESOURCE	SOURCE	IDENTIFIER
Antibodies		
TruStain fcX (anti-mouse CD16/32)	BioLegend	Cat# 101319, RRID:AB_1574973
anti-mouse/human B220 (clone RA3-6B2) AlexaFluor-594	BioLegend	103254, RRID:AB_2563229
anti-mouse CD3 (clone 17A2) AlexaFluor 488	BioLegend	100212, RRID:AB_493530
anti-mouse CD3ε (clone 145-2C11) PE-eFluor 610	eBioscience	61-0031, RRID:AB_2574514
anti-mouse CD4 (GK1.5) AlexaFluor 700	eBioscience	56-0041, RRID:AB_493999
anti-mouse CD8α (53-6.7) APC-eFluor 780	eBioscience	47-0081, RRID:AB_1272185
anti-mouse/human CD11b (M1/70) AlexaFluor 700	eBioscience	56-0112, RRID:AB_657585)
anti-mouse CD11c (N418) APC-eFluor 780	eBioscience	47-0114, RRID:AB_1548663
anti-mouse CD19 (eBio1D3) APC-eFluor 780	eBioscience	47-0193, RRID:AB_10853189
anti-mouse CD19 (eBio1D3) PE	eBioscience	12-0193, RRID:AB_657661
anti-mouse CD19 (eBio1D3) PE-eFluor 610	eBioscience	61-0193, RRID:AB_2574536
anti-mouse CD40 (1C10) PerCP-eFluor 710	eBioscience	46-0401, RRID:AB_2573677
anti-human CD40L (TRAP) PE	BD Pharmingen	555700
anti-mouse CD40L (MR1) PE	eBioscience	12-1541, RRID:AB_465887
anti-mouse CD44 (IM7) APC-eF780	eBioscience	47-0441
anti-mouse CD45 (30-F11) BV605	BioLegend	103139, RRID:AB_2562341
anti-mouse CD45 (30-F11) PE-Cy7	eBioscience	25-0451, RRID:AB_469625
anti-mouse CD45.1 (A20) PE-eFluor610	eBioscience	61-0453
anti-mouse CD45.2 (104) PE-Cy7	eBioscience	25-0454
anti-mouse CD62L (MEL14)	eBioscience	56-0621
anti-mouse CD69 (H1.2F3) FITC	BioLegend	104505, RRID:AB_313108

anti-mouse CD80 (16-10A1) PE	eBioscience	12-0801, RRID:AB_465753
anti-mouse CD86 (GL1) PE-Cy7	eBioscience	25-0862, RRID:AB_2573372
anti-mouse CD103 (2E7) BV711	BioLegend	121435
anti-mouse CXCL9 (MIG-2F5.5) PE	BioLegend	515604
anti-human EGFR (Cetuximab) APC	MSKCC Antibody Core	
anti-mouse F4/80 (BM8) APC	eBioscience	17-4801, RRID:AB_469452
anti-mouse Foxp3 (FJK-16s) PE	eBioscience	12-5773, RRID:AB_465936
anti-mouse IFNγ (XMG1.2) PE-Cy7	eBioscience	25-7311, RRID:AB_1257211
anti-mouse IL-2 (JES6-5H4)	eBioscience	17-7021
anti-mouse IL-4 (11B11) PerCPeF710	eBioscience	46-7041
anti-mouse IL-12p40 (C17.8) PE	eBioscience	12-7123, RRID:AB_466185
anti-mouse IL-17A (eBio17B7) APC	eBioscience	17-7177
anti-mouse Ly-6G/Ly-6C (Gr-1) (RB6-8C5) PE-eFluor 610	eBioscience	61-5931, RRID:AB_2574639
anti-mouse Ly-6G/Ly-6C (Gr-1) (RB6-8C5) PE-Cy7	eBioscience	25-5931, RRID:AB_469662
anti-mouse MHC class I (MHC-I) H-2Kd (SF1-1.1.1) PerCP-eFluor 710	eBioscience	46-5957, RRID:AB_10735380
anti-mouse MHC class II (MHC-II) I-A/I-E (M5/114.15.2) BV510	BioLegend	107635, RRID:AB_2561397
anti-human Myc-tag (9B11) AlexaFluor 647	Cell Signaling	2233S, RRID:AB_10693328
anti-mouse Thy1.1 (HIS51) APC	eBioscience	17-0900, RRID:AB_469420
anti-mouse Thy1.2 (30-H12) BV510	BioLegend	105307, RRID:AB_313178
anti-mouse TNFα (MP6-XT22) BV510	BioLegend	506339, RRID:AB_2563127
Anti-		
Chemicals, Peptides, and Recombinant Proteins		
LPS from *E.coli* O55:B5	Sigma-Aldrich	L2880

Cell Stimulation Cocktail (plus Protein Transport Inhibitors)	eBioscience	00-4975
LIVE/DEAD Fixable Violet Dead Cell Stain Kit	Thermo Fisher	L34955
RetroNectin Recobminant Human Fibronectin Fragment	Takara	T100B
cOmplete EDTA-free Protease Inhibitor Cocktail	Roche	04693159001
Cyclophosphamide monohydrate	Sigma-Aldrich	C0768
D-Luciferin, Potassium Salt (Proven and Published)	Gold Biotechnology	LUCK-1G
Recombinant human IL-2 (Proleukin/Aldesleukin)	Prometheus Therapeutics & Diagnostics	NDC 65483-116-07
Recombinant mouse GM-CSF	Peprotech	315-03
Critical Commercial Assays		
Foxp3/Transcription Factor Staining Buffer Set	eBioscience	00-5523-00
EasySep™ Mouse T Cell Isolation Kit	Stemcell Technologies	19851
EasySep™ Mouse B cell Isolation Kit	Stemcell Technologies	19854
Fixation/Permeabilization Solution Kit	BD Biosciences	554714
123count eBeads Counting Beads	eBioscience	01-1234-42
Luminex Mouse TH17 Assay	Millipore	MTH17MAG-47K
Proteome Profiler Mouse Cytokine Array Kit, Panel A	R&D Systems	ARY006
ELISA^{PRO} kit Mouse IL-12 (p70)	Mabtech	3456-1 HP-2
Mouse IFN-γ ELISpot^{PLUS}	Mabtech	3321-4HPW-2
MEGAshortscript T7 Transcription Kit	Thermo Fisher	AM1354
MEGAclear Transcription Clean-Up Kit	Thermo Fisher	AM1908
Experimental Models: Cell Lines		
Human: Phoenix-ECO	ATCC	CRL-3214, RRID:CVCL_H717

Mouse: A20 lymphoma cell line	ATCC	TIB-208, RRID:CVCL_1940
Mouse: A20.GFPluc	This study	N/A
Mouse: A20.CD19-KO	This study	N/A
Mouse: A20.CD40-KO	This study	N/A
Mouse: A20.MHCII-KO	This study	
Mouse: A20.B2M-KO	This study	N/A
Mouse: ID8.*VegfA-Defb29*	Laboratory of Jose R. Conejo-Garcia	N/A
Mouse: Eμ-ALL01	Laboratory of Michel Sadelain	N/A
Mouse: NIH/3T3	ATCC	CRL-1658
Mouse: NIH/3T3.hCD19	This study	
Experimental Models: Organisms/Strains		
Mouse: BALB/cAnN	Charles Rivers	CR: 028; RRID:MGI:5654849
Mouse: CBy.PL(B6)-*Thy1*^{a}/ScrJ	The Jackson Laboratory	JAX: 005443; RRID:IMSR_JAX:005443
Mouse: CNCr.129P2-*Cd40*^{tm1Kik}/J	The Jackson Laboratory	JAX: 002927; RRID:IMSR_JAX:002927
Mouse: CByJ.SJL(B6)-*Ptprc*^{a}/J	The Jackson Laboratory	JAX: 006584
Mouse: C.129S-*Batf3*^{tm1Kmm}/J	The Jackson Laboratory	JAX: 013756
Mouse: C57BL/6J	The Jackson Laboratory	JAX: 00664; RRID: IMSR_JAX:000664
Oligonucleotides		
CleanCap™ Cas9 mRNA (modified)	Trilink Biotech	Cat# L-7206
gRNA *Cd19*	AUUCAAACUGC UCCCCCGAGUU UUAGAGCUAGA AAUAGCAAGUU AAAAUAAGGCU AGUCCGUUAUC AACUUGAAAAA GUGGCACCGAG UCGGUGC	N/A

gRNA *Cd40*	CCUCGGCUGUG CGCGCUAUGUU UUAGAGCUAGA AAUAGCAAGUU AAAAUAAGGCU AGUCCGUUAUC AACUUGAAAAA GUGGCACCGAG UCGGUGC	N/A
gRNA *B2m*	GUGAGUAUACU UGAAUUUGAGU UUUAGAGCUAG AAAUAGCAAGU UAAAAUAAGGC UAGUCCGUUAU CAACUUGAAAAA GUGGCACCGAG UCGGUGC	N/A
gRNA *H2-Ab1 (MHC-II)*	GTGCGCTACGA CAGCGACGTGU UUUAGAGCUAG AAAUAGCAAGU UAAAAUAAGGC UAGUCCGUUAU CAACUUGAAAAA GUGGCACCGAG UCGGUGC	N/A
gRNA *H2-Eb2 (MHC-II)*	GTGGGAGTGAA TGCCACATGGU UUUAGAGCUAG AAAUAGCAAGU UAAAAUAAGGC UAGUCCGUUAU CAACUUGAAAAA GUGGCACCGAG UCGGUGC	N/A
Recombinant DNA		

Plasmid: SFG	This study	N/A
Software and Algorithms		
GraphPad Prism v7	GraphPad	https://www.graphpad.com/scientific-software/prism/
FlowJo Version 10	FlowJo LLC	https://www.flowjo.com/
SparkControl	Tecan	https://lifesciences.tecan.com/multimode-plate-reader?p=Software
CaseViewer	3D Histech	https://www.3dhistech.com/caseviewer
FIJI/ImageJ		https://imagej.net/Fiji/Downloads

CHAPTER 3

Engineering CAR T Cells to Overexpress CD40L

Introduction

To investigate the potential of CAR T cells to actively recruit endogenous members of the immune system, we relied on a syngeneic immunecompetent mouse model. Murine A20 cells are cancerous cells isolated from an aged (>15 months) BALB/cAnN mouse with a spontaneously developed neoplasm (Kim et al., 1979). After in vivo passaging, the A20 cell line was established and characterized as IgM^-, IgG^-, IgA^-, MHC-II^+ (I-Ad), MHC-I^+ (H-2Kd), FcR^+, and complement $receptor^+$ (Kim et al., 1979), with CD19, CD20, B220, and CD40 surface expression characterizing A20 cells as B cell lineage-derived (Figure 3.1A). This cell line was chosen as the first tumor model to test CD40L-modified CD19-targeted CAR T cells. After i.v. injection, the A20.GL cells (transduced to express a GFP-luciferase fusion protein to allow in vivo tracking) disseminate systemically to several lymphoid and non-lymphoid organs, such as the spleen, lymph nodes, bone marrow, and liver (Kim et al., 1979) (Figures 3.1B-3.1D), recapitulating aspects of late-stage B cell malignancies.

Targeting of tumor cells is achieved through genetic engineering of murine T cells to express an anti-mouse CD19 CAR T cell with or without concomitant overexpression of CD40L. Characterization of these genetically engineered T cells and their antitumor efficacy is described in the following chapter.

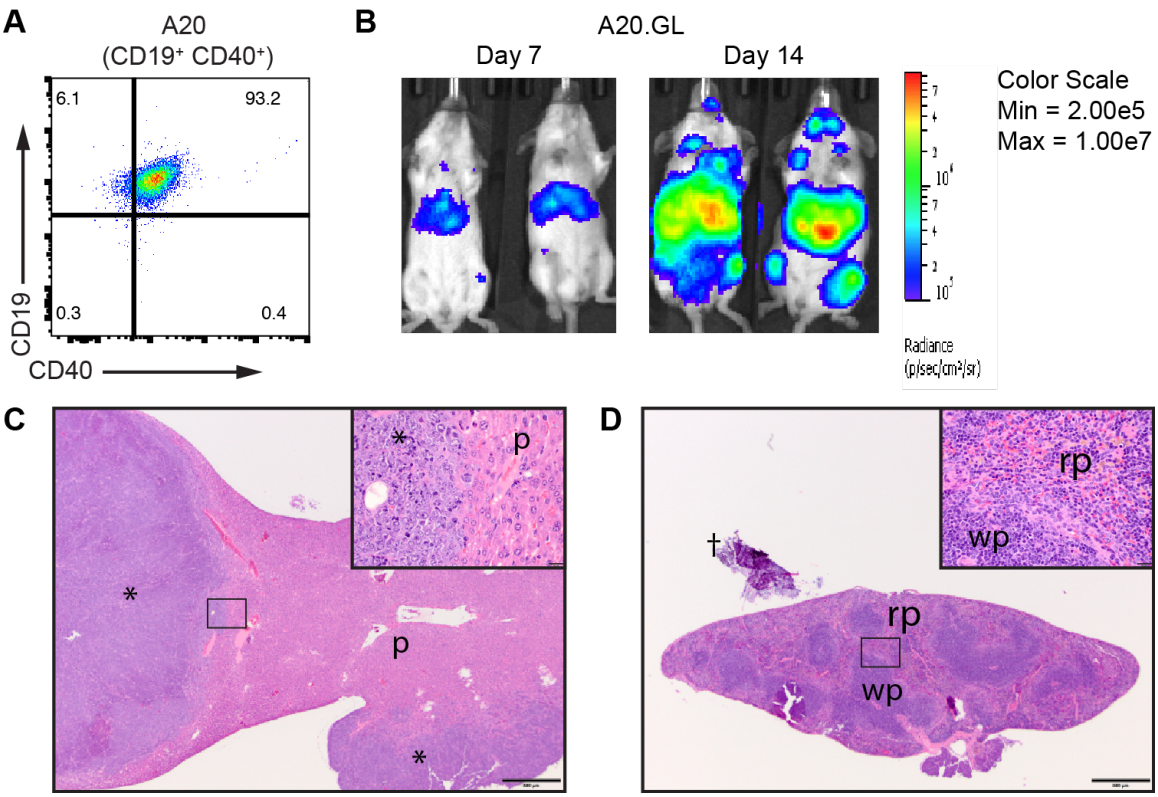

Figure 3.1. Characterization of the A20 lymphoma model
(A) Surface expression of CD19 and CD40 on A20 lymphoma cells by flow cytometry.
(B) Bioluminescence images of two representative mice on day 7 and 14 after being injected intravenously with A20.GL cells on day 0.
(C and D) Hematoxylin and eosin stains of liver (C) and spleen (D) of a moribund mouse harboring A20 lymphoma after i.v. injection. Tumor growth in liver visible as nodules. No tumor growth in spleen. Boxed-in regions are shown at higher magnification. Scale bar, 500 or 20 μm. *, tumor; †, artefact; p, liver parenchyma with hepatocytes; rp, red pulp; wp, white pulp. Adapted from Kuhn et al. (2019), *Cancer Cell*, 35(3):473-488.

Results

Genetic Engineering of T cells with Chimeric Antigen Receptors and CD40L

A previously generated anti-mouse CD19 scFv (Davila et al., 2013) was fused to a myc-tag, the murine CD28 transmembrane and intracellular domains, and the CD3ζ intracellular domain to generate a murine second-generation CAR (m1928z, Figure 3.2A). The self-cleaving P2A element between the CAR and murine CD40L allowed expression of both transgenes from one expression cassette driven by the same promoter (m1928z-CD40L, Figures 3.2A and 3.2B). Stable transgene expression in murine T cells is achieved by γ-retroviral transduction of murine T cells. The 5' LTR of the Moloney Mouse Leukemia Virus (MoMLV) drives expression of the transgene downstream after stable genomic integration. Addition of splice acceptor (SA) and splice donor (SD) sites flanking the packaging signal ψ enables splicing of the RNA transcript, resulting in removal of the complex secondary structure encoding the packaging signal ψ and subsequent efficient translation of the spliced RNA transcript (Krall et al., 1996).

As expected, anti-CD19 CAR T cells specifically lysed the $CD19^+$ A20 lymphoma (Figure 3.2C) and Eμ-ALL01 leukemia cell lines (Figure 3.2D), but not $CD19^-$ ID8 cells (Figure 3.2E). 4h11-28z CAR T cells served as negative controls. The 4h11 scFv recognizes the retained ectodomain of human MUC16 ($hMUC16^{Ecto}$), a glycosylated mucin overexpressed in ovarian cancer (Koneru et al., 2015). Constitutive CD40L expression conveyed no additional benefit in short-term cytotoxicity (Figures 3.2C and 3.2D), nor did it affect CAR-mediated effector cytokine release by T cells upon antigen encounter (Figure 3.2F). CRISPR/Cas9-mediated knockout (KO) of CD19 in A20 cells (A20.CD19-KO) prevented CD19-targeted CAR T cells from target lysis (Figure 3.2G). However, CAR T cells expressing CD40L – m1928z-CD40L and 4h11-28z-CD40L – still lysed the A20.CD19-KO cells at a low efficiency (Figure 3.2G). The antigen-independent lysis by the $CD40L^+$ CAR T cells was dependent on tumor CD40 expression, as neither $CD19^+$ $CD40^-$ Eμ-ALL01 cells, nor A20 cells lacking CD40

(A20.CD40-KO) were lysed by the CD40L-expressing off-target CAR T cell 4h11-28z-CD40L (Figures 3.2D and 3.2H).

The function of the CD28 signaling domain was validated by crosslinking CARs containing different costimulatory domains on transduced T cells and measuring subsequent IL-2 production by intracellular staining of the cytokine. The m19DEL construct has the extracellular anti-CD19 scFv, myc-tag, and CD28 transmembrane domain, but no intracellular costimulatory domains (Figure 3.3A). The m19z construct is referred to as the “first-generation” CAR with the intracellular CD3ζ costimulatory domain fused to the C-terminus of m19DEL and serves as the negative control, whereas the “second-generation” m1928z CAR construct incorporates the CD28 intracellular domain and allows IL-2 production in CAR T cells after anti-myc antibody-mediated receptor crosslinking (Figure 3.3B), akin to surface stimulation of CD3 and CD28 on non-modified T cells with αCD3/28 microbeads (Figure 3.3C).

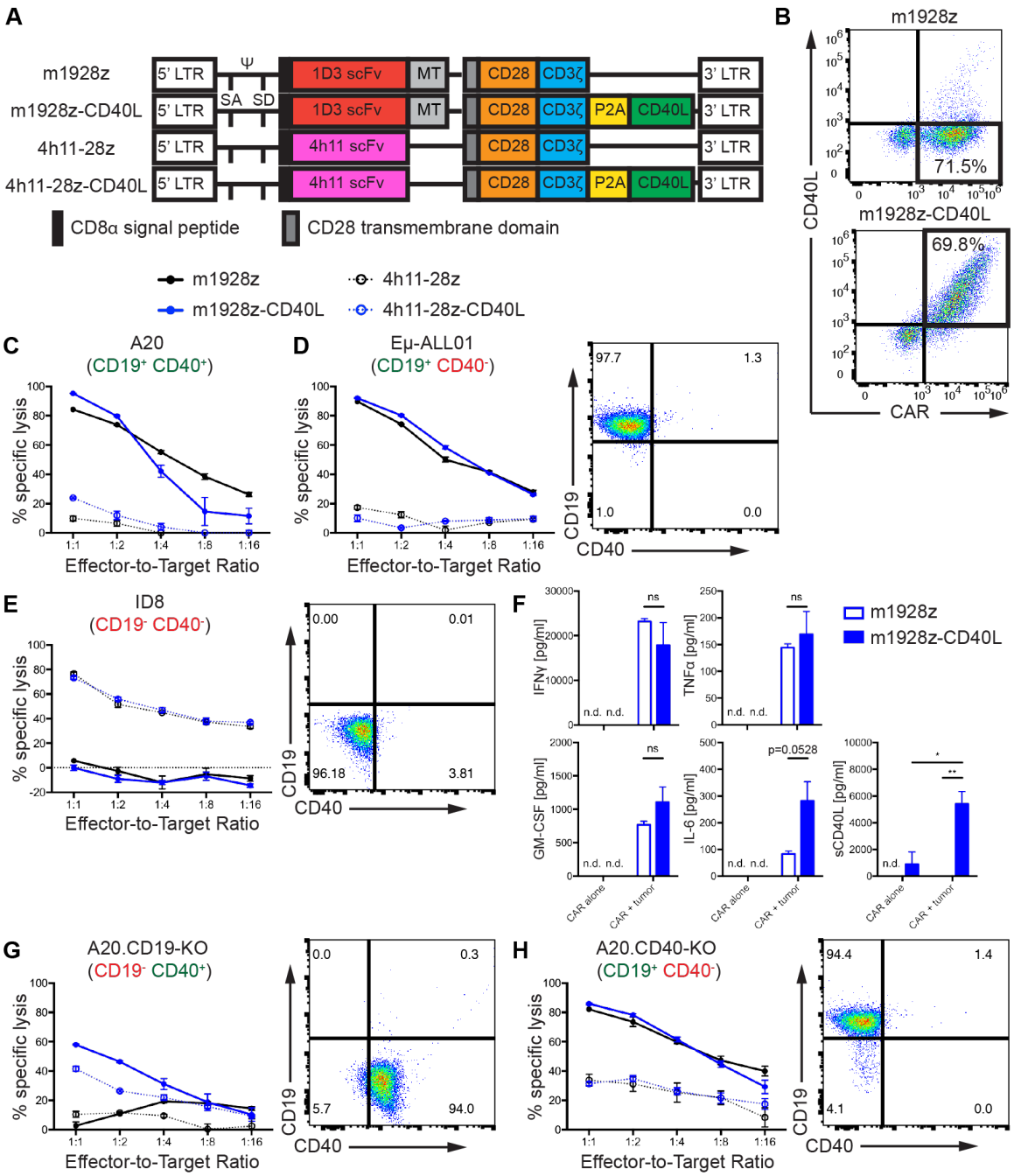

Figure 3.2. Genetic engineering of murine T cells with chimeric antigen receptors (CARs) and CD40L

(A) Transgene cassettes encoding CARs with or without CD40L. The 1D3 scFv binds murine CD19 and the 4h11 scFv binds the ectodomain of human MUC16, serving as a negative control throughout this study.

(B) Transgene surface expression after retroviral transduction of mouse T cells analyzed by flow cytometry.

(C-E) In vitro cytotoxicity of CAR T cells was assessed using a 16 hr bioluminescence assay. $CD19^+$ $CD40^+$ A20 (C), and $CD19^+$ $CD40^-$ Eμ-ALL01 (D) cells were used as targets. $CD19^-$ $CD40^-$ $hMUC16^+$ ID8 (E) cells served as a negative control. Plots are representative of two independent

experiments. Data are means ± SEM. Dot plots of Eu-ALL01 (D) and ID8 (E) cells show surface expression of CD40 and CD19.
(F) m1928z or m1928z-CD40L CAR T cells were co-cultured with or without $CD19^+$ A20 tumor cells. Supernatants were collected after 24 hr and cytokine production was measured by Luminex. Data are means ± SEM. *p<0.05, **p<0.01, ns, non-significant (Student's t-test).
(G and H) In vitro cytotoxicity of CAR T cells was assessed using a 16 hr bioluminescence assay against A20 cells with KO of CD19 (I) or CD40 (J). Plots are representative of two independent experiments. Data are means ± SEM. Dot plots of A20.CD19-KO (F) and A20.CD40-KO (G) cells show surface expression of CD40 and CD19.
LTR, long terminal repeats; MT, myc tag; P2A, P2A element; SA, splice acceptor; scFv, small chain variable fragment; SD, splice donor; Ψ, packaging signal. Adapted from Kuhn et al. (2019), *Cancer Cell*, 35(3):473-488.

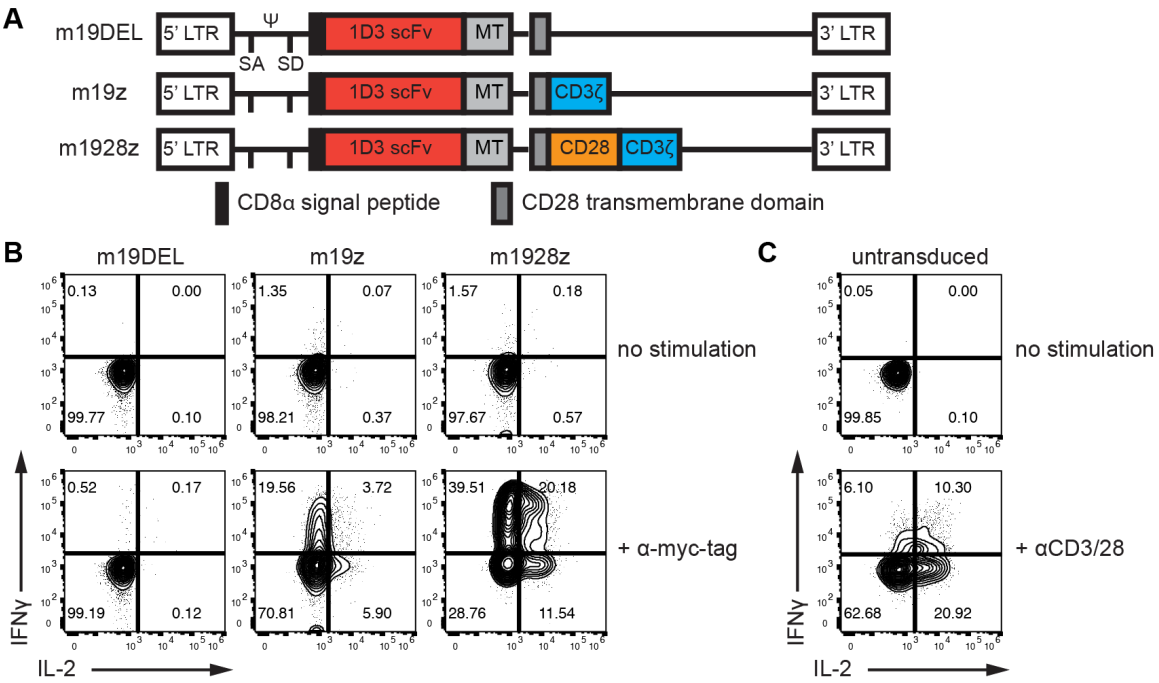

Figure 3.3. Validation of the CD28 signaling domain
(A) Construct maps encoding CARs with different intracellular signaling domains. The m19DEL construct lacks both CD28 and CD3ζ signaling domains. The "first-generation" m19z encodes for the CD3ζ signaling domain and the "second-generation" m1928z construct encodes for both CD28 and CD3ζ signaling domains.
(B) Murine T cells were retrovirally transduced with the different constructs depicted in (A) and the CAR was crosslinked with plate-bound α-myc-tag antibody for 6 hr. Cytokine production of IFNγ and IL-2 was measured by intracellular flow cytometry.
(C) Murine T cells were cultured with or without αCD3/28 Dynabeads for 6 hr at a 1:2 bead-to-T-cell-ratio. Cytokine production of IFNγ and IL-2 was assessed by intracellular flow cytometry.
LTR, long terminal repeats; MT, myc tag; SA, splice acceptor; scFv, small chain variable fragment; SD, splice donor; Ψ, packaging signal.

m1928z-CD40L CAR T cells circumvent tumor immune escape via antigen downregulation through CD40/CD40L-mediated cytotoxicity

Anti-CD19 CAR therapy has produced tumor relapse in select leukemia patients with $CD19^-$ tumor outgrowth (Park et al., 2018). Thus, we wanted to investigate if the dual cytotoxic effect of m1928z-CD40L CAR T cells would still ensure tumor cell lysis in settings of immune escape via antigen downregulation on the tumor cell surface or outgrowth of $CD19^-$ tumor cells. Long-term co-culture of $CD19^+$ GFP^+ A20 cells with m1928z CAR T cells led to downregulation of cell surface CD19 and outgrowth of $CD19^-$ tumor cells by day 21 that could not be targeted and eliminated by the m1928z CAR T cells (Figure 3.4A). Co-culture of $CD19^+$ GFP^+ A20 cells with m1928z-CD40L CAR T cells also led to downregulation of cell surface CD19, as demonstrated by the presence of a small fraction of GFP^+ $CD19^-$ cells at day 1 of co-culture (Figure 3.4A). However, m1928z-CD40L CAR T cells were able to eliminate these CAR-antigen-negative tumor cells and prevent their eventual outgrowth. This effect was dependent on tumor CD40 expression, as m1928z-CD40L CAR T cells were unable to eliminate the $CD19^+$ $CD40^-$ A20.CD40-KO tumor cells (Figure 3.4B). The CD40/CD40L-mediated cytotoxicity alone was sufficient to target the tumor cells, as off-target 4h11-28z-CD40L CAR T cells also completely eliminated A20 cells (Figures 3.4C and 3.4D). These results demonstrate the ability of $CD40L^+$ CAR T cells to circumvent tumor immune escape by antigen downregulation through CD40/CD40L-mediated cytotoxicity in settings of tumor CD40 expression.

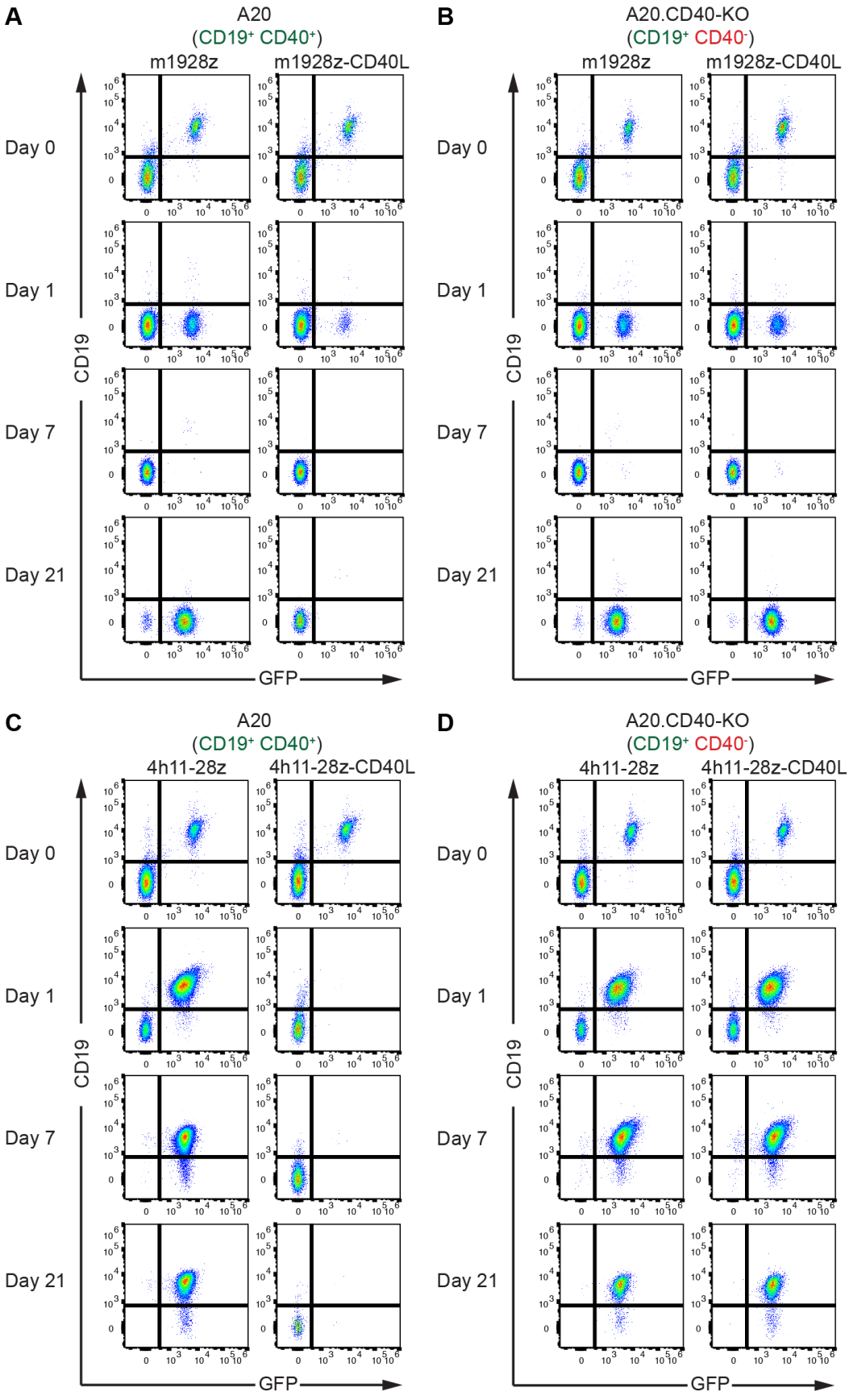
A
A20
(CD19+ CD40+)
m1928z
m1928z-CD40L
B
A20.CD40-KO
(CD19+ CD40-)
m1928z
m1928z-CD40L
C
A20
(CD19+ CD40+)
4h11-28z
4h11-28z-CD40L
D
A20.CD40-KO
(CD19+ CD40-)
4h11-28z
4h11-28z-CD40L
Day 0
Day 1
Day 7
Day 21
CD19
GFP

Figure 3.4. m1928z-CD40L CAR T Cells circumvent tumor immune escape via antigen downregulation through CD40/CD40L-mediated cytotoxicity
(A and B) $CD19^+$ $CD40^+$ GFP^+ A20 cells (A) or $CD19^+$ $CD40^-$ GFP^+ A20 cells (B) were co-cultured at a 1:1 ratio with m1928z or m1928z-CD40L CAR T cells. Percentage of GFP^+ tumor cells and CD19 surface expression was assessed over time by flow cytometry. Shown is one of 3 independent experiments.
(C and D) Same as (A and B), except that 4h11-28z or 4h11-28z-CD40L CAR T cells were co-cultured with A20 (C) or A20.CD40-KO (D) cells. Shown is one of 3 independent experiments. Adapted from Kuhn et al. (2019), *Cancer Cell*, 35(3):473-488.

m1928z-CD40L CAR T cells function in vivo without preconditioning

We next wanted to evaluate the efficacy of m1928z-CD40L CAR T cells in eradicating systemic $CD19^+$ disease. Others have previously reported that preconditioning with cyclophosphamide (Cy) enables complete eradication of $CD19^+$ tumors by T cells transduced to express an anti-CD19 CAR with the CD3ζ domain and lacking any co-stimulatory domains in an immunecompetent mouse model (Cheadle et al., 2010). Here, we noticed that second-generation m1928z CAR T cells conveyed improved survival in mice bearing systemic A20 lymphoma when preconditioned with Cy one day before ACT, leading to 20% long-term survival (Figure 3.5A). Treatment with a single injection of m1928z-CD40L CAR T cells after Cy preconditioning improved long-term survival significantly to 100% (Figure 3.5A, $p < 0.01$).

These results prompted us to assess the necessity of preconditioning for m1928z-CD40L CAR T cell function since our lab has previously reported that IL-12-secreting first-generation anti-CD19 CAR T cells can eradicate systemic tumors without prior conditioning (Pegram et al., 2012). Additionally, obviating the need for preconditioning in cancer patients could potentially alleviate adverse events, as higher doses of lymphodepleting agents have been associated with exacerbated toxicity symptoms in the clinical setting (Hay et al., 2017). After ACT of CD19-targeted CAR T cells, we used the presence/absence of endogenous $CD19^+$ B cells as a biomarker for anti-CD19 CAR T cell in vivo functional persistence (Figure 3.5B). Cy preconditioning was necessary for successful in vivo persistence of m1928z CAR T cells in fully immunecompetent mice (Figure 3.5C), whereas m1928z-CD40L CAR T cells induced long-term B cell aplasia without preconditioning. These results demonstrate the improved in vivo efficacy and functional cell engraftment of m1928z-CD40L CAR T cells in the absence of preconditioning.

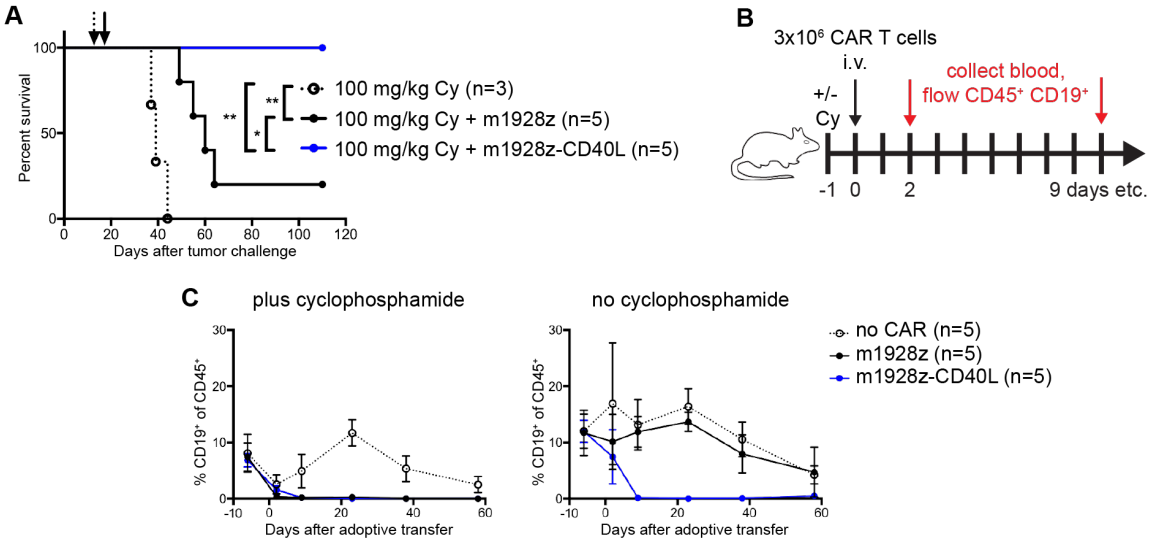

Figure 3.5. m1928z-CD40L CAR T cells function in vivo without preconditioning
(A) Kaplan-Meier survival plots of BALB/c mice that were injected with 5x10^6 A20.GL cells i.v. on day 0. On day 13, mice were given 100 mg/kg cyclophosphamide (Cy; dotted arrow). One day later, mice were left untreated or treated with 3x10^6 m1928z or m1928z-CD40L CAR T cells i.v. (solid arrow) (n = 3-5 mice per group). *p < 0.05, **p < 0.01 by logrank (Mantel-Cox) test.
(B) Experimental layout for (C).
(C) Non-tumor-bearing mice were preconditioned with (left) or without (right) Cy and treated as outlined in (B). Mice were bled at indicated time points and the percentage of CD19$^+$ B cells in the CD45$^+$ population in the peripheral blood was assessed by flow cytometry. Means ± SEM are shown (n=5/group). Data is plotted as mean ± SEM and is representative of two independent experiments. Adapted from Kuhn et al. (2019), *Cancer Cell*, 35(3):473-488.

m1928z-CD40L CAR T cells display improved antitumor response in murine CD19$^+$ disease models independent of CD40 expression on the tumor

A20 cells were transduced with a GFP-luciferase fusion gene (A20.GL) to allow in vivo tracking of tumor burden. As described above, A20 cells injected intravenously (i.v.) into mice predominantly seed in the liver and bone marrow (Figures 3.1B), causing a distended abdomen and hind limb paralysis due to progressive tumor growth. Whereas m1928z CAR T cell treatment without preconditioning did not increase survival of A20.GL tumor-bearing mice, presumably due to lack of successful functional engraftment (Figure 3.5B), m1928z- CD40L CAR T cell treatment without preconditioning delayed the onset of tumor-causing symptoms and significantly enhanced survival in these mice (Figure 3.6A). Whole-body bioluminescence imaging (BLI) of mice challenged with luciferase-expressing A20.GL cells showed no delay of tumor outgrowth in mice treated with m1928z CAR T cells (Figure 3.6B). Eventually all m1928z-treated mice succumbed to overt tumor outgrowth without any survival benefit compared to untreated mice (Figures 3.6A and 3.6B). m1928z-CD40L CAR T cell treatment delayed tumor outgrowth in all mice and improved survival (Figures 3.6A and 3.6B). The majority of mice subsequently relapsed – all with CD19$^+$ disease (Figure 3.6C).

The enhanced antitumor effect of m1928z-CD40L CAR T cells was not entirely dependent on tumor CD40 expression, as they also enhanced survival of mice challenged with A20.CD40-KO cells (Figure 3.6D), and not limited to the A20 lymphoma model in BALB/c mice. C57BL/6 mice challenged with the murine leukemia cell line Eμ-ALL01 (Davila et al., 2013) also benefited from a single injection of m1928z-CD40L CAR T cells, with 46% of all treated mice surviving long-term (Figure 3.6E). The Eμ-ALL01 cell line is CD19$^+$ CD40$^-$, demonstrating again that the increased antitumor efficacy of m1928z-CD40L CAR T cells does not entirely depend on tumor CD40 expression, despite the CD40/CD40L-mediated cytotoxicity of these CAR T cells (Figure 3.4).

The extracellular domain of CD40L contains membrane proximal integrin binding and cleavage sites that are recognized by the matrix metalloproteinases

ADAM10 and ADAM 17, resulting in the release of soluble CD40L from CD40L expressing T cells (Figure 3.1H) (Yacoub et al., 2013). Masuta et al. have shown that introducing mutations in either the integrin binding or the cleavage site can disrupt cleavage of CD40L from the cell surface (Masuta et al., 2007). Deletion of the integrin binding and cleavage site generated a non-cleavable CD40L (ncCD40L) molecule that is expressed on the surface of T cells after transduction to similar levels as the conventional CD40L (Figure 3.6F), but is detectable at 4-to-8-fold lower levels in the supernatant of transduced cells (Figure 3.6G). To test, if sustained expression of CD40L with reduced cleavage from the CAR T cell surface improves antitumor response, A20 tumor-bearing mice were treated with the conventional CD40L-modified CAR T cells or with the ncCD40L-modified CAR T cells. Whereas m1928z-ncCD40L CAR T cell treatment improved survival of mice challenged with A20 cells compared to m1928z CAR T cells (Figure 3.6H), m1928z-CD40L treatment was superior compared to m1928z-ncCD40L CAR T cells, implying that cleaving of the CD40L molecule from the cell surface is necessary for the $CD40L^{+}$ CAR T cell to exert full antitumor efficacy.

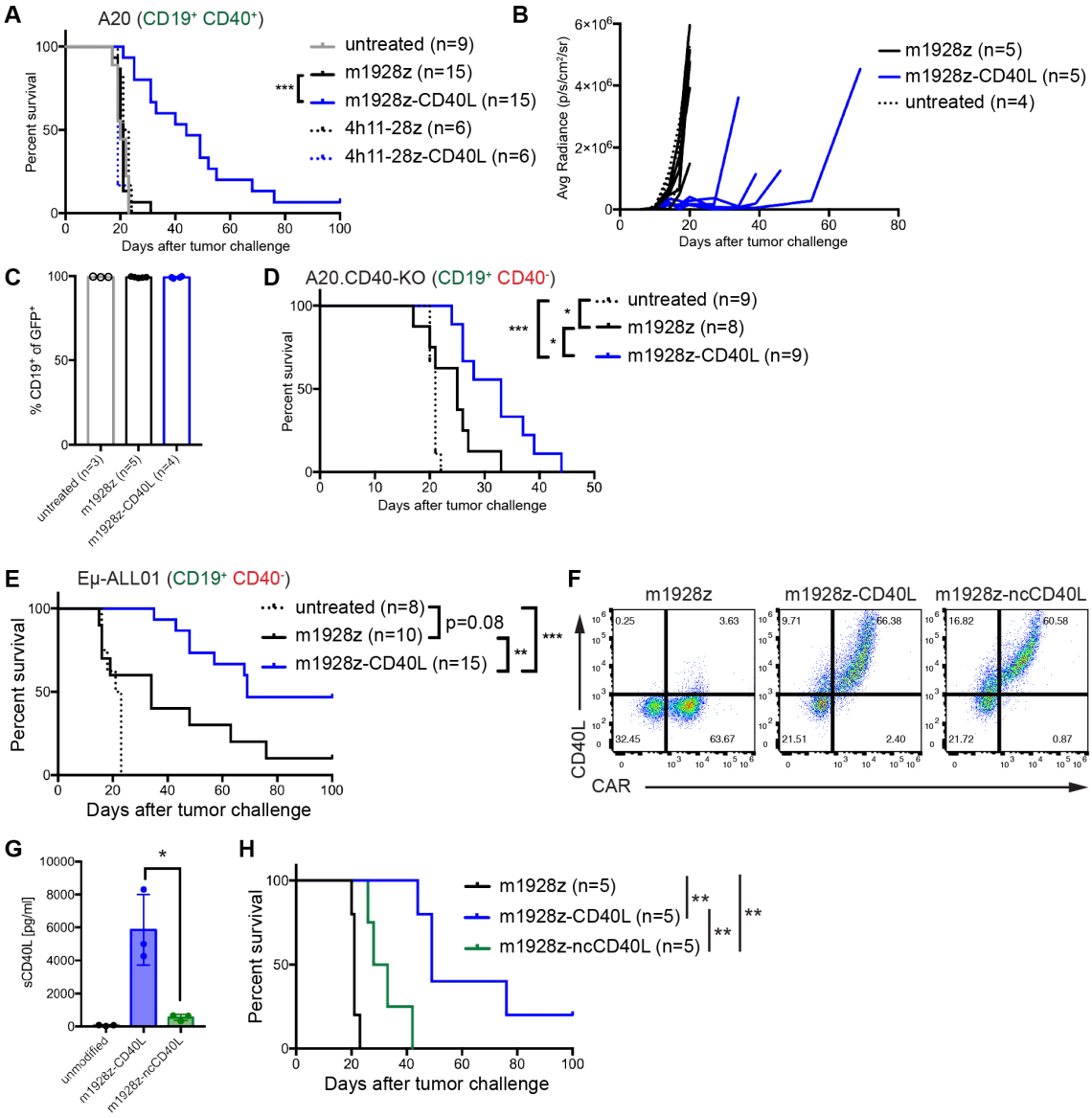

Figure 3.6. m1928z-CD40L CAR T cells display improved antitumor response in murine CD19$^+$ disease models independent of CD40 surface expression on the tumor

(A) Survival of BALB/c mice injected with 1x10^6 A20.GL tumor cells i.v. on day 0 and treated with 3x10^6 CAR T cells i.v. on day 7 without preconditioning (n=6-15/group, pooled from 3 independent experiments).

(B) Tumor burden of A20.GL injected mice was monitored using bioluminescence imaging (average radiance, photons / s / cm^2 / sr) after treatment with CAR T cells (n=4-5 /group). One of three representative experiments is shown.

(C) BALB/c mice were injected with 1x10^6 A20.GL cells (GFP$^+$) i.v. and then either left untreated or treated with 3x10^6 m1928z or m1928z-CD40L CAR T cells i.v. on day 7. At time of death, GFP$^+$ tumor cells were analyzed for surface CD19 expression by flow cytometry (n=3-5 / group).

(D) Same as in (A), except that mice were injected with 1x10^6 A20.CD40-KO tumor cells (n=8-9/group, pooled from two independent experiments).

(E) Survival of C57BL/6 mice injected with 1x10^6 CD19$^+$ CD40$^-$ Eμ-ALL01 leukemia cells i.v. on day 0 and treated with 1-2x10^6 CAR T cells i.v. on day 7 without preconditioning (n=8-15, pooled from two independent experiments).

(F) Transgene expression after retroviral transduction of mouse T cells analyzed by flow cytometry.
(G) Media supernatant of 3T3 cells transduced with m1928z-CD40L or m1928z-ncCD40L constructs was collected after 24 hr and probed for sCD40L by Luminex analysis. Each dot represents one experimental replicate. *p<0.05 (Student's t test).
(H) Survival of BALB/c mice injected with $1x10^6$ A20.GL cells i.v. and treated with $3x10^6$ m1928z, m1928z-CD40L, or m1928z-ncCD40L CAR T cells i.v. on day 7. *p<0.05, **p<0.01, ***p<0.001 by a log-rank (Mantel-Cox) test (A, D, E, and H). Adapted from Kuhn et al. (2019), *Cancer Cell*, 35(3):473-488.

m1928z-CD40L CAR T cell treatment is safe in preclinical setting

Anti-CD19 CAR T cell treatment in humans leads to cytokine release syndrome (CRS) in the majority of patients (Park et al., 2018). Whereas cytokine secretion by activated CAR T cells is an expected event, maintenance of severe CRS via immunesuppressive glucocorticoids and/or the anti-IL-6 receptor monoclonal antibody tocilizumab are essential to ensure patient safety (Davila et al., 2014). To assess how constitutive expression of CD40L in CAR T cells can influence systemic cytokine production in mice, serum cytokine levels were analyzed after CAR T cell treatment. Only m1928z-CD40L CAR T cells increased IFNγ and TNFα serum levels in tumor-bearing mice (Figure 3.7A). The CAR expression alone (m1928z) or CD40L expression with an irrelevant CAR (4h11-28z- CD40L) did not affect systemic effector cytokine levels (Figure 3.7A). Other effector cytokines, such as IL-2 and granulocyte macrophage colony-stimulating factor (GM-CSF) were not elevated any time after CAR T cell transfer (Figure 3.7A). We also observed no systemic increase in IL-6 or soluble CD40L (sCD40L) in m1928z-CD40L CAR T cell treated mice (Figure 3.7A), consistent with the localized release of sCD40L at the tumor site from the cell surface of $CD40L^+$ CAR T cell.

Other preclinical reports have observed diverse toxicities upon anti-CD40 antibody therapy, namely perivascular infiltrates in the liver and lung with fatal hepatotoxicity, as well as thrombocytopenia (Byrne et al., 2016; Knorr et al., 2018). Upon pathological analysis, tumor-bearing mice receiving $3x10^6$ m1928z-CD40L CAR T cells displayed moderate multifocal perivascular mononuclear cell infiltration in the lung and liver of unknown significance (Figure 3.7B). The same multifocal perivascular cell infiltrate was observed in *Cd40*$^{-/-}$, but only to a minimal to mild degree. However, no necrosis or thrombotic events were detected in any tissue, not in wild-type, nor in *Cd40*$^{-/-}$ mice. Platelet counts remained normal and transaminase (ALT and AST) serum levels remained low in m1928z-CD40L CAR T cell treated mice, indicating absence of thrombocytopenia and hepatocyte cell damage (Figure 3.7C). Furthermore, non-tumor-bearing mice receiving CAR T cells at 10 to 100 times the clinical dose displayed no outward signs of toxicity.

Mice receiving $1x10^7$ m1928z-CD40L had an average weight loss of 7.4% (±2.2%) on day 3 after cell transfer, which recovered back to baseline at day 5 (Figure 3.7D). Together, these results show the superior and safe in vivo antitumor effect of $CD40L^+$ CAR T cells in $CD19^+$ disease models.

To test the possibility of controlling the expression level of surface CD40L after gene transfer, human T cells were retrovirally transduced with either of two different constructs that encode an internal ribosomal entry site (IRES) (E.p.1928z.i.CD40L) or the "self-cleaving" T2A peptide upstream of the CD40L transgene (E.p.1928z.t.CD40L) (Figure 3.8). Both constructs also encode for truncated epidermal growth factor receptor (EGFRt) as an internal control of gene transfer efficiency, allowing comparison of normalized CD40L surface expression between the two different constructs ($GeoMFI_{CD40L}$ / $GeoMFI_{EGFRt}$ = $Norm_{CD40L}$). Absolute and $Norm_{CD40L}$ expression at baseline, i.e. after gene transfer and without CAR stimulation, was higher in T cells transduced with the E.p.1928z.t.CD40L construct (Figure 3.8B). CAR stimulation after co-culture of E.p.1928z.i.CD40L or E.p.1928z.t.CD40L CAR T cells with CD19-expressing 3T3 cells led to an increase of surface CD40L expression in both groups (Figure 3.8C), with E.p.1928z.t.CD40L CAR T cells still displaying higher CD40L levels than E.p.1928z.i.CD40L CAR T cells (Figure 3.8D). Thus, surface CD40L expression on CAR T cells can be engineered to lower or higher levels by using different intergenic elements in the transgene expression cassette.

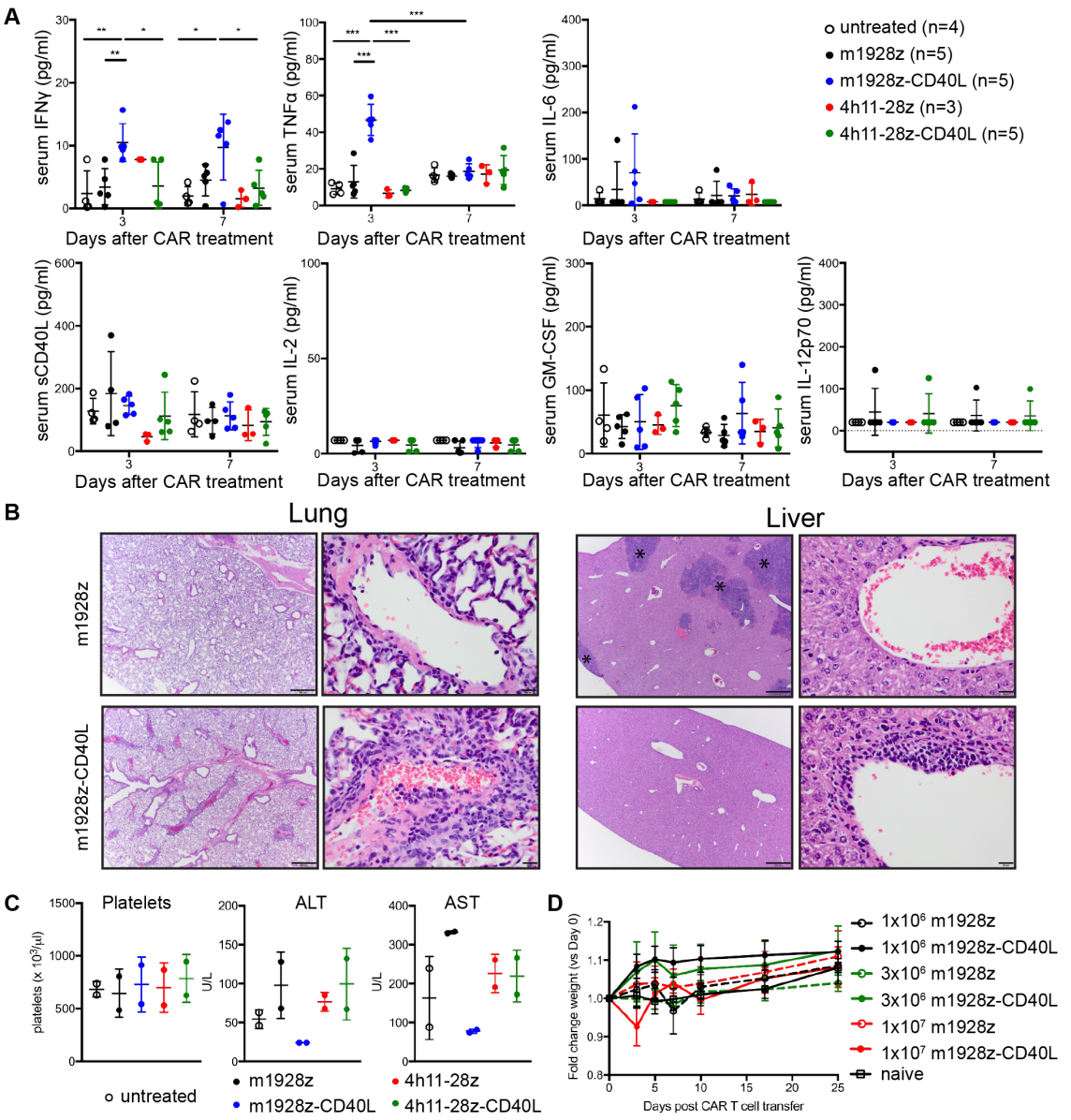

Figure 3.7. m1928z-CD40L CAR T cell treatment is safe in preclinical setting
(A) Serum levels of IFNγ, TNFα, IL-6, sCD40L, IL-2, GM-CSF, and IL-12p70 in A20.GL tumor-bearing mice treated with $3x10^6$ CAR T cells i.v. (n=3-5/group) were measured on days 3 and 7 after CAR treatment by Luminex. Data is plotted as mean ± SEM and is representative of two independent experiments.
(B) Hematoxylin and eosin stains of lung (left) and liver (right) of BALB/c mice treated with $3x10^6$ m1928z (top) or m1928z-CD40L (bottom) CAR T cells on day 7 after being injected i.v. with $1x10^6$ A20.GL cells. Mice were sacrificed and analyzed on day 7 after CAR T cell transfer. One of two representative mice per group and organ is shown. Scale bar in low magnification image (left), 500 μm. Scale bar in high magnification (right), 20 μm. *, tumor.
(C) BALB/c mice were injected with $1x10^6$ A20.GL cells i.v. and then either left untreated or treated with $3x10^6$ of indicated CAR T cells i.v. on day 7. At day 14, mice were analyzed for platelet counts, alanine aminotransferase (ALT), and aspartate aminotransferase (AST) levels in the peripheral blood. Data is plotted as mean ± SD with two mice per group. U, unit; L, liter.

(D) The fold change of body weight of BALB/c mice was plotted after mice received $1x10^6$, $3x10^6$, or $1x10^7$ m1928z or m1928z-CD40L CAR T cells i.v. (n=5 mice/group). Body weight measurement at day 0 was normalized to 1. Mean ± SD is plotted over time. Adapted from Kuhn et al. (2019), *Cancer Cell*, 35(3):473-488.

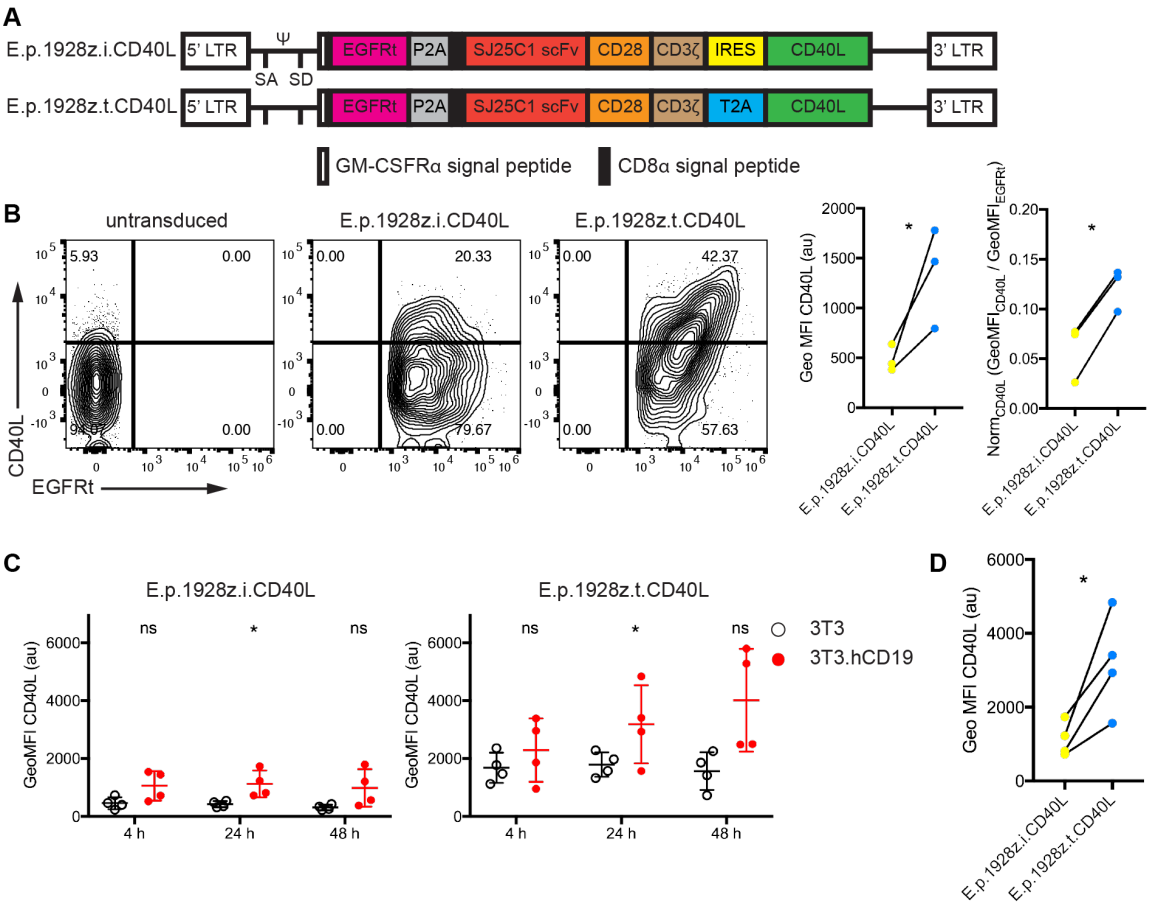

Figure 3.8. Surface level CD40L expression on human CAR T cells can be controlled by choice of intergenic element

(A) Schematic of construct maps encoding gene elements with intergenic IRES or T2A elements. Truncated EGFR (EGFRt) lacks the extracellular ligand binding domain and is separated by the "self-cleaving" P2A element from the second-generation CAR construct. The SJ25C1 scFv recognizes human CD19 and is fused to the CD28 and CD3ζ signaling domains. The CD40L transgene is separated from the CAR cassette by either an internal ribosome entry site (IRES; E.p.1928z.i.CD40L) or the "self-cleaving" T2A element (E.p.1928z.t.CD40L).

(B) Contour plots of retrovirally transduced human T cells with the two constructs depicted in (A). Surface expression of CD40L and EGFRt was analyzed by flow cytometry (pre-gate $EGFR^+$). Quantification of absolute and normalized CD40L surface expression for both constructs is plotted on the right. Each pair of dots represents one donor transduced with either the IRES (yellow) or the T2A (blue) encoding construct.

(C) CAR T cells were co-cultured with CD19-negative (3T3) or CD19-overexpressing murine fibroblasts (3T3.hCD19). At indicated time points, surface CD40L was measured by flow cytometry. Each dot represents one donor and mean ± SD of 4 donors is plotted.

(D) Surface CD40L expression after 24 hr of CAR T cell stimulation on 3T3.hCD19 cells. Each pair of dots represents one donor transduced with either the IRES (yellow) or the T2A (blue) containing construct.

*p<0.05, ns, non-significant (Student's t-test). LTR, long terminal repeats; GeoMFI, geometric mean fluorescence intensity; SA, splice acceptor; scFv, small chain variable fragment; SD, splice donor; Ψ, packaging signal.

Validation of biological function of transgenically expressed CD40L

T cell activation through mitogens or TCR crosslinking leads to a transient increase of CD40L surface expression (Casamayor-Palleja et al., 1995). This allows binding of CD40L to its cognate receptor CD40 on APCs, mainly DCs and B cells, which serves as a survival, proliferation, and maturation signal as displayed by upregulation of T cell co-stimulatory molecules CD80 and CD86 (Ranheim and Kipps, 1993). $CD19^+$ hematological malignancies arise from the B cell lineage and can express CD40 on their cell surface (Figure 3.1A). Forced expression of CD40L in chronic lymphocytic leukemia (CLL) tumor cells via intranodal CD40L gene delivery by an adenovirus increased co-stimulatory molecule expression on the tumor cells and resulted in clinical responses (Castro et al., 2012), demonstrating the feasibility of turning tumor cells into antigen-presenting stimulatory cells. Co-culture of A20 cells with $CD40L^+$ T cells induced upregulation of CD80 and CD86 (Figure 3.9A). A20.CD40-KO cells did not respond to $CD40L^+$ T cells (Figure 3.9B), indicating that this effect is dependent on CD40/CD40L interactions. CAR T cells recognize antigen independently of pMHC:TCR interactions, thus we wanted to evaluate if constitutive expression of CD40L on T cells is sufficient for APC activation. Bone marrow-derived DCs (BMDCs) upregulated CD80, CD86, and MHC-II and secreted IL-12 when co-cultured with $CD40L^+$ T cells (Figures 3.9C and 3.9D), indicative of DC licensing. Altogether, these results demonstrate upregulation of T cell co-stimulatory markers on tumor cells and licensing of $CD40^+$ professional APCs by $CD40L^+$ CAR T cells.

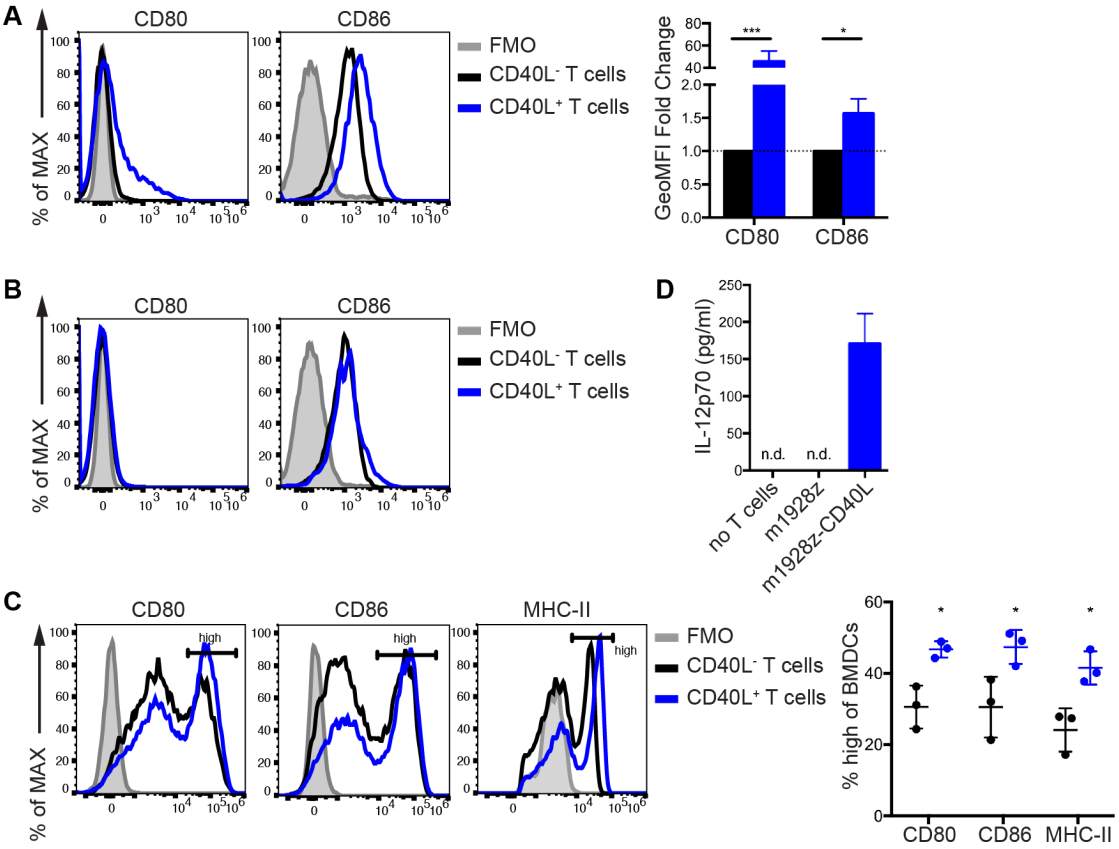

Figure 3.9. Validation of biological function of transgenically expressed CD40L
(A) Representative histograms of flow cytometry analysis of CD80 and CD86 expression on A20 cells co-cultured for 48 hr with $CD40L^+$ or $CD40L^-$ T cells. Graph summarizes results of 3 independent experiments as geometric mean fluorescence intensity (GeoMFI) fold-change (mean ± SEM; $CD40L^-$ T cells normalized to 1). *p<0.05, ***p<0.001 (Student's t-test).
(B) Same as in (A), but this time T cells were co-cultured with A20.CD40-KO cells. Results are representative of two independent experiments.
(C) Representative histograms of flow cytometry analysis of CD80, CD86, and MHC-II on BMDCs co-cultured for 48 hr with $CD40L^+$ or $CD40L^-$ T cells. Graph summarizes percentage of CD80hi, CD86hi, and MHC-IIhi BMDCs of 3 independent experiments (mean ± SD). *p<0.01 (Student's t-test).
(D) IL-12p70 concentration in the supernatant from cultured cells in (C) was measured by Luminex. Graph represents mean ± SD of experimental triplicates. One of two representative experiments is shown. n.d., not detected. Adapted from Kuhn et al. (2019), *Cancer Cell*, 35(3):473-488.

Characterization of transgenically expressed CD40L on CAR T cells

We wanted to evaluate if constitutive surface expression of CD40L could impart an autocrine or juxtacrine effect on T cells. Others have reported that a transgenic murine $CD8^+$ T cell line expresses CD40 on its surface (Bourgeois et al., 2002) suggesting that CD40/CD40L interactions on T cell surfaces could lead to T cell stimulation. Following reports, however, have shown that conditional CD40 KO in $CD8^+$ T cells had no detrimental effect on $CD8^+$ T cell-dependent immune responses and T cell memory formation in an influenza model (Lee et al., 2003). We could not detect any CD40 surface expression on stimulated T cells (Figure 3.10A). Additionally, constitutive CD40L expression did not induce effector cytokine production (Figure 3.1H), nor increase proliferation or survival of murine T cells (Figure 3.10B). The lack of an autocrine or juxtacrine proliferative signal through CD40L was also observed in human T cells transduced to overexpress human CD40L (Figure 3.10C). *Cd40*$^{-/-}$ m1928z- CD40L CAR T cells had no impaired antitumor effect in vivo (Figure 3.10D), ruling out a potential direct CD40/CD40L effect on the CAR T cells and arguing that there is no necessary autocrine or juxtacrine effect mediated by CD40/CD40L interactions on T cells in our system.

Further characterization of m1928z vs. m1928z-CD40L CAR T cells showed that constitutive CD40L expression has no effect on the CD4-to-CD8 ratio in the transduced T cell product (Figure 3.11A), nor on CD62 ligand (CD62L) and CD44 expression as markers for naïve (T_n, $CD62L^{hi}$ $CD44^{lo}$), memory (T_{mem}, $CD62L^+$ $CD44^{hi}$), effector (T_{eff}, $CD62L^-$ $CD44^{hi}$) T cells (Figure 3.11B). Also, T helper subset differentiation was similar between transduced m1928z and m1928z-CD40L CAR T cells (Figure 3.11C), with CAR T cells predominantly secreting Th1 subset-associated cytokines. Finally, to assess the contribution of CD4 and CD8 CAR T cells in the improved antitumor response in m1928z-CD40L-treated mice (Figure 3.6A), A20 tumor-bearing mice were selectively injected with either only $CD4^+$ or $CD8^+$ m1928z-CD40L CAR T cells. Wherein $CD4^+$ m1928z-CD40L CAR T cells alone provided no survival benefit, $CD8^+$ m1928z-CD40L CAR T cells protected mice from tumor relapse (Figure 3.11D). $CD8^+$ m1928z CAR T

cell treatment also conveyed a survival benefit compared to untreated mice, albeit all mice eventually died from overt disease outgrowth; indicating the necessity of added CD40L expression on CAR T cells for improved antitumor efficacy, even when only adoptively transferring cytotoxic $CD8^+$ T cells.

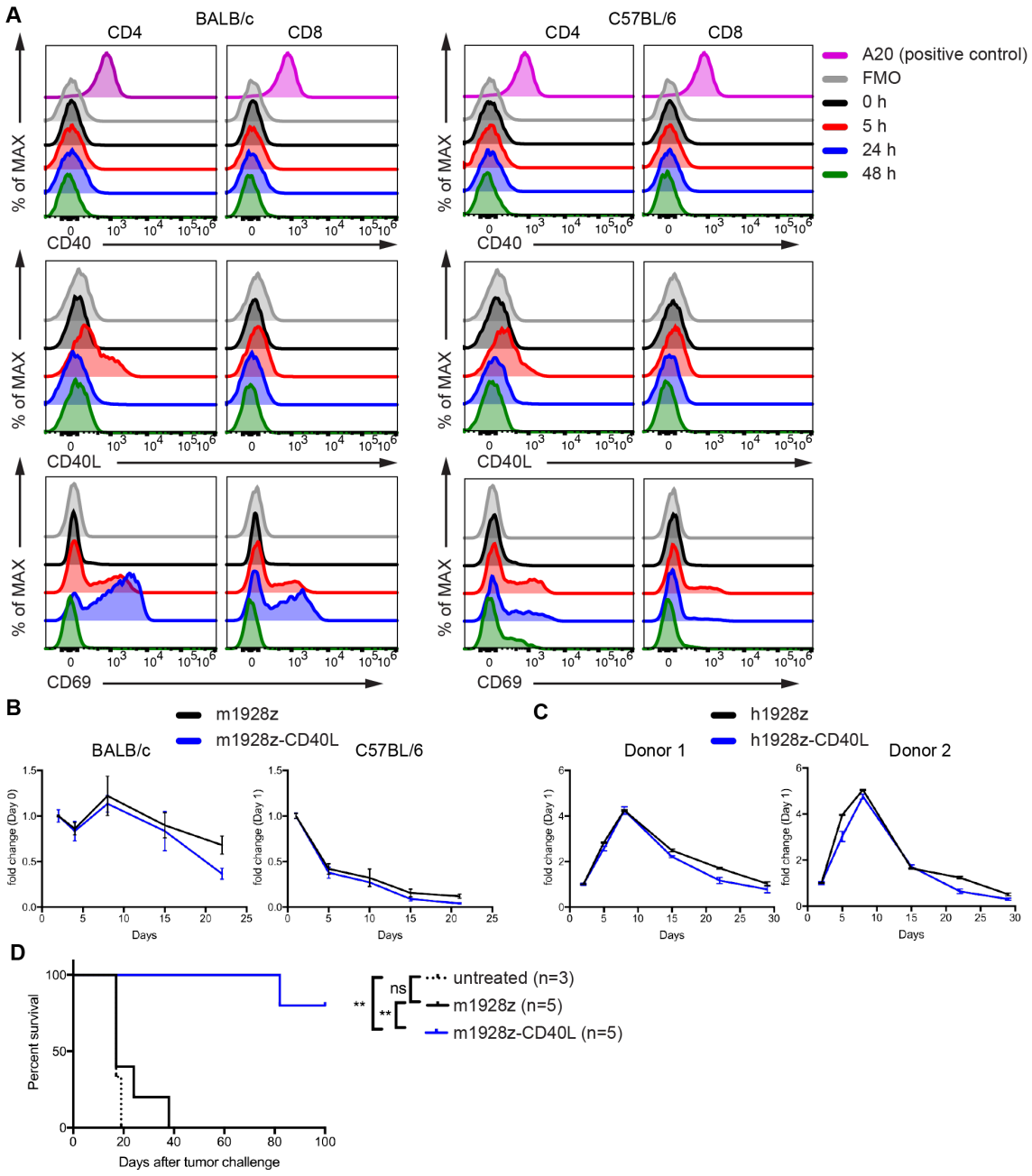

Figure 3.10. Characterization of transgenically expressed CD40L on CAR T cells

A) Splenic $CD3^+$ T cells from BALB/c (left) or C57BL/6 (right) mice were magnetically isolated through negative selection and then cultured in complete media and stimulated with CD3/28 beads and rhIL-2 (100 IU/ml). Cells were collected at different time points, fixed, and stored. After collection of the last time point, all samples were surface stained and analyzed. Cell surface expression of CD40, CD40L, and CD69 (positive control) was measured by flow cytometry on $CD4^+$ (left) and $CD8^+$ (right) T cells. One representative of two independent experiments is shown.

(B) CAR T cells from BALB/c (left) or C57BL/6 (right) mice were cultured in complete media without any supportive cytokines or stimulation. Relative cell numbers were counted at indicated time points. Experimental triplicates are summarized as mean ± SEM. One representative of three or two independent experiments is shown.

(C) Human CAR T cells transduced with the h1928z or h1928z-CD40L CAR construct were cultured in complete media without any supportive cytokines or stimulation. Relative cell numbers were counted at indicated time points. Experimental triplicates are summarized as mean ± SEM. Biological duplicates from two different donors are plotted on separate graphs.
(D) Survival of BALB/c mice injected with $1x10^6$ A20.GL cells i.v. on day 0 and treated with $3x10^6$ *Cd40*$^{-/-}$ CAR T cells i.v. on day 7 (n=5/group). **p < 0.01 by a logrank (Mantel-Cox) test. Adapted from Kuhn et al. (2019), *Cancer Cell*, 35(3):473-488.

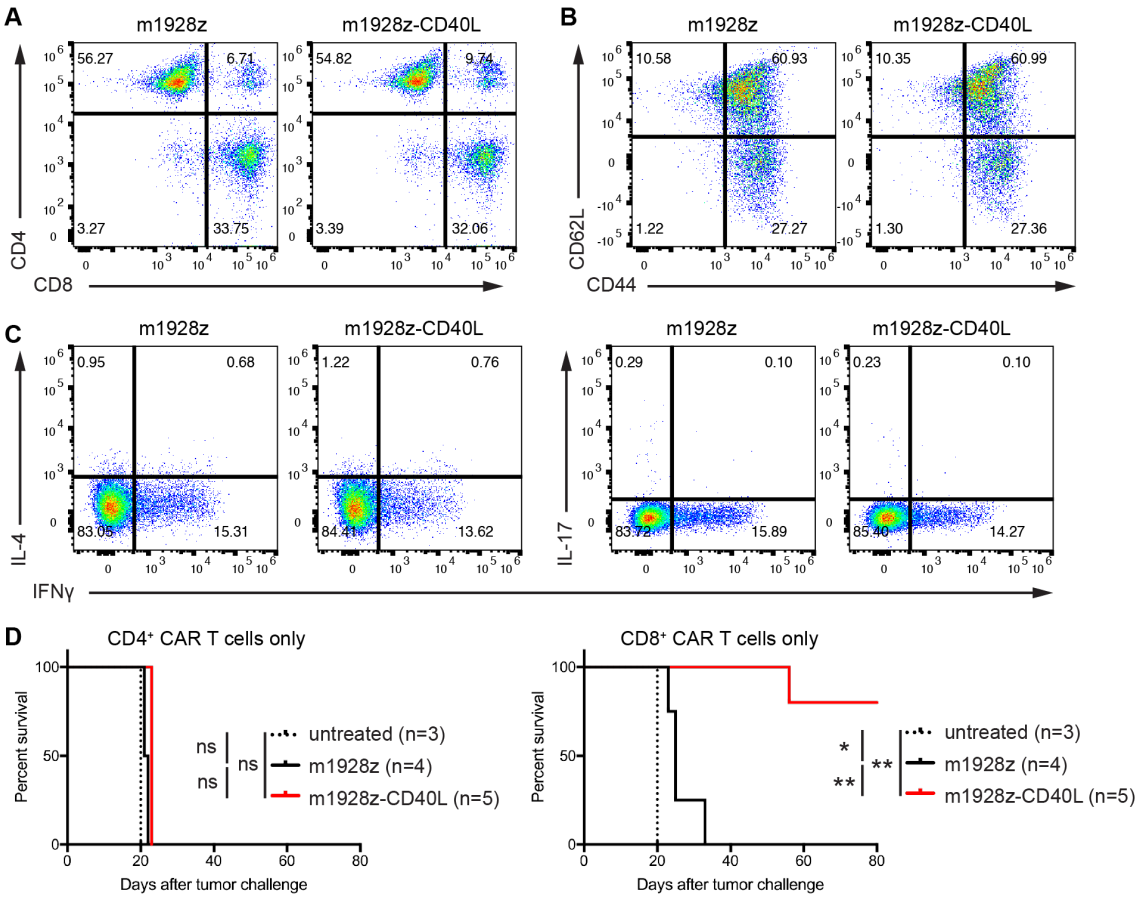

Figure 3.11. CD40L overexpression in CAR T cells does not change CD4/CD8-ratio, memory, or T_{helper} cell phenotype

(A) Flow cytometry dot plots displaying percentage of $CD4^+$ and $CD8^+$ T cells in m1928z and m1928z-CD40L CAR T cell products after transduction. One of three representative experiments is shown.

(B) Flow cytometry dot plots displaying surface expression of CD62L and CD44 in m1928z and m1928z-CD40L CAR T cell products after transduction. One of two representative different experiments is shown.

(C) m1928z or m1928z-CD40L CAR T cells were stimulated with PMA/Ionomycin for 4 hr. Cytokine production was measured by intracellular staining and analyzed by flow cytometry. Dot plots are gated on $CD4^+$ T cells and show production of IFNγ and IL-4 (left) or IL-17 (right).

(D) Survival of BALB/c mice injected with $1x10^6$ A20.GL tumor cells i.v. on day 0 and treated with $3x10^6$ $CD4^+$ (left) or $CD8^+$ (right) CAR T cells i.v. on day 7 (n=4-5/group).

Discussion

The direct cytotoxic effect of CD40/CD40L interactions on CD40-expressing tumor cells in short- (Figure 3.1) and long-term (Figure 3.3) co-culture assays highlight mechanism of protection by $CD40L^+$ CAR T cells against antigen-negative tumor outgrowth. CD40 engagement on resting B cells leads to proliferation and upregulation of Fas, which makes them susceptible to Fas-mediated apoptosis after CD40-mediated activation (Garrone et al., 1995). The sensitization to Fas-mediated apoptosis by CD40 engagement is also true for cancer cells (Dicker et al., 2005). However, both pro- and anti-apoptotic effects have been described for CD40/CD40L interactions on transformed cells, depending on the mode of engagement. Low-level constitutive engagement on $CD40^+$ tumor cells can promote survival and cell proliferation (Baxendale et al., 2005; Pham et al., 2002), whereas transient activation can have the opposite effect. Tumors from the B cell lineage express high levels of cell surface CD40 and engagement can have pro-apoptotic effects on ALL, CLL, and multiple myeloma cell lines (Tong and Stone, 2003). Constitutive ERK activation or mutated p53 in tumor cells has been associated with susceptibility to CD40 signaling-induced apoptosis (Hollmann et al., 2006), whereas CD40 stimulation in APCs via CD40L promotes survival through induction of anti-apoptotic Bcl-xL via the nuclear factor kB (NF-kB) pathway (Ouaaz et al., 2002). CD40 expression has also been observed on several epithelial cancers, such as breast, ovarian, and lung carcinomas and melanoma (Elgueta et al., 2009). There, transient activation of the CD40 signaling pathway through sCD40L in vivo had growth-inhibitory effects on human breast cancer cells (Hess and Engelmann, 1996; Wingett et al., 1998), demonstrating the antitumor effect of CD40/CD40L interactions across different tumor types. This provides a rationale for the use of $CD40L^+$ CAR T cells in different cancer settings due to the additional CD40/CD40L-mediated tumor cell killing despite CAR-mediated antigen downregulation and/or outgrowth of antigen-negative escape variants.

The effect CD40/CD40L interactions have on transformed cells raises the issue of potential detrimental effects impinging on physiological $CD40^+$ tissues.

Preclinical and clinical experience using agonistic anti-CD40 antibodies has documented adverse events; manifested by fatal liver toxicity, drop in platelet levels, and moderate CRS (Knorr et al., 2018; Vonderheide, 2018). Whereas we observed no such adverse events in our system, we did detect perivascular infiltration in lung and liver (Figure 3.10B). The significance of this event is unknown, but potentially explained by CD40 expression on endothelial cells (Elgueta et al., 2009) and their subsequent activation upon encountering m1928z-CD40L CAR T cells form the bloodstream. In the clinical setting, we would argue for treating patients starting at low doses and then escalating the cell numbers under strict clinical supervision and analysis of blood biomarkers for liver damage (AST and ALT) and CRS (IL-6 and fever). Encouragingly, we neither observed an increase in these markers in our preclinical system (Figure 3.10), nor detected any visible toxic effects on mice injected with m1928z-CD40L CAR T cells at doses 10-to-100-fold above the conventional clinical doses normalized to body weight (Figure 3.10E).

Besides controlling the applied CAR T cell dose, we can control CD40L expression levels via modifications of intergenic elements in the transgene construct (Figure 3.8). By positioning the CAR transgene upstream of the CD40L transgene in the expression cassette, we can insert an IRES or 2A element between the two genes. This leads to low or high CD40L surface levels on the T cell, whereas a consistent CAR expression level is maintained. Use of an IRES element results in lower expression levels compared to the use of a 2A element. Additionally, in a multicistronic vector, positioning a gene towards the end of the expression cassette leads to lower expression (Liu et al., 2017). This allows further tuning of relative gene expression between CAR and CD40L. Together, this permits design of engineered CAR T cells that express relatively low or high levels of CD40L, potentially mitigating toxicities.

It was previously reported that retroviral overexpression of CD40L in murine bone marrow or thymic cells led to thymic lymphoproliferative disease in mice (Brown et al., 1998). The authors suggest that constitutive expression of CD40L in developing T cells contributes to the dysregulated proliferation in the thymus.

We did not see any evidence of lymphoproliferative disease in over 40 mice treated with m1928z-CD40L CAR T cells that were monitored for up to 2 years, arguing that CD40L over-expression in mature T cells does not have the same effect. Furthermore, besides the absence of any lymphoproliferative phenotype, we also did not observe any abnormal differentiation in CD40L-modified CAR T cells, as both murine m1928z and m1928z-CD40L CAR T cells displayed the same ratios of $CD4^+$, $CD8^+$, naïve, and memory T cells, and $CD4^+$ T-helper subtypes (Figure 3.11). Introduction of suicide/elimination switches in the clinic should be considered to improve safety and combat potential CD40L-mediated lymphoproliferation in human CAR T cells (Bonifant et al., 2016). Suicide/elimination switches can be used to deplete the adoptively transferred cell product when deemed necessary by a clinician. One example is the iCasp9 molecule, which is an artificial caspase molecule that is expressed in the cell product and can be activated by addition of a small molecule. This leads to homodimerization of the iCasp9 molecule and subsequent activation of the apoptotic pathway in the iCasp9-expressing cells (Di Stasi et al., 2011). A different strategy for depleting engineered T cells is to also express the extracellular domain of EGFR (EGFRt) on their surface. This enables antibody-mediated elimination of T cells after injection of the clinically approved and EGFR-specific antibody cetuximab (Wang et al., 2011).

Therapeutic interventions should maximize efficacy and minimize toxicity. CAR T cell treatment in clinical trials at different treatment centers has produced unanticipated toxicities that have not been previously observed in mice, such as CRS and neurotoxicity, highlighting the difficulty of translating therapy-induced adverse events between mouse and human (Park et al., 2018). The severity of these toxicities is potentially correlated with the intensity of lymphodepleting preconditioning (Hay et al., 2017). Encouragingly, m1928z-CD40L CAR T cells did not require preconditioning for successful in vivo antitumor function (Figure 3.5), potentially alleviating previously seen adverse events in humans by reducing or eliminating preconditioning regimens. In addition, sparing preconditioning could help to maintain the endogenous lymphoid and myeloid cell

compartments, allowing them to aid in the antitumor response of $CD40L^+$ CAR T cells.

CHAPTER 4

CD40L$^+$ CAR T Cells License APCs in vivo

Introduction

In the previous chapter we could demonstrate the safe and improved antitumor response of CD40L-modified CAR T cells compared to CAR T cells without CD40L overexpression (Figure 3.6), as well as the ability of CD40L-modified CAR T cells to induce DC licensing in vitro (Figure 3.9). The underlying hypothesis explaining the improved antitumor response states that CD40$^+$ host cells are licensed through CD40L$^+$ CAR T cells upon ACT and in turn recruit additional endogenous immune effectors to assist in tumor cell recognition and eradication. This chapter will investigate the in vivo licensing of APCs by CD40L$^+$ CAR T cells, and is based on known biology describing the involvement of CD40$^+$ APCs in the antitumor response.

CD40 protein is predominantly expressed in cells belonging to the hematopoietic system, namely DCs, monocytes, and B cells (Van Kooten and Banchereau, 2000). Low levels of CD40 expression have also been observed on non-hematopoietic cells, such as endothelial cells, some epithelial cells, and fibroblasts (Van Kooten and Banchereau, 2000). The importance of CD40 expression on non-hematopoietic cells is still relatively unknown. The lack of any gross organ abnormalities in *Cd40*$^{-/-}$ mice in non-pathological conditions suggests CD40 is mainly important in the hematopoietic system. The involvement and function of APCs in an effective antitumor response is well documented, where especially DCs are instructive in T cell priming (Broz et al., 2014; Engelhardt et al., 2012; Spranger et al., 2017). The importance of functional DCs in an effective antitumor response is further supported by observations describing lack of tumor control in settings of DC dysfunction (Gabrilovich, 2004).

In the context of tumor progression, macrophages are thought to fall along a polarization axis spanning from an activated M1 antitumor phenotype on one side, to an alternatively activated M2 pro-tumor phenotype on the other side (Qian and Pollard, 2010). One study has found that antibody-mediated CD40

activation on macrophages in a murine pancreatic tumor model induces non-durable tumor regression, which is dependent on CD40-activated macrophages (Beatty et al., 2011). Finally, as the third member of hematopoietic APCs, CD40-activated B cells are neglected in this study for further analysis as they are eradicated when mice are injected with CD19-targeted CAR T cells (Figure 3.5C).

In combination with chemotherapy and/or radiation, monoclonal agonistic CD40-targeted antibodies have been used in the preclinical setting to successfully treat pancreatic and bladder cancer (Beatty et al., 2011; Byrne and Vonderheide, 2016; Sandin et al., 2013), but the use of agonistic CD40-targeted antibodies as a single agent has so far met with less success in the clinic, where objective tumor response rates have been below 25% (Vonderheide and Glennie, 2013). Here, we demonstrate that m1928z-CD40L CAR T cells can, in addition to their antigen-specific cytotoxicity, also license $CD40^+$ APCs in vivo with the potential of priming endogenous non-CAR T cells to aid in the antitumor response. The aspect of non-CAR T cell priming is explored in the following chapter 5. The licensing of APCs through T cells is usually dependent on the presentation of peptide-MHC (pMHC) antigen on the APC and its recognition by the TCR on a $CD4^+$ T cell. This leads to the formation of an immunological synapse between APC and T cell, resulting in TCR-mediated signaling and activation of the T cell. Early activation signals, such as CD40L, are expressed on the cell surface and bind to constitutively expressed CD40 on the APC. This CD40/CD40L interaction, as a response to the initial pMHC:TCR recognition, is necessary for efficient licensing of the APC. Successfully licensed APCs increase surface expression of antigen-presenting molecules (such as MHC), co-stimulatory molecules (such as CD80 and CD86, as well as TNF-related surface molecules), adhesion molecules (such as ICAM-1), and secrete cytokines (such as IL-12) to prime and engage T cells in an antigen-specific immune response. Thus, this chapter investigates the ability of CD40L-expressing genetically engineered CAR T cells to invert the relationship between DCs and T cells,

wherein the CAR T cells function as the initiator of APC maturation independently of pMHC:TCR interactions.

Results

m1928z-CD40L CAR T cells promote APC maturation in vivo

Taking advantage of our syngeneic mouse model, we investigated if $CD40L^+$ CAR T cells could license APCs in vivo. A20.GL tumor-bearing mice received ACT 7 days after tumor inoculation to model established systemic disease, followed by analysis of activation and maturation markers on tumor-resident myeloid cells in the liver (Figures 4.1A). Whereas there was a brief detectable upregulation of the co-stimulatory marker CD86 on DCs and macrophages on day 1 and 3 after m1928z-CD40L CAR T cell treatment (Figure 4.1B), no indications of sustained licensing of these cell populations was observed. This is supported by comparable levels of CD86, MHC-II, and CD40 in both m1928z and m1928z-CD40L treated mice (Figures 4.1B-4.1D). Thus, an interaction between $CD40L^+$ CAR T cells and $CD40^+$ APCs did not occur at sufficiently high levels to induce APC licensing at the primary tumor site and prompted the analysis of APCs in lymphoid tissue.

The spleen was chosen for lymphoid tissue analysis at day 7 after ACT because no A20 tumor cells are detectable at this time point (Figure 3.1D). Here, m1928z-CD40L CAR T cell treatment increased surface expression of the activation/maturation markers CD86, MHC-II, and CD40 on both splenic DCs and macrophages (Figures 4.2B-4.2D). CD86 upregulation on DCs and macrophages was observed at early time points (days 1 and 2) and remained high until day 7 (Figure 4.2B). Changes in MHC-II levels induced by m1928z-CD40L treatment were observed at later time points, with the highest levels detectable on day 7 in both DCs and macrophages (Figure 4.2C). Low level upregulation was seen for CD40, wherein m1928z-CD40L treatment did significantly affect CD40 expression in DCs early (day 3), compared to m1928z alone, and late (day 7) on macrophages (Figure 4.2D). Furthermore, the licensing of DCs was also observed in celiac and portal lymph nodes (Figure 4.2E), the lymph nodes

draining the liver where the A20 tumor nodules reside (Barbier et al., 2012) (Figure 3.1D). Lymph-node resident DCs displayed higher levels of CD80, CD86, and MHC-II in m1928z-CD40L treated mice, albeit not to a statistically significant margin for CD86 (Figure 4.2E). Collectively, m1928z-CD40L CAR T cells promoted APC licensing in vivo by inducing upregulation of co-stimulatory and maturation markers.

Besides the immunophenotypical changes that were observed and described above, we next thought to examine how CAR T cell treatment changes the immune cell infiltrate in the tumor and the spleen. Fluorescent microscopic images revealed infiltration of CAR T cells into B and T cell zones of lymphoid organs (Figure 4.3A and 4.3B), with m1928z-CD40L CAR T cell treated mice having no detectable B cell zones in lymph nodes due to B cell aplasia.

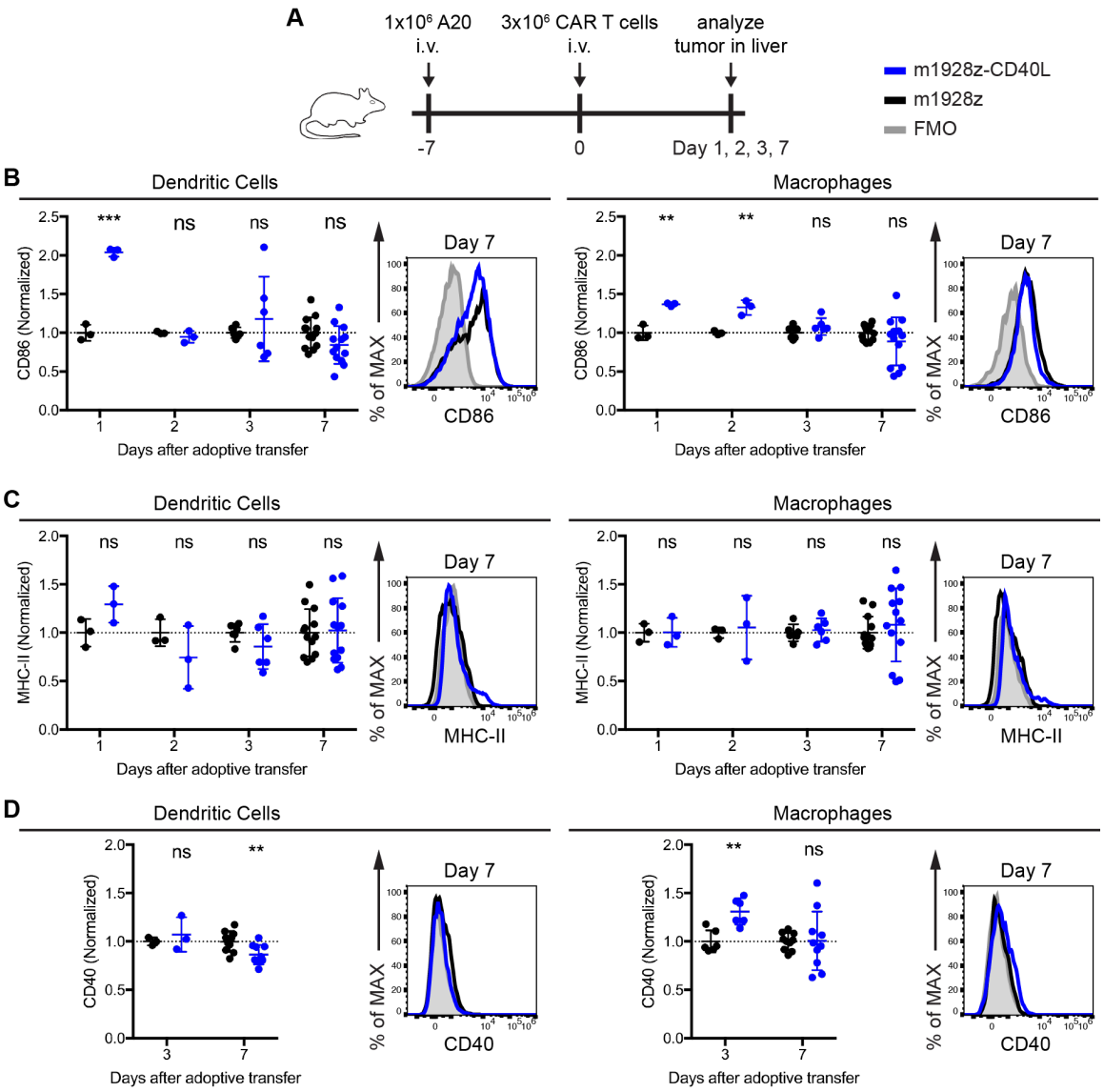

Figure 4.1. m1928z-CD40L CAR T cells do not license tumor-resident myeloid cells
(A) Experimental layout for B-D.
(B) Normalized surface expression of CD86 on CD11b$^-$ CD11c$^+$ DCs (left) and CD11b$^+$ F4/80$^+$ macrophages (right) at indicated time points (CD45$^+$ CD3$^-$ CD19$^-$ Gr-1$^-$ pre-gates; m1928z normalized to 1). Representative overlay histograms depict surface expression on day 7.
(C) Normalized surface expression of MHC-II on DCs (left) and macrophages (right) at indicated time points (m1928z normalized to 1). Representative overlay histograms depict surface expression on day 7.
(D) Normalized surface expression of CD40 on DCs (left) and macrophages (right) at indicated time points (m1928z normalized to 1). Representative overlay histograms depict surface expression on day 7.
Each dot represents one mouse (n=3-13/group). Data is plotted as mean ± SEM and is representative of 1-3 independent experiments. **p<0.01, ***p<0.001 (Student's t test). FMO, fluorescence minus one; ns, non-significant. Adapted from Kuhn et al. (2019), *Cancer Cell*, 35(3):473-488.

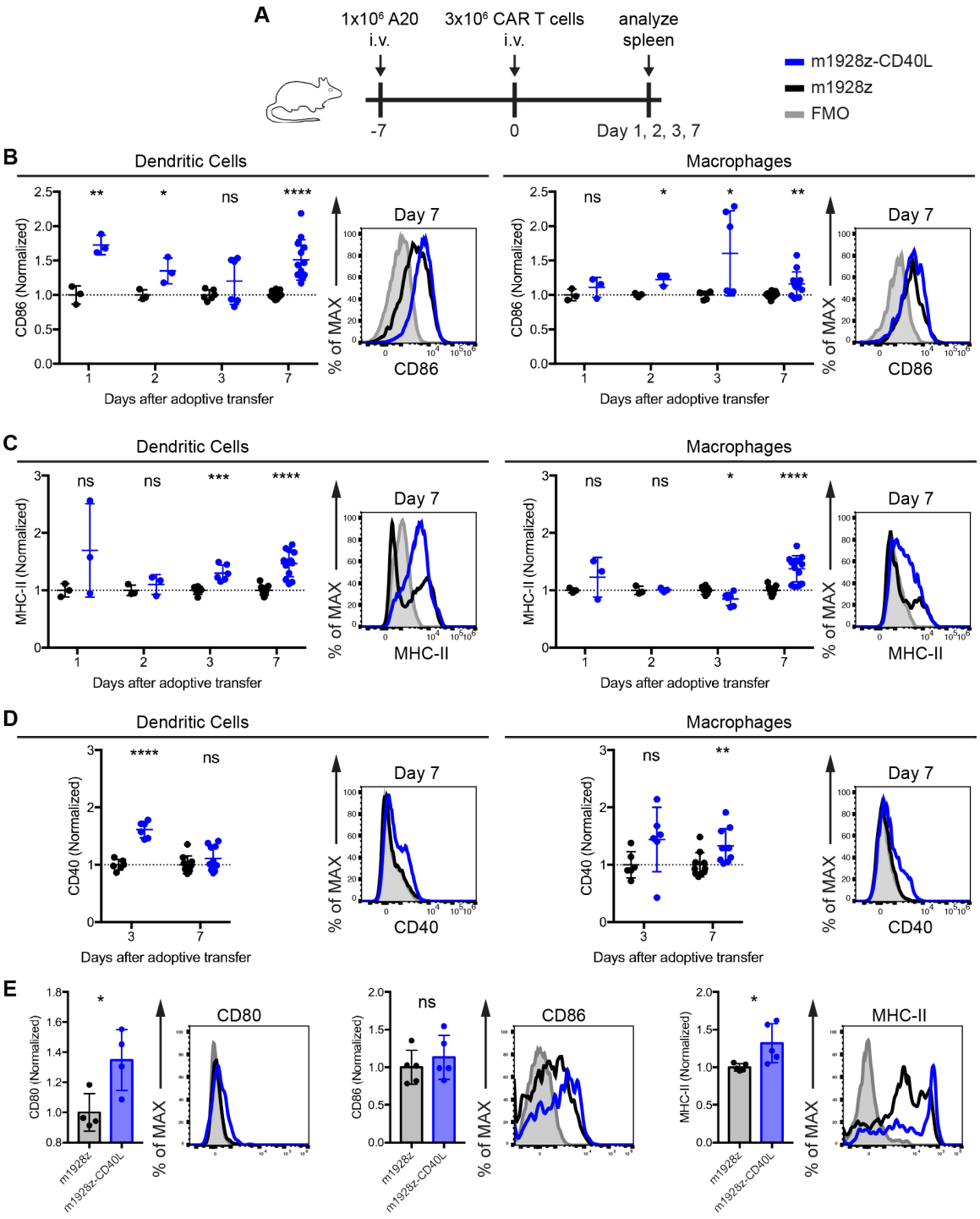

Figure 4.2. m1928z-CD40L CAR T cells license splenic myeloid cells
(A) Experimental layout for B-D.
(B) Normalized surface expression of CD86 on CD11b^{-} CD11c^{+} DCs (left) and CD11b^{+} F4/80^{+} macrophages (right) at indicated time points (CD45^{+} CD3^{-} CD19^{-} Gr-1^{-} pre-gates; m1928z normalized to 1). Representative overlay histograms depict surface expression on day 7.
(C) Normalized surface expression of MHC-II on DCs (left) and macrophages (right) at indicated time points (m1928z normalized to 1). Representative overlay histograms depict surface expression on day 7.

(D) Normalized surface expression of CD40 on DCs (left) and macrophages (right) at indicated time points (m1928z normalized to 1). Representative overlay histograms depict surface expression on day 7.
(E) Normalized surface expression of CD80, CD86, and MHC-II on DCs in tumor-draining lymph nodes (pooled celiac and portal lymph nodes) of A20 tumor-bearing mice on day 6 after CAR T cell treatment (m1928z is normalized to 1). Overlay histograms depict representative surface expression from one sample.
Each dot represents one mouse (n=3-13/group). Data is plotted as mean ± SEM and is representative of 1-3 independent experiments. *p<0.05, **p<0.01, ***p<0.001, ****p<0.0001 (Student's t test). FMO, fluorescence minus one; ns, non-significant. Adapted from Kuhn et al. (2019), *Cancer Cell*, 35(3):473-488.

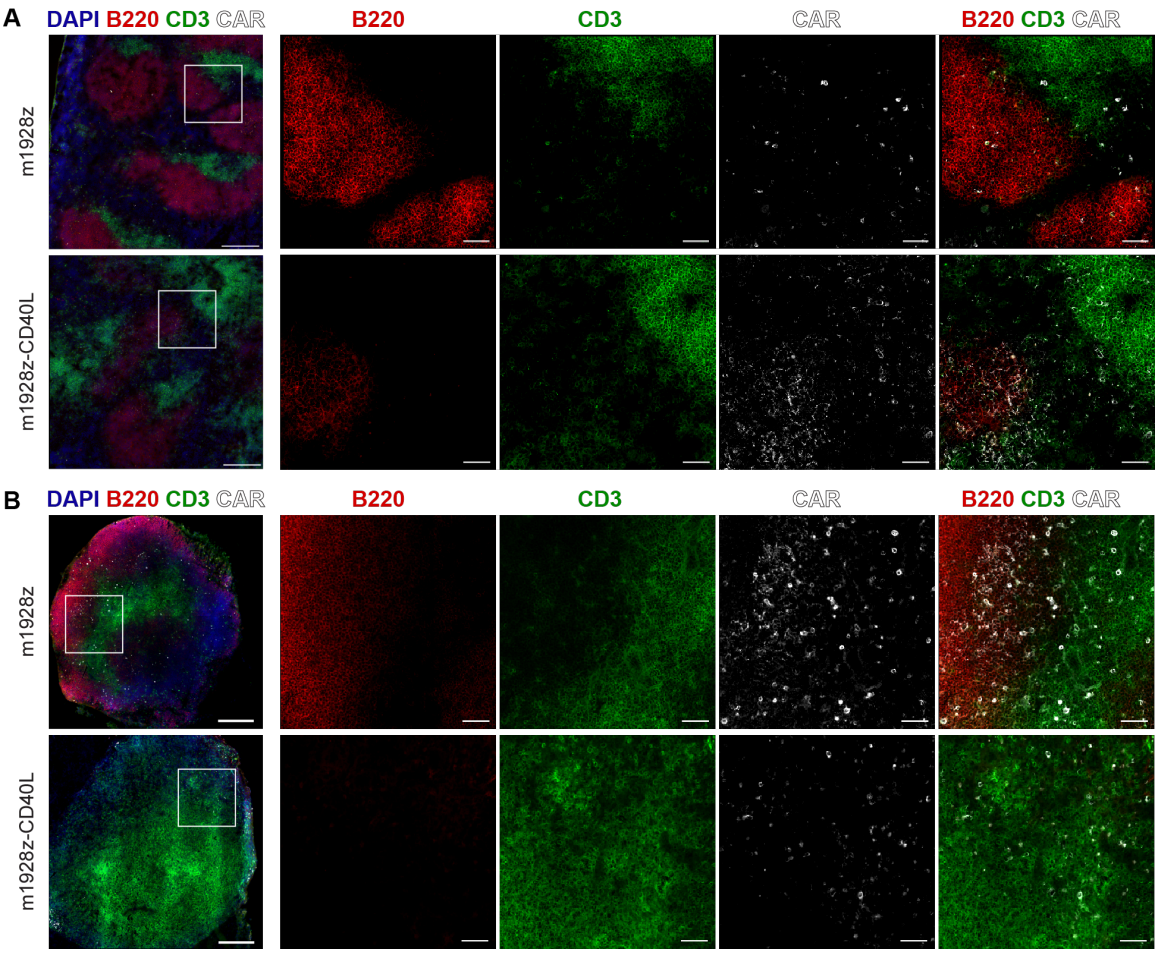

Figure 4.3. m1928z-CD40L CAR T cells infiltrate lymphoid tissue and deplete B cell zones
BALB/c mice were injected i.v. with $1x10^6$ A20.GL cells followed by ACT of $3x10^6$ CAR T cells 7 days after tumor challenge. The spleens and tumor-draining (hepatic & celiac) lymph nodes of the mice were analyzed 7 days after ACT.
(A) Immunofluorescent staining for DAPI (blue), B220 (red), CD3 (green), and CAR (white) in spleens of m1928z (top) or m1928z-CD40L (bottom) CAR T cell treated mice. One of two representative spleens is shown per cohort. Individual antibody stains at higher magnification of boxed-in region are shown on the right. Scale bar, 250 or 50 μm.
(B) Same analysis as in (A), except that tumor-draining lymph nodes were analyzed. One of two representative lymph nodes is shown per cohort. Individual antibody stains at higher magnification of boxed-in region are shown on the right. Scale bar, 250 or 50 μm. Adapted from Kuhn et al. (2019), *Cancer Cell*, 35(3):473-488.

Local pro-inflammatory cytokine release after m1928z-CD40L CAR T cell treatment

Upon CD40/CD40L-mediated cell licensing, myeloid cells upregulate activation markers – as seen above in Figure 4.2 – and are also instructed to release immunestimulatory signal molecules (Caux et al., 1994; Cella et al., 1996). To assess if m1928z-CD40L CAR T cell treatment can instruct myeloid cells to secrete such signal molecules in vivo, splenic lysates of CAR treated mice were analyzed by a cytokine/chemokine protein array. The spleen was chosen as the site of analysis because m1928z-CD40L CAR T cells induced the most pronounced degree of licensing we could detect in splenic myeloid cells (Figures 4.2B-4.2D). Thirteen of 40 proteins analyzed were detected at high levels (Figure 4.4A). m1928z-CD40L CAR T cell treatment mediated significantly higher levels of the IL-1 receptor antagonist IL-1Ra (Figure 4.4B), which is protective of severe CRS (Giavridis et al., 2018). Also, monocytic (CCL3 and CCL5) and lymphocytic (CXCL9 and CXCL10) chemoattractants were present at higher levels following m1928z-CD40L CAR T cell treatment (Figure 4.4B). The remaining 8 detectable proteins were present at similar levels between the two treatment cohorts. These data provide evidence that CAR T cells can provide a pro-inflammatory milieu and potentially facilitate expansion of immune effectors.

The lymphocyte-attracting chemokines CXCL9 and CXCL10 are responsible for $CD4^+$ T cell, $CD8^+$ T cell, and natural killer (NK) cell trafficking by binding to CXCR3 on their cell surface (Griffith et al., 2014). In antiviral host responses, CXCL9 production is attributed to stromal and myeloid cells in lymphoid tissue following IFNγ stimulation (Kastenmüller et al., 2013; Sung et al., 2012). This leads to recruitment of Th1 $CD4^+$ and cytotoxic $CD8^+$ T cells, followed by subsequent priming of these cells to function in viral control (Nakanishi et al., 2009). In a murine breast cancer model, de Mingo Pulido et al. showed that CXCL9 is produced by intratumoral DCs. Inhibition of its biological function by blocking its cognate receptor CXCR3 on lymphoid cells decreased an immunotherapy-based antitumor response (de Mingo Pulido et al., 2018). To assess if the higher levels of CXCL9 in m1928z-CD40L treated mice in our

system can also be attributed to its production by intratumoral DCs, tumor- and spleen-resident APCs were stained intracellularly for CXCL9 protein. Intriguingly, m1928z-CD40L CAR T cell treatment stimulated CXCL9 production in splenic macrophages (Figure 4.4C), whereas no CXCL9 protein was detected in tumor-resident APCs at day 7.

Stimulation of human and murine DCs with CD40L showed that CD40/CD40L interaction is sufficient to induce IL-12 release (Cella et al., 1996; Koch et al., 1996). IL-12 instructs $CD4^+$ T cells to differentiate into IFNγ-producing Th1 cells (Teng et al., 2015) and has tumor-protective effects when combined with CAR T cell therapy (Pegram et al., 2012). Here, we wanted to investigate if m1928z-CD40L CAR T cells could stimulate in vivo production of IL-12 in myeloid cells. m1928z-CD40L CAR T cell treatment significantly increased IL-12p40 production in splenic DCs, but not tumor-resident DCs, as measured by ex vivo intracellular staining (Figure 4.4D). IL-12p40 production was specific to $CD11b^-$ $CD11c^+$ splenic DCs in mice receiving $CD40L^+$ CAR T cells. $CD11b^+$ $F4/80^+$ macrophages in the same mice were IL-12-negative (Figure 4.4D). Cumulatively, these results demonstrated that splenic $CD40^+$ macrophages and DCs could be instructed to produce the immunestimulatory molecules CXCL9 and IL-12, respectively, upon m1928z-CD40L CAR T cell treatment.

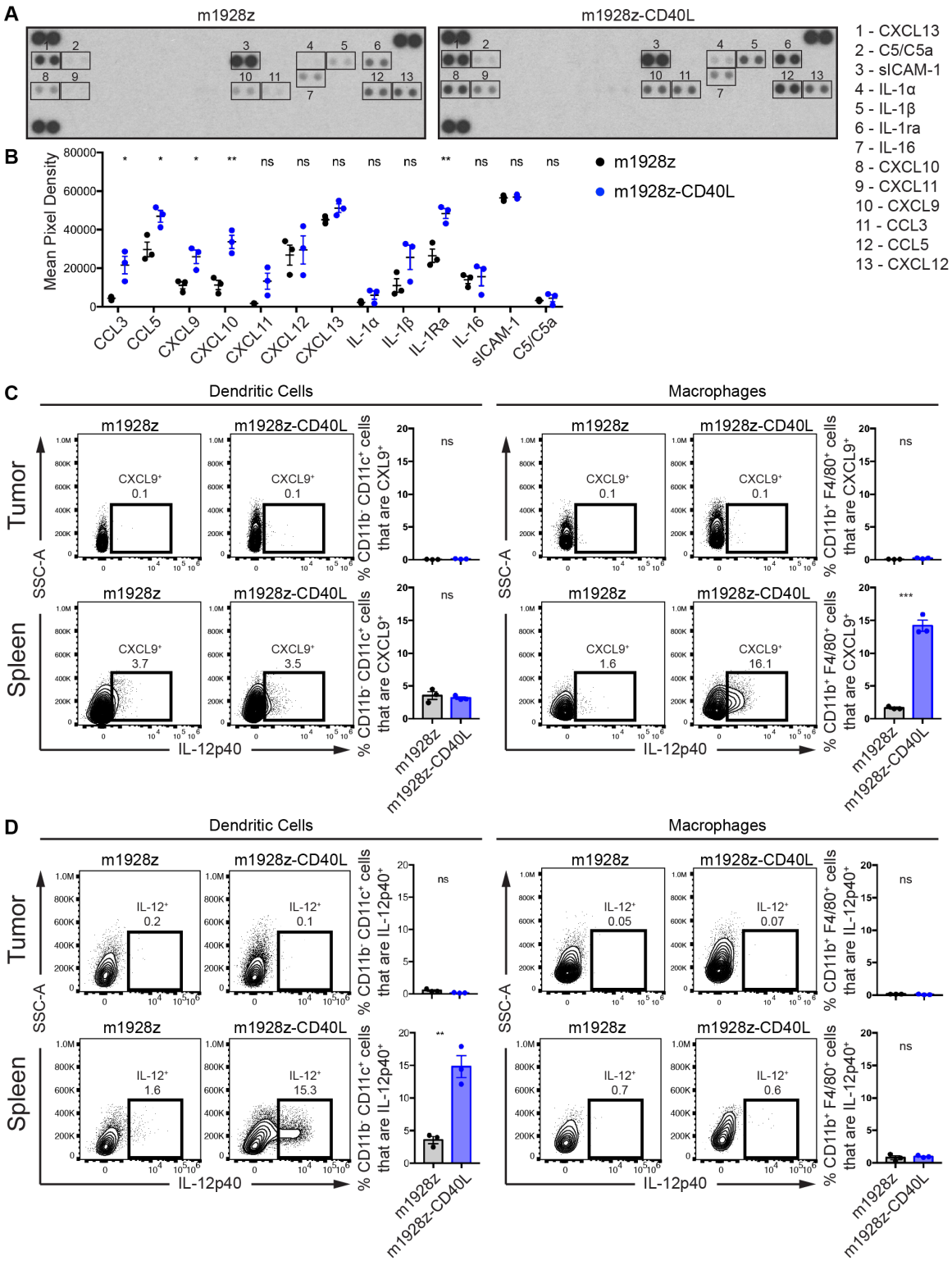

Figure 4.4. Local pro-inflammatory cytokine release after m1928z-CD40L CAR T cell treatment.

(A) BALB/c mice were injected i.v. with 1x10^6 A20.GL cells followed by ACT of 3x10^6 CAR T cells 7 days after tumor challenge. Array of 40 proteins taken from the supernatant of homogenized spleens of m1928z or m1928z-CD40L CAR T cell treated mice 7 days after ACT.

(B) Quantification of significantly changed cytokines in (A) (n=3 mice/group). One of two representative experiments is shown.
(C) Intracellular flow cytometry of DCs (left) and macrophages (right) for CXCL9 production in tumor (top) and spleen (bottom) of mice treated with m1928z or m1928z-CD40L CAR T cells. Boxed-in regions highlight CXCL9-producing cells. One representative plot per treatment condition is shown. Frequency of $CXCL9^{+}$ DCs or macrophages is plotted on the right (n=3/group).
Each dot represents one mouse. Data is plotted as mean ± SEM. *p<0.05, **p<0.01, ***p<0.001 (Student's t test). ns, non-significant.
(D) Intracellular flow cytometry of DCs (left) and macrophages (right) for IL-12p40 production in tumor (top) and spleen (bottom) of mice treated with m1928z or m1928z-CD40L CAR T cells. Boxed-in regions highlight IL-12p40-producing cells. One representative plot per treatment condition is shown. Frequency of $IL\text{-}12p40^{+}$ DCs or macrophages is plotted on the right (n=3/group; representative of 2 different experiments). Adapted from Kuhn et al. (2019), *Cancer Cell*, 35(3):473-488.

Further, m1928z-CD40L CAR T cells changed the cellular composition of the tumor compared to m1928z CAR T cells (Figure 4.5). More DCs, $CD4^+$ and $CD8^+$ T cells infiltrated the tumor after mice were injected with m1928z-CD40L CAR T cells (Figures 4.5A and 4.5B). Intriguingly, the tumor-resident $CD4^+$ $Foxp3^+$ T regulatory (Treg) cell fraction was also slightly elevated in $CD40L^+$ CAR-treated mice (Figure 4.5B), resulting in similar $CD8^+$-to-Treg ratios (Figure 4.5C). No significant difference in CAR T cell tumor infiltration was observed between the two treatment cohorts (Figure 4.5D). Focusing on the lymphoid tissue, more macrophages and DCs were recruited to the spleen after mice received m1928z-CD40L CAR T cells (Figure 4.5E), indicative of engagement of $CD40^+$ APCs in lymphoid organs. Splenic lymphoid populations were also strongly altered after CAR treatment. In m1928z-CD40L CAR T cell- treated mice, more CAR^- $CD4^+$ and $CD8^+$ T cells localized to the spleen (Figure 4.5F). This coincided with a favorable $CD8^+$-to-Treg ratio in the spleen (Figure 4.5G) and an increase of m1928z-CD40L CAR T cells (Figure 4.5H).

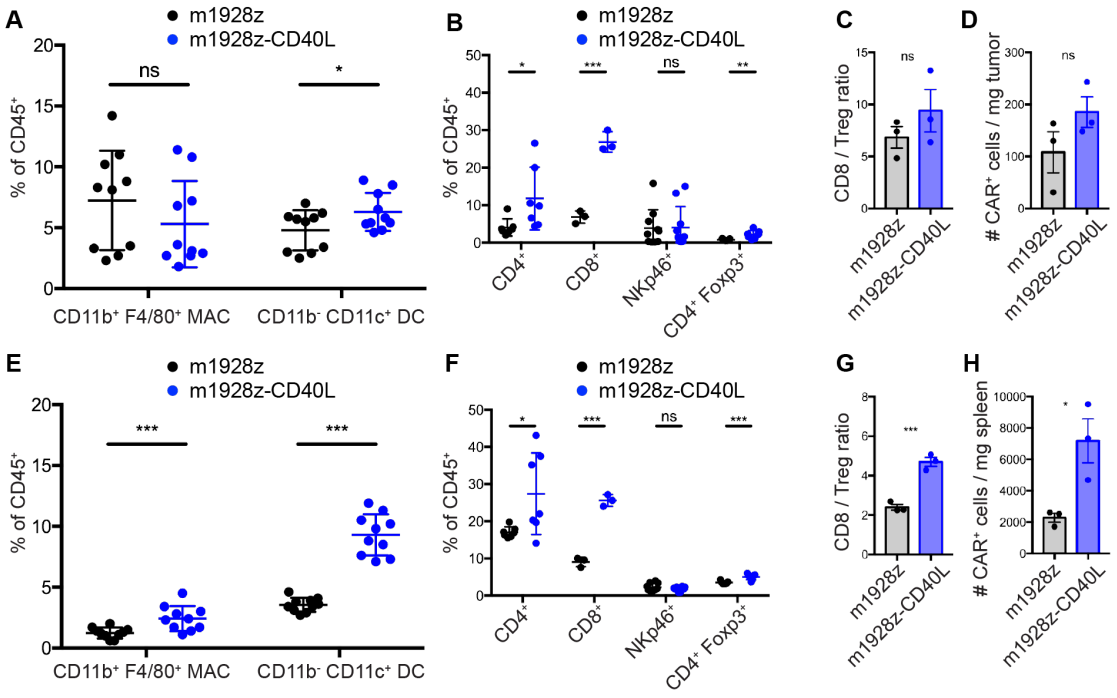

Figure 4.5. m1928z-CD40L CAR T cell treatment promotes the recruitment of immune effectors

Quantification of different immune cell populations in A20 tumor-bearing mice 7 days after being treated with $3x10^6$ CAR T cells.

(A) Frequency of macrophages (MAC) and dendritic cells (DC) as percentage of $CD45^+$ cells in tumor tissue.

(B) Frequency of $CD4^+$ T cells, $CD8^+$ T cells, $NKp46^+$ lymphocytes, and Treg cells ($CD4^+$ $Foxp3^+$) as percentage of $CD45^+$ cells in tumor tissue.

(C) The $CD8^+$ / Treg cell ratio in tumor tissue.

(D) Quantification of CAR^+ T cells per mg of tumor tissue.

(E-H) Same as in (A-D), except that immune populations were analyzed in the spleen.

Each dot represents one mouse. Data is plotted as mean ± SEM and is representative of 2-3 independent experiments. *p<0.05, **p<0.01, ***p<0.001 (Student's t test). ns, non-significant. Adapted from Kuhn et al. (2019), *Cancer Cell*, 35(3):473-488.

m1928z-CD40L CAR T cell-induced expansion and maturation of DCs is dependent on host CD40 expression

Having demonstrated the superior antitumor response of m1928z-CD40L CAR T cells compared to m1928z CAR T cells (Figure 3.6A) and the capability of $CD40L^+$ CAR T cells to license DCs in vivo (Figures 4.2), we wanted to evaluate if these effects are necessitated by host expression of CD40, the cognate receptor of CD40L. We hypothesized that the $CD40L^+$ CAR T cells activate host immune cells via CD40/CD40L interactions to enhance the immune response. Thus, we challenged CD40-deficient mice with A20 tumor cells before CAR T cell treatment. We used the A20.CD40-KO cell line to avoid any potential tumor rejection due to recognition of CD40 as foreign in the *Cd40*$^{-/-}$ mice. Here, m1928z-CD40L CAR T cells lost their protective effect (Figure 4.6A), implying that $CD40L^+$ CAR T cells need to engage with $CD40^+$ cells in the host to exert their improved antitumor response.

To ensure that CAR T cells in *Cd40*$^{-/-}$ mice do not have an inherent defect in cytotoxicity, we tested their capacity to induce B cell aplasia after preconditioning. Similar to WT host mice (Figure 3.5C), both m1928z and m1928z-CD40L CAR T cells induced complete B cell aplasia in *Cd40*$^{-/-}$ mice when preconditioned with cyclophosphamide (Figure 4.6B). These data demonstrated that lack of host CD40 expression does not impair CD19-targeted CAR T cell function.

Additionally, we noticed that m1928z-CD40L CAR T cells in A20 tumor-bearing *Cd40*$^{-/-}$ mice did not license DCs or macrophages to mature, as evidenced by a lack of CD86 and MHC-II upregulation in the spleen (Figure 4.6C). IL-12p40 production by DCs was also dependent on CD40 expression, as no IL-12p40 was detected in splenic DCs after CAR T cell treatment (Figure 4.6D). Importantly, *Cd40*$^{-/-}$ DCs are capable of IL-12 production. Stimulating bone marrow-derived DCs (BMDCs) of both WT and *Cd40*$^{-/-}$ mice with the toll-like receptor 4 agonist lipopolysaccharide (LPS) leads to IL-12 release (Figure 4.6E). In line with the absence of APC licensing in *Cd40*$^{-/-}$ mice, these mice also lacked

significant differences in immune cell infiltrates when comparing m1928z and m1928z-CD40L CAR T cell treated mice in tumor tissue or spleen (Figure 4.6F).

Together, these results demonstrate the necessity of host *Cd40* expression for the improved antitumor response through m1928z-CD40L CAR T cell treatment and the mechanism of in vivo APC licensing by these CAR T cells.

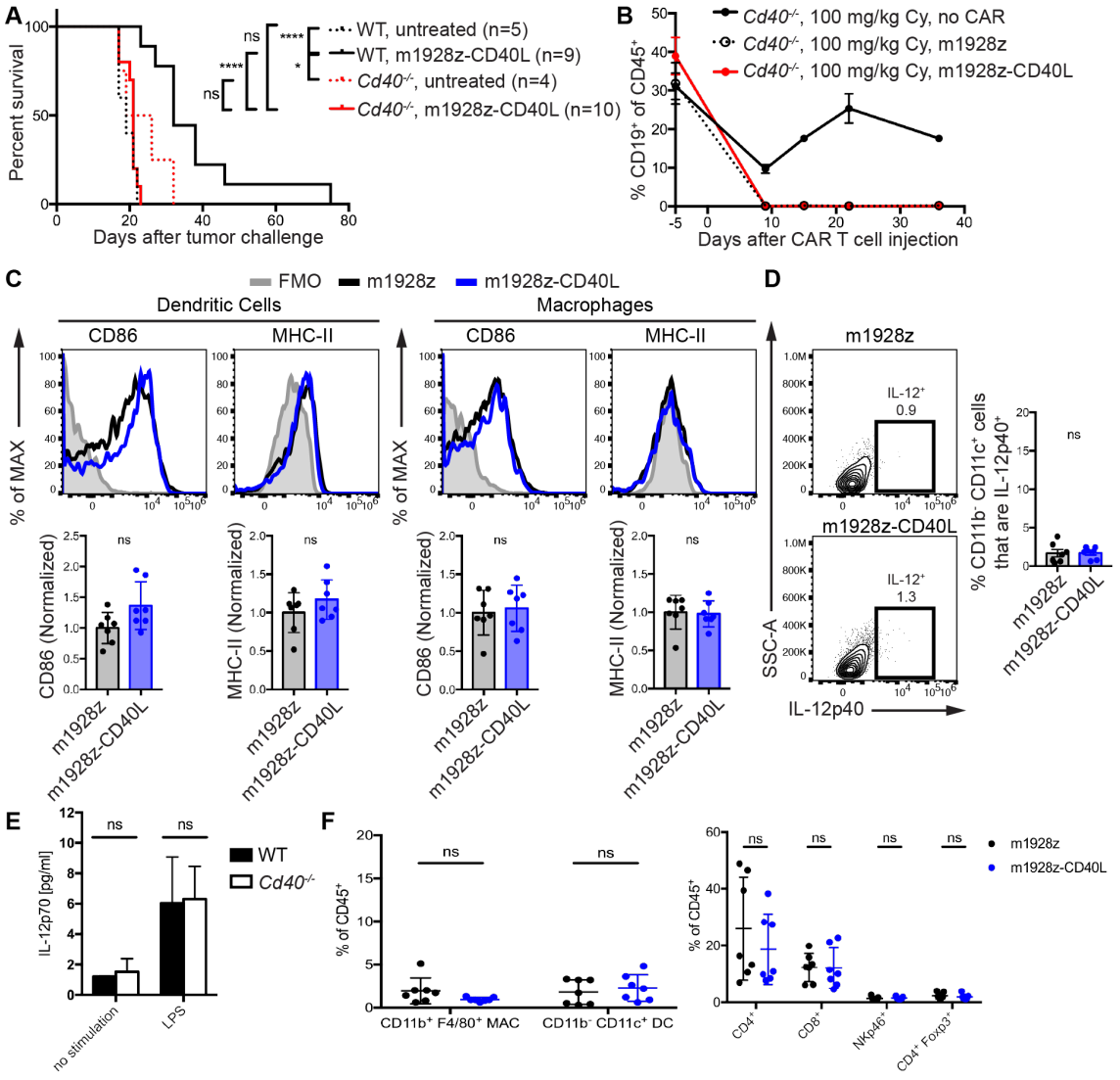

Figure 4.6. m1928z-CD40L CAR T cell antitumor efficacy and licensing of DCs is dependent on host *Cd40* expression

(A) Survival of WT or *Cd40*$^{-/-}$ BALB/c mice injected with 1x10^6 A20.CD40-KO cells i.v. and treated with 3x10^6 m1928z-CD40L CAR T cells i.v. on day 7. Graph summarizes two independent experiments (n=4-10/group). *p<0.05, ****p<0.0001 by log-rank (Mantel-Cox) test.

(B) *Cd40*$^{-/-}$ Mice were preconditioned with Cy on day -1 and received 3x10^6 m1928z or m1928z-CD40L CAR T cells i.v. on day 0. Peripheral blood was collected at indicated time points and the percentage of CD19$^+$ B cells of CD45$^+$ cells was assessed by flow cytometry. Means ± SEM are shown (n=3/group). One of two representative experiments is shown. Cy, cyclophosphamide.

(C) Surface expression of CD40, CD86, and MHC-II on CD11b$^-$ CD11c$^+$ DCs (CD45$^+$ CD3$^-$ CD19$^-$ Gr-1$^-$ pre-gates) in spleen tissue of *Cd40*$^{-/-}$ mice 7 days after CAR T cell treatment. Quantification of surface marker expression is plotted underneath the histograms (n=7/group, m1928z normalized to 1).

(D) Intracellular flow cytometry of DCs for IL-12p40 production in spleen of mice on day 7 after m1928z or m1928z-CD40L CAR T cells treatment. Boxed regions highlight IL-12p40-producing DCs. One representative plot per treatment condition is shown. Frequency of IL-12p40$^+$ DCs is plotted on the right (n=7/group).

(E) IL-12p70 production of WT and *Cd40*$^{-/-}$ BMDCs stimulated with LPS (1 ug/ml) for 24 hr was measured by ELISA sandwich assay. Data is plotted as mean ± SD (n=3).
(F) Fraction of macrophages (MAC), dendritic cells (DC), CD4^{+} T cells, CD8^{+} T cells, NKp46^{+} lymphocytes, and Treg cells (CD4^{+} Foxp3^{+}) as a percentage of CD45^{+} cells in spleen tissue of mice on day 7 after m1928z (black) or m1928z-CD40L (blue) CAR T cell treatment (n=7 mice per group).
Data is the summary of two independent experiments and plotted as mean ± SEM. ns, non-significant (Student's t-test). Adapted from Kuhn et al. (2019), *Cancer Cell*, 35(3):473-488.

Discussion

CAR T cells can be modified to license APCs in vivo via CD40/CD40L-mediated stimulation. This CAR T cell-to-APC crosstalk results in production of immunestimulatory chemokines and cytokines, and is responsible for a superior antitumor response.

Previous reports have demonstrated that combining checkpoint blockade with chemotherapy expands and activates cross-presenting DCs at tumor site and tumor-draining lymph nodes (tdLNs), leading to an enhanced antitumor $CD8^+$ T cell response (de Mingo Pulido et al., 2018; Salmon et al., 2016). In our analyses, m1928z-CD40L CAR T cell treatment did not trigger the activation of tumor-resident DCs, as DCs in the tumor mass of those mice had no increased CD40, CD86, or MHC-II surface expression. Despite a lack of sustained APC licensing at the tumor site, we did notice increased $CD4^+$ and $CD8^+$ T cell tumor infiltration in m1928z-CD40L CAR T cell-treated mice. Lack of increased TIL presence, cytokine production, splenic APC cell activation, and IL-12 production in *Cd40*$^{-/-}$ mice implies that m1928z-CD40L CAR T cells mediate these effects through the licensing of APCs in lymphoid organs.

Leveraging the CD40 pathway for an improved antitumor response is actively being investigated. Agonistic CD40 monoclonal antibodies (mAbs) have been used in tumor-bearing mice with success. There it was noticed that anti-CD40 mAb therapy as a single agent is only effective in immunogenic tumors carrying viral antigens (van Mierlo et al., 2002) or transiently effective in less immunogenic transgenic autochthonous pancreatic model (Beatty et al., 2011). Thus, attempts to combine agonistic anti-CD40 antibodies with chemotherapy are explored in patients (Beatty et al., 2013) and have already been shown to induce more robust responses in pancreatic mouse models (Byrne and Vonderheide, 2016). Here, we combine CD40/CD40L stimulation with the cytotoxic capabilities of CAR T cells. Whereas Byrne et al. predominantly saw intratumoral myeloid cell activation and T cell infiltration; we primarily saw APC activation in the spleen and tdLNs, and not at the primary tumor site. This

difference could be attributed to the different modalities of delivering CD40 stimulation. After ACT, CAR T cells presumably accumulate at anatomical sites with high antigen density. Therefore, $CD40L^+$ anti-CD19 CAR T cells would predominantly seed to the lymphoid tissue, a site with an abundant $CD19^+$ B cell population, and engage with $CD40^+$ DCs there. This was supported by a 20-fold increase in m1928z-CD40L CAR T cell numbers in the spleen compared to the liver.

The use of IL-12 in cancer immunotherapy has been pursued in the past. IL-12 is considered a pleiotropic cytokine with a wide range of biological activity in the immune system. Several immunestimulatory effects have been attributed to IL-12, such as the promotion of lymphocyte effector function, promotion of MHC-I expression on tumor cells, induction of CXCL9, 10, and 11 secretion to attract lymphocytes to the tumor site, and remodeling of tumor vasculature and stroma to enhance recruitment of T cells (Lasek et al., 2014). However, systemic administration of recombinant IL-12 in clinical settings have caused severe side effects and even deaths (Lasek et al., 2014). This halted the use of recombinant IL-12 as a monotherapy in cancer immunotherapy. A safer route of IL-12 administration was identified by local/intratumoral injection of IL-12 encoding DNA in combination with electroporation (Daud et al., 2008). Other strategies are based on genetically engineering tumor-infiltrating T cells (TILs) or CAR T cells to secrete IL-12, anticipating local cell-based delivery of the cytokine to the tumor site and have demonstrated antitumor efficacy in animal models (Chmielewski et al., 2011; Pegram et al., 2012). In patients, the autologous adoptive transfer of isolated TILs from melanoma patients after being transduced with an activation-induced nuclear factor of activated T cells (NFAT) promoter driving IL-12 production caused severe dose-limiting toxicities associated with high IL-12 and IFNγ serum levels (Zhang et al., 2015). These findings further highlight the narrow therapeutic index of therapeutically used IL-12, calling for improved design of IL-12-based immunotherapies. Using intravital imaging, a recent report elegantly depicts intratumoral IL-12 production by DCs in mice treated with anti-

PD1-based immune checkpoint blockade (Garris et al., 2018). There, IL-12 production was restricted to DCs and necessary for anti-PD1 treatment efficacy.

Our results also show specific IL-12 production in splenic DCs by intracellular flow cytometry after m1928z-CD40L CAR T cell treatment, whereas no IL-12 is detected in the cytokine array as a readout of local IL-12 production on the level of an organ (Figure 4.4A), nor in the serum of m1928z-CD40L CAR T cell treated mice as a readout of systemic IL-12 level increases (Figure 3.7A). The lack of IL-12 detection outside of the microenvironment of spleen-resident DCs suggests the presence of a close-by sink, such as activated T cells known to upregulate surface IL-12R expression (Trinchieri, 2003), which would be primed to produce IFNγ. T cell activation in this context is examined in the following chapter 5. In the A20 tumor model, the spleen is just one of several anatomical sites expressing the anti-CD19 CAR antigen, namely endogenous B cells present in germinal centers, whereas the liver is the predominant site of A20 tumor cell seeding and growth (Figure 3.1D). As we did not detect any IL-12 production in the tumor present in the liver, use of a locally growing tumor – instead of a systemic A20 lymphoma model – would help to delineate if the spleen acts as a sink for m1928z-CD40L CAR T cells, potentially explaining the licensing of APCs at that site, or if CD40L-modified CAR T cells are capable of inducing APC maturation and IL-12 production in the tumor microenvironment as well.

Furthermore, the importance of IL-12 production by DCs and its effect on IL-12R expressing lymphocytes on the improved antitumor response would require more careful analysis. The use of tumor-bearing *Il-12p40*$^{-/-}$ mice would prevent IL-12 and IL-23 production in host DCs after m1928z-CD40L CAR T cell treatment and would be informative in deciphering their roles in the improved antitumor response. However, since the IL-12p40 subunit is part of both IL-12 and IL-23 cytokine heterodimers, elucidating an unequivocal role of IL-12 in lymphocyte priming after m1928z-CD40L CAR T cell treatment would require a different strategy. Whereas the IL-23 cytokine signals via binding of IL-23R and IL-12Rβ1 subunits, IL-12 exclusively signals by binding to the IL-12Rβ1 and IL-12Rβ2 subunits of the IL-12 receptor (Teng et al., 2015). Thus, lymphocytes in

Il12rb2$^{-/-}$ mice would be unresponsive to m1928z-CD40L CAR T cell-mediated IL-12 production by DCs. This would allow testing the relevance of IL-12 signaling on the lymphocyte population.

Besides IL-12 in DCs, m1928z-CD40L CAR T cells also stimulated CXCL9 production in macrophages. In the antiviral response, microscopic staining of CXCL9 in lymph nodes identified stromal cells and macrophages as producers of the lymphocyte-attracting chemokine (Kastenmüller et al., 2013; Sung et al., 2012). There, lymph-borne viruses were taken up by sentinel macrophages at the entry of the lymph node and predominantly recruit CXCR3^{+} central memory CD8^{+} T cells via CXCL9/CXCR3 stimulation. Importantly, CXCL9 production by the macrophages is dependent on IFNγ release from the recruited CD8^{+} T cells, resulting a positive feedback loop between the APC and the T cell. The next chapter will investigate potential IFNγ sources, with both CAR T cells and endogenous T cells being the most likely candidates, potentially explaining the increased CXCL9 production in splenic macrophages upon m1928z-CD40L CAR T cell treatment. Whereas we detected CXCL9 protein in macrophages, similar to its production in an antiviral response, de Mingo Pulido et al. detected CXCL9 mRNA and protein production specifically in breast tumor-residing DCs – and not macrophages – after αTIM-3 treatment (de Mingo Pulido et al., 2018). Additionally, they demonstrated that increased *CXCL9* mRNA levels in human breast cancer tissue correlates with an improved response to chemotherapy. The question, if CXCL9 production in m1928z-CD40L CAR T cell treated mice is also necessary for the observed improved antitumor response in our lymphoma model, prompts further investigation. The use of a CXCR3 blocking antibody – blocking the receptor for CXCL9 on CXCR3^{+} lymphocytes – and/or CXCR3-deficient (*Cxcr3*$^{-/-}$) CAR T cells could help to elucidate if systemic blocking of the biological function of CXCL9 and/or targeted-deletion in CAR T cells can abrogate the CAR T cell-mediated antitumor response.

CHAPTER 5

Recruitment and Activation of endogenous Immune Effectors by m1928z-CD40L CAR T Cell Treatment

Introduction

Most T cell-based immunotherapies are focused on directly increasing the number of tumor-targeted T cells by adoptively transferring T cells into patients, removing immune-inhibitory checkpoints that act on the endogenous repertoire of the polyclonal T cell population, redirecting the endogenous T cell population to the tumor via bispecific antibodies, and/or genetically engineered T cells with chimeric antigen receptors that allow supraphysiological antitumor T cell responses. All these strategies directly manipulate and redirect immune responses on the T cell level. With the findings in the previous chapter of in vivo APC licensing after m1928z-CD40L CAR T cell treatment, this chapter investigates if the APC licensing mediates priming of an endogenous T cell antitumor response. Unlike most conventional immunotherapies targeting T cell activation, m1928z-CD40L CAR T cell treatment potentially leads to recruitment and activation of these additional immune effectors with the help of APCs.

Conventional DCs (cDCs), as opposed to plasmacytoid DCs (pDCs), are the most potent antigen-presenting cells and can be further subdivided into cDC1 and cDC2 populations (Merad et al., 2013). cDCs express high levels of MHC-II and CD11c in both humans and mice. The transcription factors BATF3, IRF8, and ID2 are essential for cDC1 development, whereas cDC2s depend on the transcription factors RELB, IRF4, and ZEB2 (Murphy et al., 2016). cDC2s are predominantly involved in initiating $CD4^+$ T cell responses against nematodes and viral infections (Gao et al., 2013; Krishnaswamy et al., 2017). So far, there is limited understanding of cDC2 function in the immune antitumor response, but a recent study has identified cDC2s in mice and humans and their involvement in $CD4^+$ T cell activation (Binnewies et al., 2019).

cDC1s express surface CD8α and CD103 (Integrin αE) in lymphoid and non-lymphoid tissue, respectively. Both lymphoid and non-lymphoid tissue cDC1s

share a very similar transcriptional profile and a central role in the adaptive immune response by cross-presenting antigen to cytotoxic $CD8^+$ T cells in antiviral and antitumor responses (Broz et al., 2014; Hildner et al., 2008; Merad et al., 2013). In humans, cDC1s are identified by CD141/BDCA3 surface expression (Jongbloed et al., 2010) and seem to be excluded from tumor tissue compared to matched, healthy tissue (Lavin et al., 2017). This suggests that cDC1s have a role in the antitumor immune response and is further supported by the finding that high levels of intratumoral $BDCA3^+$ cDC1s correlate with responsiveness to anti-PD-1 immunotherapy in melanoma patients (Barry et al., 2018). Thus, the aim of several preclinical tumor transplantation studies was to increase the accumulation of tumor-resident cDC1s, where it was noted that NK cell-derived Flt3 ligand (FLT3L) and other cDC1 chemoattractants stimulated cDC1 recruitment to the tumor and controlled further tumor growth (Barry et al., 2018; Böttcher et al., 2018). The accumulation of tumor-resident cDC1s improved $CD8^+$ T cell expansion and responses to anti-PD-L1 treatment (Salmon et al., 2016).

T cell-mediated antitumor responses are well characterized and can be based on recognition of non-mutated cancer-related antigens or neoantigens derived from mutated proteins (Rosenberg and Restifo, 2015; Schumacher and Schreiber, 2015). The antigen is recognized by the TCR of the $CD4^+$ or $CD8^+$ T cell on presented MHC-II or MHC-I, respectively. The importance of $CD8^+$ T cell-mediated tumor control through pMHC-I:TCR interactions is highlighted by the observation that MHC-I or β2M loss in tumor cells – both resulting in the absence of antigen presentation on the cancer cell surface – leads to tumor immune evasions and subsequent tumor outgrowth in patients (Tran et al., 2016; Zaretsky et al., 2016). Still, long-term survival for up to 10 years has now been described in a subset of patients with metastatic disease who were treated with T cell-mobilizing immunotherapies (Postow et al., 2018). Similar results have been described for B-ALL patients treated with anti-CD19 CAR T cells in a long-term follow up (Park et al., 2018). However, some patients relapse with CAR-antigen-negative disease at later time points. Thus, a sustained antitumor response that

is based on the highly cytotoxic effector function of the CAR T cell, plus the recruitment of cytotoxic non-CAR T cells recognizing tumor cell-specific antigens is explored in this chapter. m1928z-CD40L CAR T cells, through the mobilization of other endogenous immune effectors, could potentially induce long-lived immune cell-based antitumor memory and, thereby, provide protection from CAR-antigen-negative tumor outgrowth.

Results

m1928z-CD40L CAR T cells produce more effector cytokines in vivo and increase the effector cytokine production of endogenous non-CAR T cells

The licensing of APCs through CD40L CAR T cells described in the previous chapter was prominent in lymphoid tissue at day 7 after ACT (Figure 4.1). Since we did not detect any profound changes in the tumor tissue, we analyzed earlier time points after ACT and quantified DC recruitment to both tumor and spleen (Figure 5.1A). Again, m1928z-CD40L CAR T cell treatment did not affect the recruitment of bulk MHC-II$^+$ CD11c$^+$ DCs to the tumor tissue over time (Figure 5.1B), whereas, compared to m1928z CAR T cell treatment, CD40L$^+$ CAR T cells induced the accumulation of splenic MHC-II$^+$ CD11c$^+$ DCs not until day 7 after ACT (Figure 5.1C). Clearly, m1928z-CD40L CAR T cell treatment has no effect on DC tumor infiltration numbers – not at earlier or later time points – nor does it affect the lymphoid compartment until one week after ACT.

Encouraged by the observation of in vivo DC licensing by m1928z-CD40L CAR T cells (Figure 4.2) and their quantitative increase at day 7 after ACT in the spleen (Figure 5.1C), we chose day 7 post ACT to test whether this DC activation can bolster the CAR T cell response and/or prime endogenous non-CAR T cells as bystanders for enhanced tumor recognition. Despite similar DC infiltration numbers and lack of licensing in the tumor (Figures 5.1B and 4.1), CD40L$^+$ CAR T cells produced significantly more IFNγ and TNFα than T cells only expressing the CAR (Figure 5.1D). The same increase in T cell effector cytokine production was seen in the spleen (Figure 5.1E). Focusing on the bystander cells, we noticed that more double-positive IFNγ$^+$ TNFα$^+$ CD3$^+$ CAR$^-$ T cells were present

in both tumor and spleen of m1928z-CD40L compared to m1928z CAR T cell-treated mice (Figures 5.1D and 5.1E).

The combination of lack of tumor-resident DC licensing with increased cytokine production of tumor-infiltrating lymphocytes prompted a more detailed analysis of potential changes in the tumor-resident DC compartment. As outlined in the introduction of this chapter, conventional DCs can be further divided into cDC1 and cDC2 subpopulations. Both subpopulations have been described to have roles in antitumor immune responses, where they control T cell immunity (Salmon et al., 2016; Spranger et al., 2017). Thus, we investigated DC subpopulations in m1928z-CD40L CAR T cell treated mice.

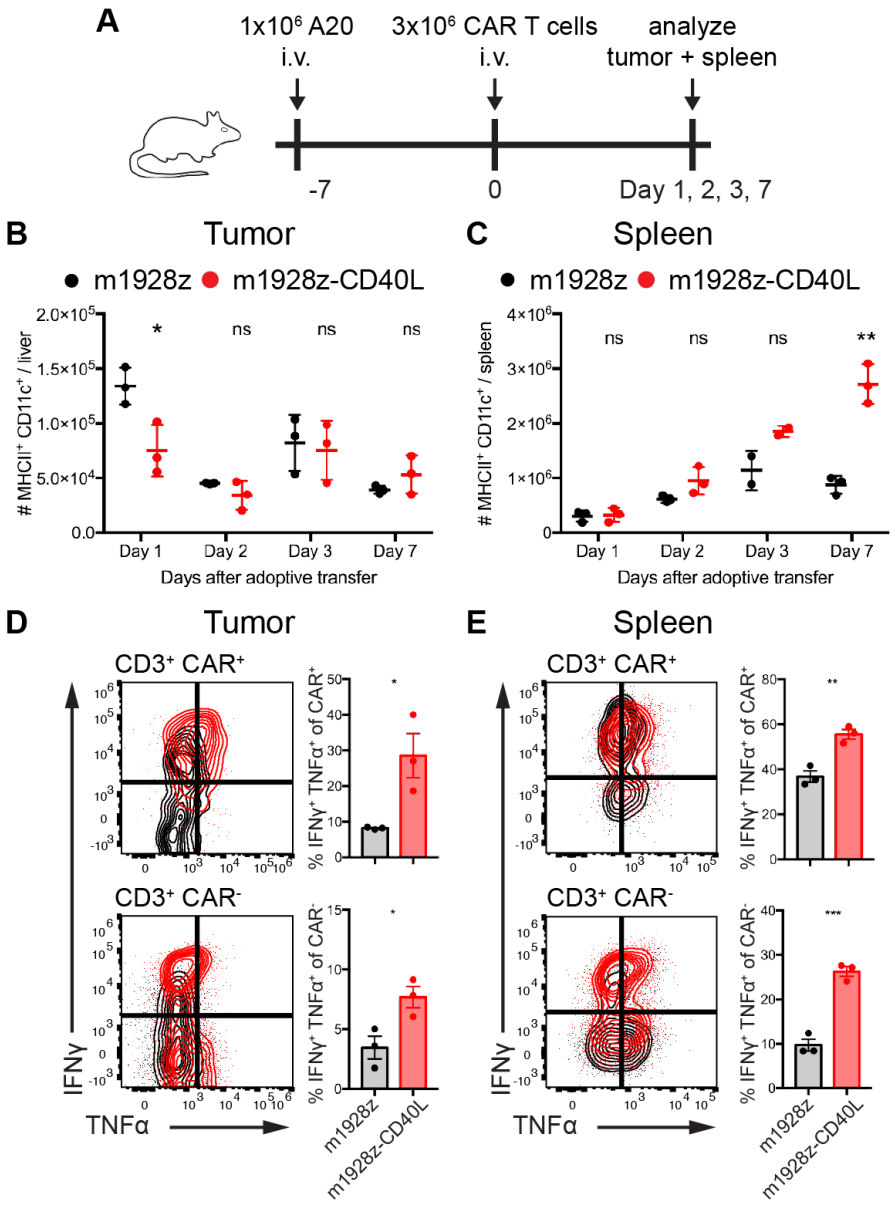

Figure 5.1. m1928z-CD40L CAR T cell recruit DCs to spleen, produce more effector cytokines in vivo, and increase effector cytokine production of endogenous non-CAR T cells

(A) Experimental layout for B-E.

(B and C) Absolute numbers of MHC-II$^+$ CD11c$^+$ DCs (CD45$^+$ Gr1$^-$ CD19$^-$ CD3e$^-$ pre-gates) in tumor (B) and spleen (C) of A20 tumor-bearing mice treated as outlined in (A). Each dot represents one mouse (n=3/group). Data is representative of two experiments and plotted as mean ± SEM.

(D and E) BALB/c mice were injected with 1x10^6 A20.GL cells i.v. and treated with 3x10^6 CAR T cells i.v. after 7 days. On day 7 after ACT, CD3$^+$ CAR$^+$ (top) and CD3$^+$ CAR$^-$ (bottom) cells (CD45$^+$ CD19$^-$ CD11b$^-$ Gr-1$^-$ pre-gate) in tumor (D) or spleen (E) were isolated and analyzed for production of IFNγ and TNFα by intracellular flow cytometry after 4 hr ex vivo stimulation with PMA/ionomycin. Overlay plots (left) and frequency IFNγ$^+$ TNFα$^+$ T cells (right) are plotted. Each dot represents one mouse (n=3/group). Data is representative of two independent experiments and plotted as mean ± SEM. ns, non-significant. *p<0.05, **p<0.01, ***p<0.001 (Student's t test). Adapted from Kuhn et al. (2019), *Cancer Cell*, 35(3):473-488.

Improved antitumor response of m1928z-CD40L CAR T cells requires presence of Batf3-expressing cDC1s

cDC1 and cDC2 populations can be immunophenotyped based on surface marker expression. Identified by high expression of the conventional DC markers MHC-II and CD11c, cDC1 populations in non-lymphoid tissue express the integrin CD103 and are $CD11b^-$, whereas cDC2s are $CD11b^+$ $CD103^-$ (Figure 5.2A). In the lymphoid tissue, the cDC1 population loses its CD103 expression and instead is identified by CD8α expression, with cDC2 cells maintaining their $CD11b^+$ $CD8\alpha^+$ status (Figure 5.2B). With this mutually exclusive surface marker expression, the frequencies of cDC1 and cDC2 populations were assessed over time. A20 lymphoma-bearing mice were treated with m1928z or m1928z-CD40L CAR T cells and changes in cDC1/2 populations were analyzed at different time points post ACT (Figures 5.2C and 5.2D). Whereas we previously did not observe a change in absolute numbers of tumor-resident DCs (Figure 5.1B), now, m1928z-CD40L CAR T cell treatment led to a relative increase in the tumor-resident cDC1 population at day 7 post ACT (Figure 5.2C). These findings, for the first time, documented a change in the myeloid cell compartment of the tumor tissue after m1928z-CD40L CAR T cell treatment. Whereas previous analyses did not detect any changes in activation status (Figure 4.1) or numbers (Figure 5.1B), m1928z-CD40L CAR T cells skew the tumor-resident cDC1-to-cDC2 ratio in favor of the cDC1 population. Curiously, the opposite skewing was observed in the spleen, where the cDC2 population dominated after m1928z-CD40L CAR T cell treatment (Figure 5.2D). These observations highlighted the effect m1928z-CD40L CAR T cells have on DC subpopulations and prompted the question of its relevance in the antitumor response.

Next, we wanted to prevent cDC1 accumulation in the tumor and, thereby, assess its necessity in the m1928z-CD40L CAR T cell-mediated antitumor response. The transcription factor BATF3 is important for the development of cDC1s, as mice lacking *Batf3* expression are deficient in $CD8\alpha^+$ DCs and tumor-resident $CD103^+$ DCs, making them more susceptible to $CD8^+$ T cell-controlled viral infections and tumor growth (Hildner et al., 2008; Spranger et al., 2017). We

challenged both wild-type and *Batf3*$^{-/-}$ mice with A20 lymphoma cells and, as expected, no CD11b^{-} CD103^{+} cDC1 cells were present in the tumor of *Batf3*$^{-/-}$ mice (Figure 5.2E). This allowed investigation of their involvement in the m1928z-CD40L CAR T cell treatment-induced antitumor response. Subsequent treatment with CAR T cells showed that m1928z-CD40L CAR T cells in *Batf3*$^{-/-}$ mice improves survival of tumor-bearing mice (Figure 5.2F), demonstrating that the cDC1 population is not solely responsible for in vivo m1928z-CD40L CAR T cell function. However, their presence in wild-type mice significantly improved survival and allowed complete tumor clearance by m1928z-CD40L CAR T cells in 40% of mice (Figure 5.2F). Taken together, the improved antitumor response of and tumor cell eradication by m1928z-CD40L CAR T cells requires the presence of cDC1 cells.

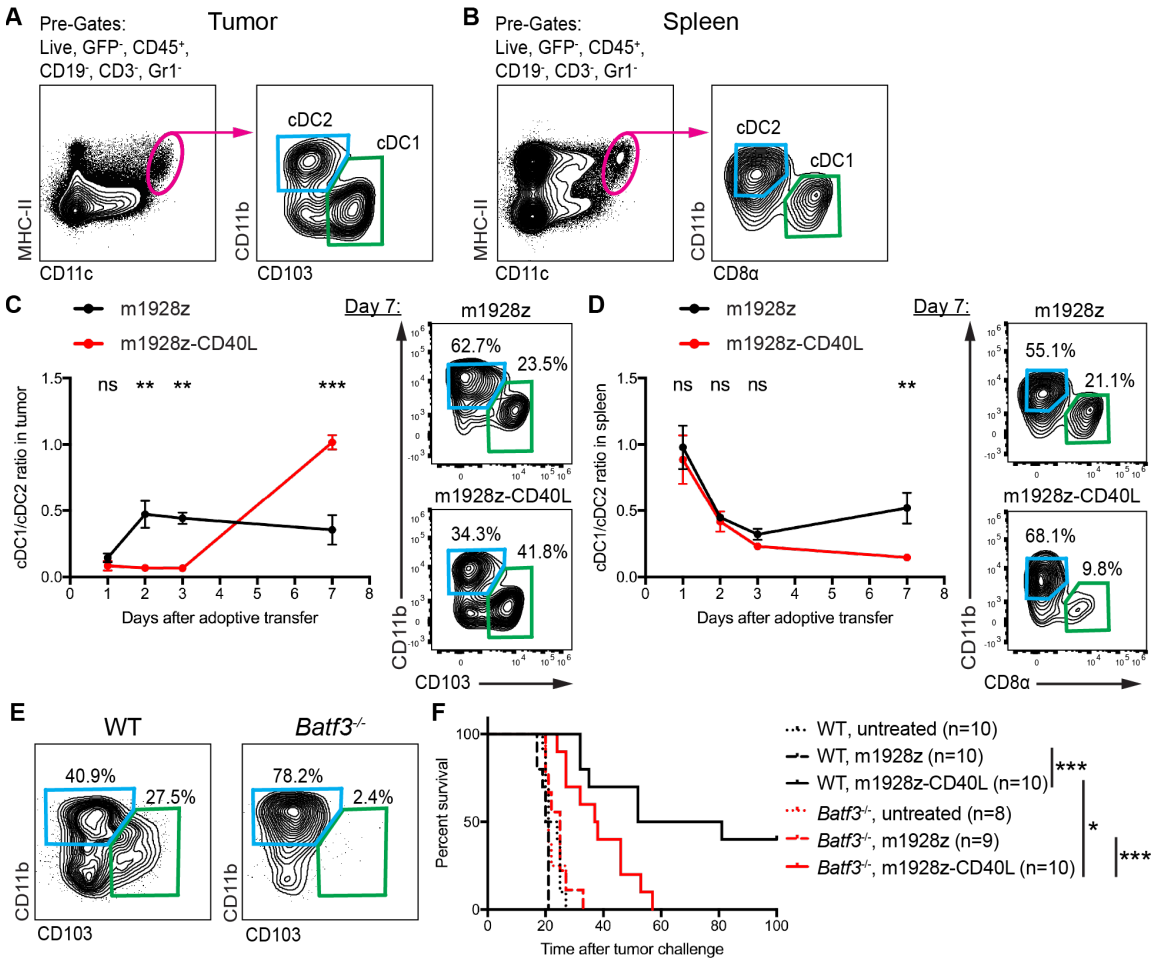

Figure 5.2. Improved antitumor response of m1928z-CD40L CAR T cells requires presence of *Batf3*-expressing cDC1

(A and B) Gating strategy for MHC-II^{+} CD11c^{+} cDC1 and cDC2 populations in tumor (A) and spleen (B).

(C and D) BALB/c mice were injected with 1x10^{6} A20.GL cells i.v. on day -7 and treated with 3x10^{6} CAR T cells on day 0. Ratios of cDC1-to-cDC2 populations in tumor (C) and spleen (D) are plotted over time. Data is plotted as mean ± SEM (n=3/group). Representative flow cytometry contour plots on day 7 of m1928z or m1928z-CD40L CAR T cell treated mice are shown on the right. *p<0.05, **p<0.01 (Student's t test).

(E) Flow cytometry contour plots of the MHC-II^{+} CD11c^{+} DC population in tumors of WT and *Batf3*$^{-/-}$ mice on day 14 after A20.GL i.v. injection.

(F) Survival of BALB/c WT or *Batf3*$^{-/-}$ mice challenged with 1x10^{6} A20.GL cells and treated with 3x10^{6} CAR T cells on day 7. *p<0.05, ***p<0.001 by a log rank (Mantel-Cox) test.

Host Cd40 expression, but not Batf3 expression, is necessary for m1928z-CD40L CAR T cell-mediated T cell cytokine production

With the increased priming of tumor-infiltrating CAR^+ and CAR^- T cells (Figure 5.1D), the accumulation of tumor-resident cDC1 population (Figure 5.2C), and an impaired antitumor response in m1928z-CD40L CAR T cell treated *Batf3*$^{-/-}$ mice (Figure 5.2F), we hypothesized that m1928z-CD40L CAR T cells prime the tumor-infiltrating T cell population through the cDC1 population. Due to the known function of cDC1 cells cross-presenting antigen to $CD8^+$ T cells, we focused on analyzing the $CD8^+$ T cell compartment. As expected, after A20 tumor challenge and CAR T cell treatment, $CD8^+$ T cells in m1928z-CD40L CAR T cell treated mice produced more IFNγ after ex vivo PMA/ionomycin stimulation (Figures 5.3A and 5.3B). However, this elevated IFNγ production was sustained in the absence of cDC1 cells in *Batf3*$^{-/-}$ mice (Figures 5.3A and 5.3B). This indicates that m1928z-CD40L CAR T cells can provide a permissive environment in vivo that allows endogenous $CD8^+$ T cells to robustly produce IFNγ independently of cDC1 cells.

To assess if absence of cDC1 cells has any effect on the adoptively transferred T cell population, which might explain the impaired antitumor response in *Batf3*$^{-/-}$ mice, IFNγ production in $CD3^+$ CAR^+ T cells was assessed. Again, more IFNγ was detected in m1928z-CD40L CAR T cells compared to m1928z CAR T cells and this difference was not affected by genetic deletion of cDC1 cells in *Batf3*$^{-/-}$ mice (Figures 5.3C and 5.3D). This suggested that cDC1 cells are not responsible for the increased effector cytokine production observed in both CAR^- and CAR^+ T cells of m1928z-CD40L CAR T cell treated mice.

In a different attempt to link the observations of in vivo APC licensing (Figure 4.2) and enhanced T cell cytokine production in m1928z-CD40L CAR T cell treated mice (Figures 5.1D and 5.1E), we focused on the most proximal interaction between CAR T cell and APC in our system: the CD40/CD40L interaction. Previous results have demonstrated that absence of host *Cd40* expression completely negated the antitumor response of m1928z-CD40L CAR T cell treatment (Figure 4.6A), highlighting the importance of the CD40/CD40L

interaction in our system. Intriguingly, absence of $CD40^+$ APCs in *Cd40*$^{-/-}$ mice also blunted the effector cytokine production of both CAR^+ and CAR^- tumor-infiltrating (Figure 5.3E) and spleen-resident T cells (Figure 5.3F). Collectively, these results demonstrate that host *Cd40* expression, but not *Batf3* expression, is necessary for CAR^+ and CAR^- T cell effector cytokine production after m1928z-CD40L CAR T cell treatment. Importantly, it suggests that DC licensing by $CD40L^+$ CAR T cells is upstream of and necessary for T cell activation in this system.

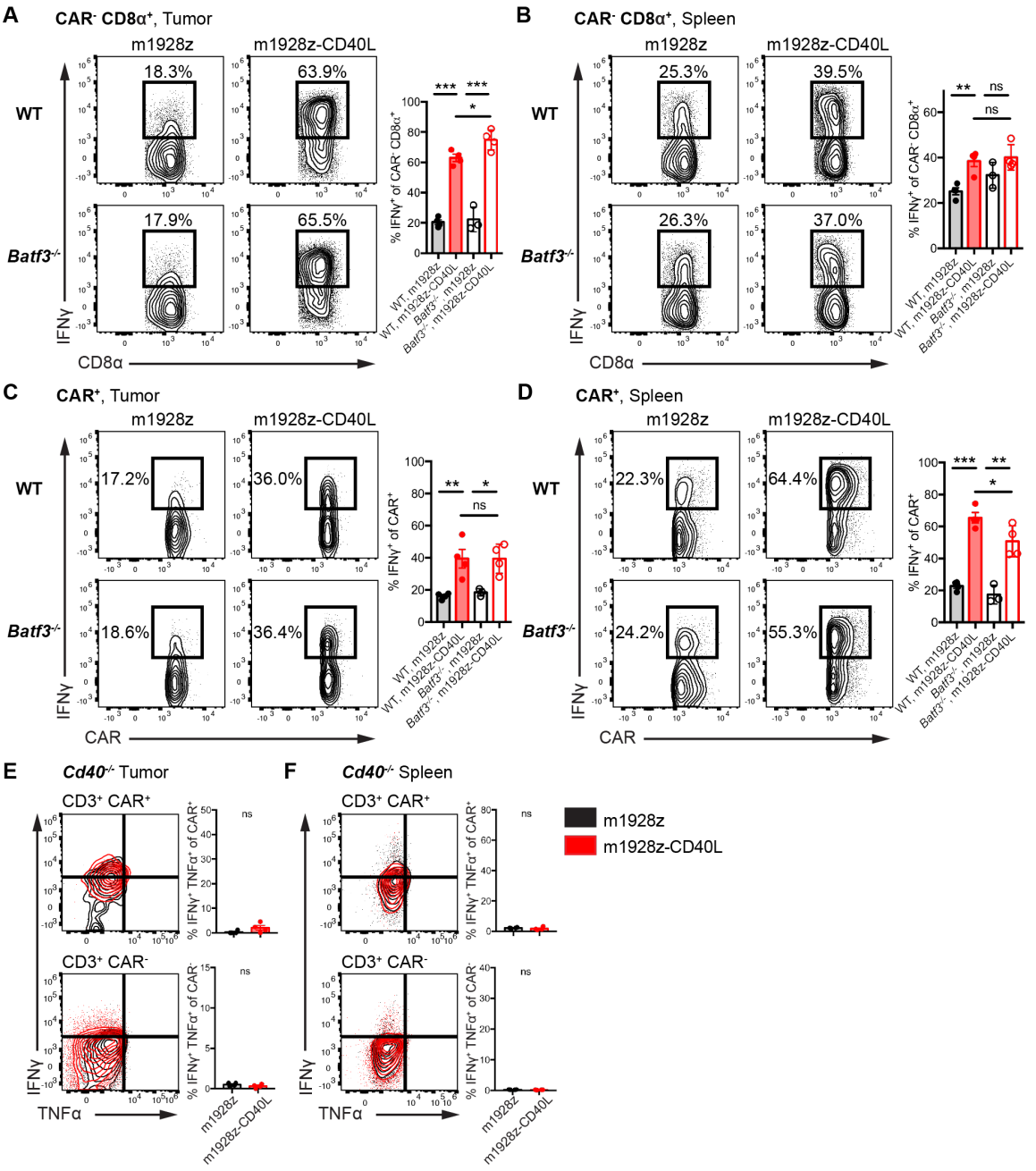

Figure 5.3. Host *Cd40* expression, but not *Batf3* expression, is necessary for m1928z-CD40L CAR T cell-mediated T cell cytokine production

BALB/c mice were injected i.v. with $1x10^6$ A20.GL cells followed by ACT of $3x10^6$ CAR T cells 7 days after tumor challenge. The tumor and spleens were analyzed 7 days after ACT.

(A and B) Flow cytometry contour plots of CAR^- $CD8^+$ T cells ($CD45^+$ $CD19^-$ $CD11b^-$ $Gr\text{-}1^-$ $CD3^+$ CAR^- pre-gates) after 4 hr ex vivo PMA/ionomycin stimulation isolated from tumor (A) and spleen (B) of WT (top) or *Batf3*$^{-/-}$ (bottom) mice. IFNγ-producing cells are highlighted by boxed-in region. Percentage of $IFN\gamma^+$ cells is summarized on the right. Each dot represents one mouse (n=3-4/group) and data is plotted as mean ± SEM. ns, non-significant. *p<0.05, **p<0.01, ***p<0.001 (Student's t test).

(C and D) Flow cytometry contour plots of CAR^+ T cells ($CD45^+$ $CD19^-$ $CD11b^-$ $Gr\text{-}1^-$ $CD3^+$ pre-gates) after 4 hr ex vivo PMA/ionomycin stimulation isolated from tumor (C) and spleen (D) of WT

(top) or *Batf3*$^{-/-}$ (bottom) mice. IFNγ-producing cells are highlighted by boxed-in region. Percentage of IFNγ^{+} cell is summarized on the right. Each dot represents one mouse (n=3-4/group) and data is plotted as mean ± SEM. ns, non-significant. *p<0.05, **p<0.01, ***p<0.001 (Student's t test).
(E and F) *Cd40*$^{-/-}$ BALB/c mice were treated as described. CD3^{+} CAR^{+} (top) and CD3^{+} CAR^{-} (bottom) cells in tumor (D) or spleen (E) were isolated and analyzed for production of IFNγ and TNFα by intracellular flow cytometry after 4 hr ex vivo stimulation with PMA/ionomycin. Overlay plots (left) and frequency IFNγ^{+} TNFα^{+} T cells (right) are plotted. Each dot represents one mouse (n=3/group). Data is representative of two independent experiments and plotted as mean ± SEM. ns, non-significant (Student's t test). Adapted from Kuhn et al. (2019), *Cancer Cell*, 35(3):473-488.

Endogenous T cells recognize and lyse tumor cells post CAR T cell treatment

The results above demonstrate the importance of the CD40/CD40L interaction between CAR T cell and APC in vivo to sustain T cell effector cytokine production. Assessment of cytokine production was done by ex vivo intracellular cytokine staining after non-specific activation of T cells by the diacylglycerol (DAG) analog PMA and the calcium ionophore ionomycin. Together, these stimulants lead to protein kinase C activation (via PMA) and calcium release (via ionomycin) in T cells and activate T cells downstream of TCR-induced activation. Thus, analysis of PMA/ionomycin stimulated cell populations provides a readout for general cell activation potential, but not a readout for cell-specific tumor recognition.

However, we wanted to assess if the increase in bystander CAR^- T cell activation translates into recruitment of endogenous T cells recognizing tumor cells specifically through their TCR. To do this, congenically marked $Thy1.1^+$ CAR T cells were adoptively transferred into A20 tumor-bearing $Thy1.2^+$ mice allowing post-treatment sorting and ex vivo analysis of endogenous $Thy1.2^+$ non-CAR T cells (Figure 5.4A). Upon restimulation of the sorted CAR^- $Thy1.2^+$ $CD4^+$ T cell population with A20 cells, we noticed that m1928z CAR T cell treatment alone led to an increase in recruitment of tumor-specific $CD4^+$ T cells as assessed by IFNγ ELIspot (Figures 5.4B and 5.4C). Importantly, the recruitment of these cells was further increased upon m1928z-CD40L CAR T cell treatment (Figures 5.4B and 5.4C). The IFNγ release in $CD4^+$ T cells was strictly dependent on pMHC:TCR interactions, because no IFNγ was detected when endogenous $Thy1.2^+$ $CD4^+$ T cells were co-cultured with MHC-II^- A20.MHCII-KO cells (Figure 5.4D).

The recognition of tumor cells via pMHC:TCR was also detected in endogenous $Thy1.2^+$ $CD8^+$ T cells. CAR T cell treatment led to IFNγ release in $Thy1.2^+$ $CD8^+$ T cells upon A20 tumor cell stimulation and this effect was potentiated when mice were treated with m1928z-CD40L CAR T cells (Figures 5.4E and 5.4F). When sorted $Thy1.2^+$ $CD8^+$ T cells were co-cultured with A20.B2M-KO cells, which lack MHC-I expression due to KO of *B2m*, no increase in IFNγ was detected (Figure

5.4G), indicating that the endogenous $CD8^+$ T cells produced IFNγ upon binding to MHC-I-peptide on A20 tumor cells via their TCR. These results demonstrate that m1928z-CD40L CAR T cells prime endogenous non-CAR T cells to recognize tumor cells through their TCR.

Finally, to test if the increased mobilization of IFNγ-producing endogenous $CD4^+$ and $CD8^+$ T cells to recognize tumor via pMHC:TCR interactions translates to more tumor cell killing, non-CAR T cell populations were assessed for their ex vivo killing capacity after CAR T cell treatment. Again, to provide enough time for the endogenous T cells to be primed, A20 tumor-bearing mice were treated with CAR T cells and 7 days after ACT endogenous T cells were isolated. Non-CAR T cells from m1928z-CD40L CAR T cell treated mice consistently lysed more CD19-negative A20.CD19-KO cells ex vivo compared to T cells from m1928z CAR T cell treated mice (Figure 5.4H). Taken together, these results demonstrate the priming effect m1928z-CD40L CAR T cells have on endogenous $CD4^+$ and $CD8^+$ T cells to recognize tumor cells through their TCR.

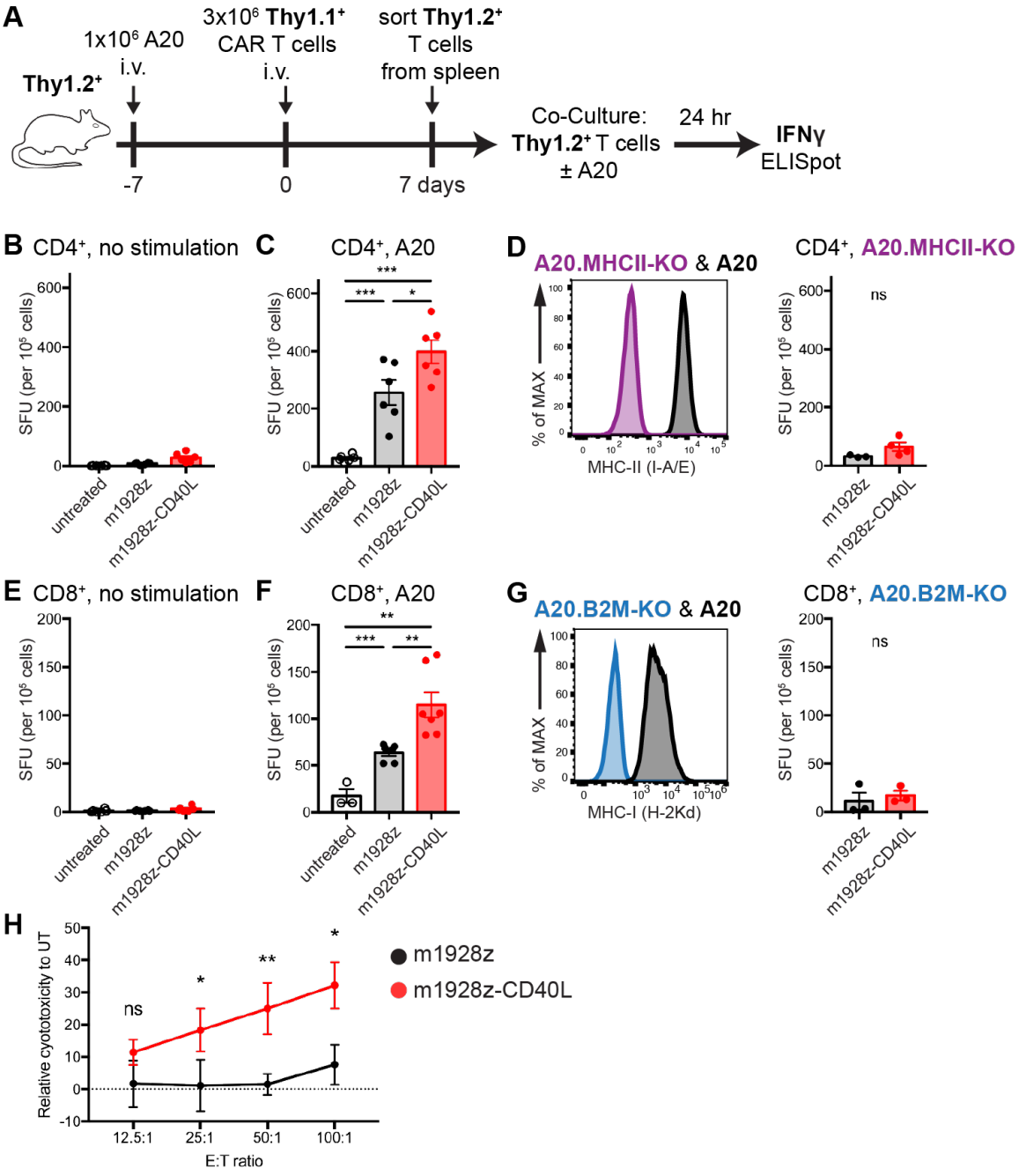

Figure 5.4. Endogenous T cells recognize and lyse tumor cells post CAR T cell treatment in a TCR-dependent manner

(A) Experimental layout for (B-G).

(B-G) Thy1.2$^+$ BALB/c mice were treated as depicted in (A). On day 7, mice were sacrificed and Thy1.2$^+$ CAR$^-$ host T cells were sorted from spleens via FACS. Sorted CD4$^+$ T cells were then cultured without any stimulation (B), stimulated by co-culturing with A20 (C) or A20.MHCII-KO (MHC-II$^-$) A20 cells (D) for 24 hr. Sorted CD8$^+$ T cells were cultured without stimulation (E), co-cultured with A20 cells (I) or A20.B2M-KO (MHC-I$^-$) cells (J) for 24 hr. IFNγ release was measured by ELISpot assay. Data are representative of one experiment (D and G) or summary of two independent experiments (B, C, E, and F) and plotted as mean ± SEM (n=3-6/group). *p<0.05, **p<0.01, ***p<0.001 (Student's t test). ns, non-significant.

(H) Ex vivo A20.CD19-KO tumor cell killing assay by endogenous T cells from mice challenged with $1x10^6$ A20 cells and treated with $3x10^6$ $CD45.1^+$ CAR T cells on day 7. Endogenous $CD45.2^+$ T cells were sorted by FACS from spleens 7 days after CAR T cell treatment and cultured with luciferase-expressing A20.CD19-KO target cells for 24 hr. CD19-negative A20.CD19-KO cells were used to exclude the possibility that contaminating CD19-targeted CAR T cells lyse the tumor via CAR-mediated cytotoxicity. Data is plotted as mean ± SEM (n=4/group). *p<0.05, **p<0.01 (Student's t test). ns, non-significant; SFU, spot forming unit. Adapted from Kuhn et al. (2019), *Cancer Cell*, 35(3):473-488.

m1928z-CD40L CAR T cells provide long-term protection against antigen-negative tumor cell growth

Having demonstrated myeloid and lymphoid cell activation induced by m1928z-CD40L CAR T cell treatment, we next asked if the activation of these immune effectors establishes functional protection against tumor outgrowth. To separate the anti-CD19 CAR T cell-mediated antitumor response from the non-CAR T cell-mediated antitumor response, we used the $CD19^-$ A20.CD19-KO cell line that escapes any m1928z-CD40L CAR T cell antitumor response (Figure 5.5A). Mice that were initially challenged with $CD19^+$ A20 cells and survived for 99+ days after m1928z-CD40L CAR T cell treatment were re-challenged with the isogenic tumor cell line lacking CD19 expression A20.CD19-KO. CAR antigen-negative ($CD19^-$) cells were used to eliminate the possibility of persisting CAR T cells inducing a direct antitumor response. All mice (5 of 5) resisted $CD19^-$ tumor outgrowth in the A20 lymphoma model (Figure 5.5B), indicating that m1928z-CD40L CAR T cell treatment provides long-term protection against antigen-negative tumor cell growth. The effect was not just limited to the BALB/c A20 tumor model, as the majority (6 of 7) of long-term surviving C57BL/6 mice that were initially injected with $CD19^+$ Eμ-ALL01 leukemia cells and subsequently cured by m1928z-CD40L CAR T cell treatment also resisted tumor challenge with $CD19^-$ Eμ-ALL01.CD19-KO cells (Figure 5.5C).

Taken together, m1928z-CD40L CAR T cells can efficiently enhance priming of lymphoid populations of the host endogenous immune system to recognize and respond to the tumor, thus widening the immune response across several different cell types; and, most importantly, provide the host with a sustained, endogenous immune response that is protective of CAR antigen-negative tumor growth after initial tumor cell clearance.

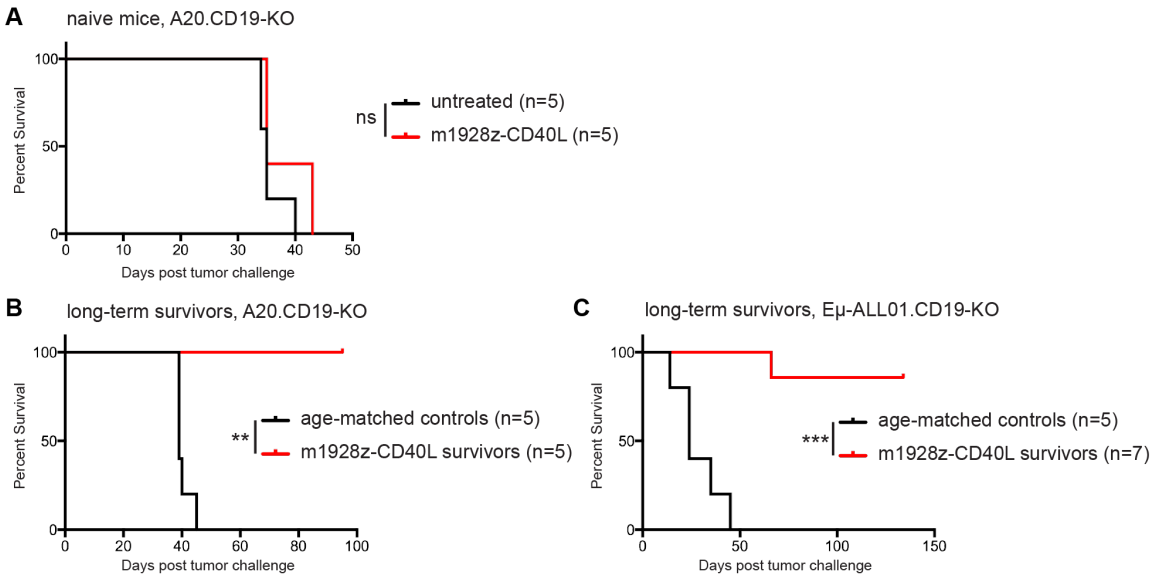

Figure 5.5. m1928z-CD40L CAR T cell treatment provides long-term memory against antigen-negative tumor cell growth

(A) Naïve BALB/c mice were injected i.v. with $5x10^5$ $CD19^-$ A20.CD19-KO lymphoma cells. On day 7, mice were either left untreated or received $3x10^6$ m1928z-CD40L CAR T cells by i.v. injection. Kaplan-Meier survival plots of n = 5 mice/group are shown. ns, non-significant

(B) Surviving BALB/c mice that were initially challenged with A20 lymphoma cells and treated with m1928z-CD40L CAR T cells were injected i.v. with $1x10^5$ $CD19^-$ A20.CD19-KO cells on day 99+. Kaplan-Meier survival plots of n = 5 mice/group are shown. **p < 0.01 by a log rank (Mantel-Cox) test.

(L) Surviving C57BL/6 mice that were initially challenged with Eμ-ALL01 leukemia cells and treated with m1928z-CD40L CAR T cells were injected i.v. with $1x10^6$ $CD19^-$ Eμ-ALL01.CD19-KO leukemia cells on day 140+. Kaplan-Meier survival plots of n = 5–7 mice/group. ***p < 0.001 by a log rank (Mantel-Cox) test. Adapted from Kuhn et al. (2019), *Cancer Cell*, 35(3):473-488.

cDC1 cells prime CD8$^+$ non-CAR T cells, which mediate the protection against antigen-negative tumor growth

Finally, we wanted to identify the cell population in the cured mice that mediates the protection against CAR-antigen-negative tumor outgrowth. The observation that lack of cDC1s in *Batf3*$^{-/-}$ mice impaired m1928z-CD40L CAR T cell treatment (Figure 5.2F) and that m1928z-CD40L CAR T cells can increase the population of CD8$^+$ T cells recognizing tumor cells via their TCR (Figures 5.4E-5.4G), prompted us to more closely ascertain the involvement of the antigen cross-presenting cDC1s in CD8$^+$ T cell priming. Furthermore, we wanted to define the role of endogenous CD3$^+$ T cells in the CAR-antigen-negative tumor cell challenge experiment.

To this end, A20 tumor-bearing wild-type or *Batf3*$^{-/-}$ mice were treated with CD45.1$^+$ CAR T cells and the endogenous CD45.2$^+$ non-CAR CD8$^+$ T cells were assayed for IFNγ release after tumor cell stimulation ex vivo (Figure 5.6A). As expected, IFNγ-ELISpot analysis showed more tumor-reactive CD8$^+$ T cells in wild-type mice treated with m1928z-CD40L CAR T cells (Figures 5.6B and 5.6C). Intriguingly, this increase in endogenous tumor-recognizing CD8$^+$ T cells was lost in *Batf3*$^{-/-}$ mice (Figures 5.6B and 5.6C). Thus, the m1928z-CD40L CAR T cell-mediated priming of endogenous CD8$^+$ T cells is dependent on the presence of cross-presenting cDC1s and implicates cytotoxic CD8$^+$ T cells in potentially being responsible for protecting mice against CAR-antigen-negative tumor cell challenge. When treated with m1928z CAR T cells, the amount of tumor-responsive CD8$^+$ T cells in *Batf3*$^{-/-}$ mice also decreased in comparison to wild-type mice (Figure 5.6C), indicating that second-generation CAR T cell treatment alone can induce CD8$^+$ T cell priming via Batf3-expressing cDC1 cells, albeit to a lesser degree.

To explore the possibility if endogenous CD4$^+$ T cells are necessary for the improved antitumor response of m1928z-CD40L CAR T cell treatment, we took advantage of the finding that CD8$^+$ CAR T cells alone, but not CD4$^+$ CAR T cells, could cure A20 tumor-bearing mice (Figure 3.11D). This allowed isolated

antibody-mediated depletion of $CD4^+$ T cells in the context of $CD8^+$ m1928z-CD40L CAR T cell treatment, to assess the role of non-CAR $CD4^+$ T cells in the antitumor response. $CD4^+$ T cells were depleted with the anti-CD4 antibody clone GK1.5 in A20 tumor-bearing mice before and after $CD8^+$ m1928z-CD40L CAR T cell treatment (Figure 5.7A). $CD4^+$ T cell depletion was confirmed by flow cytometry in the peripheral blood of GK1.5-treated mice with a different anti-CD4 antibody clone (RM4-5) on the day of ACT (day 7) and at a later time point (day 21) to make sure that no $CD4^+$ T cells are present that could potentially aid during the initial antitumor CAR T cell response (Figure 5.7B). Survival of CD4-depleted mice demonstrated that $CD4^+$ T cells are not necessary for the improved antitumor response through m1928z-CD40L CAR T cell treatment (Figure 5.7A).

Focusing on the $CD8^+$ T cell compartment, antibody-mediated depletion of $CD8^+$ T cells before and/or after ACT would also lead to depletion of $CD8^+$ T cells in the CAR T cell product, due to the long half-life of the depletion antibody and its systemic persistence. This would make it impossible to attribute the observed results to either the endogenous $CD8^+$ T cell population or the adoptively transferred CAR T cells. To circumvent this problem, we decided to investigate the contribution of $CD8^+$ T cells to the memory response against CAR-antigen-negative tumor cell challenge (Figure 5.5). Again, long-term surviving mice that were initially cured from A20 tumor challenge by m1928z-CD40L CAR T cells were injected with CAR-antigen-negative A20.CD19-KO cells to exclude any CAR T cell-mediated antitumor response by persisting CAR T cells. Nineteen mice that were tumor free by bioluminescent imaging at day 50+ after initial luciferase-expressing A20 tumor challenge were separated into two cohorts. Ten of 19 mice were $CD8^+$ T cell-depleted by intraperitoneal injection with anti-CD8 antibody clone 2.43 (Figure 5.7C). The remaining 9 mice received the IgG control antibody. Complete $CD8^+$ T cell depletion was confirmed (Figure 5.7D) and growth of luciferase-expressing A20.CD19-KO tumor cells was measured over time (Figure 5.7E). Mice cured from primary A20 tumor challenge that were depleted of $CD8^+$ T cells were not able to control A20.CD19-KO tumor outgrowth,

unlike the IgG control mice (Figure 5.7E). This resulted in a lack of survival due to disease progression (Figure 5.7F). All relapsed mice died from outgrowth of $CD19^-$ tumor cells, indicating that $CD8^+$ T cell depletion did not cause reemergence of residual $CD19^+$ tumor cells from the first tumor challenge (Figure 5.7G). Further, these results imply that the endogenous $CD8^+$ T cell population that gets primed by cross-presenting cDC1s to recognize the tumor cells after m1928z-CD40L CAR T cell treatment is responsible for controlling CAR-antigen-negative tumor cell outgrowth.

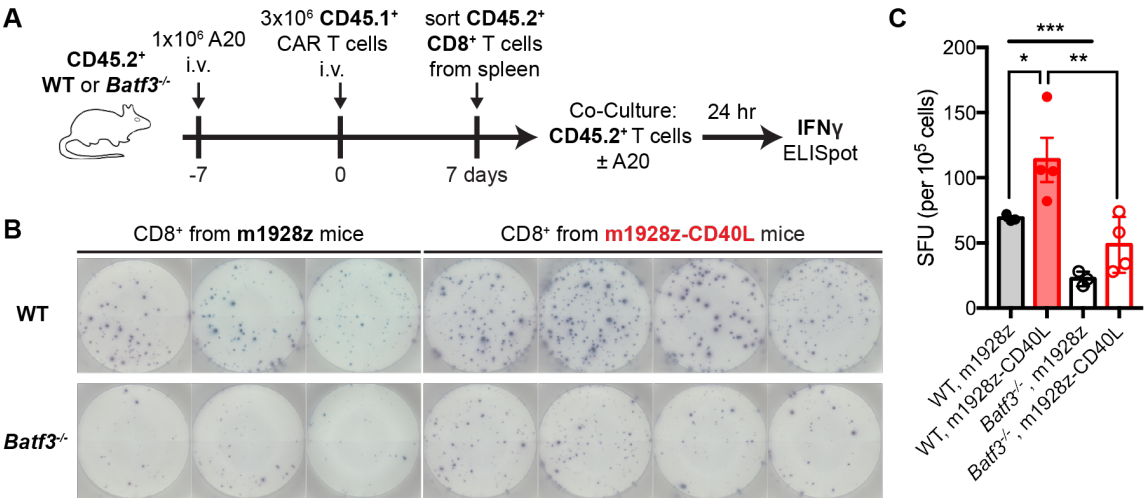

Figure 5.6. *Batf3*-expressing cDC1 cells are necessary for increased priming of CD8$^+$ non-CAR T cells in m1928z-CD40L CAR T cell treated mice

(A) Experimental scheme for (B and C).

(B) Individual IFNγ-capture ELISpot wells of 1x10^5 CD45.2$^+$ CD8$^+$ non-CAR T cells co-cultured with 1x10^5 A20 cells for 24 hr after being sorted from spleens of WT (top) or *Batf3*$^{-/-}$ (bottom) mice that were treated with m1928z or m1928z-CD40L CAR T cells.

(C) Quantification of (B). Each dot is one mouse (n=3-4/group) and data is plotted as mean ± SEM. *p<0.05, **p<0.01, ***p<0.001 (one-tailed Student's t test). SFU, spot forming unit.

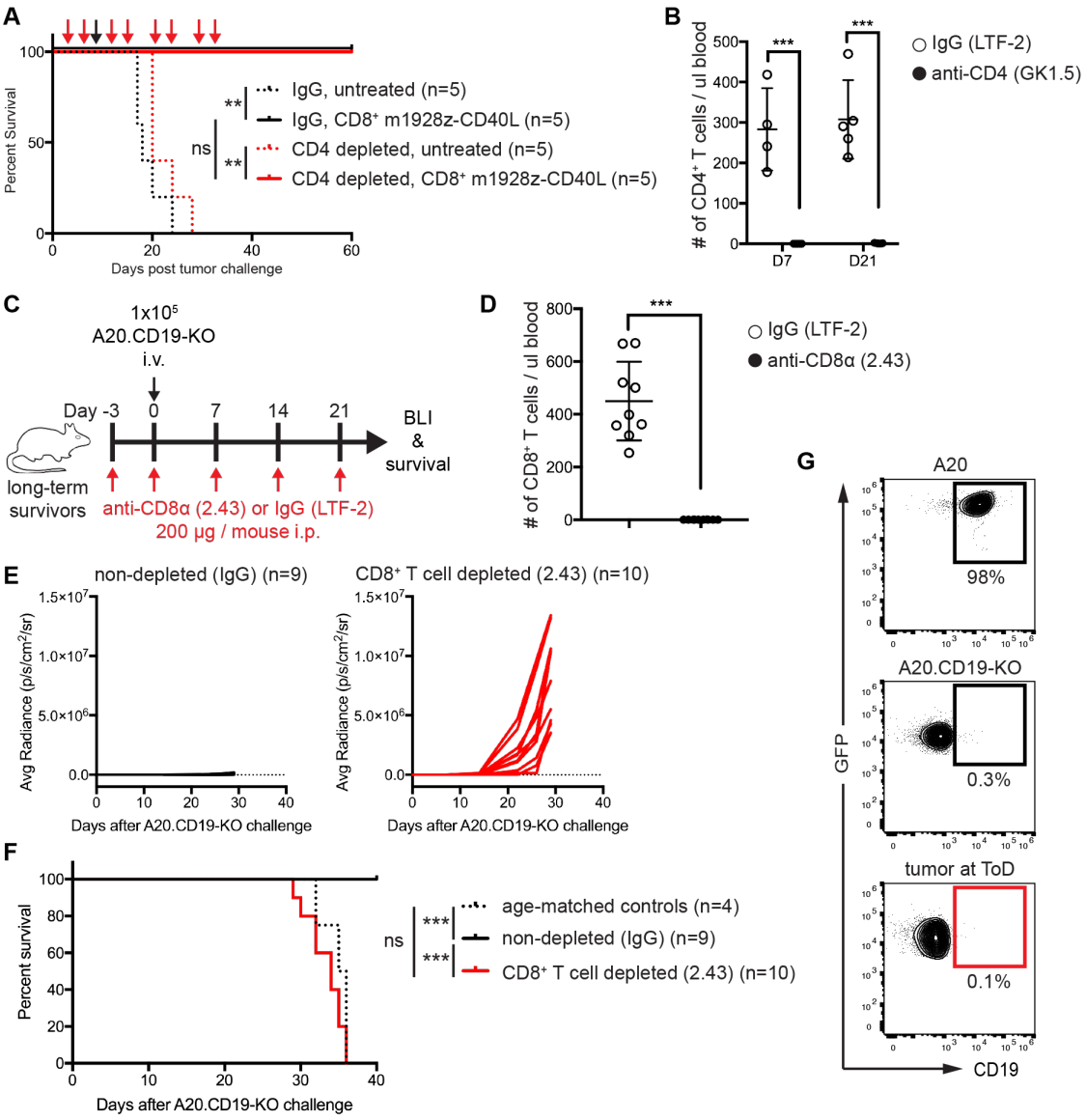

Figure 5.7. CD8$^+$ T cells are necessary for m1928z-CD40L CAR T cell-mediated protection against antigen-negative tumor growth

(A) Survival of naïve BALB/c mice injected with 1x10^6 A20 cells i.v. and either left untreated, or injected with 3x10^6 CD8$^+$ m1928z-CD40L CAR T cells i.v. on day 7 (black arrow). For CD4$^+$ T cell depletion, two cohorts of mice received 200 µg of anti-CD4 depletion antibody (GK1.5) by i.p. injection 2x per week for 4 weeks (red arrows). n=5 mice/group, **p<0.01 by log-rank (Mantel-Cox) test. ns, non-significant.

(B) Peripheral blood of m1928z-CD40L CAR T cell treated mice from (A) was collected retroorbitally and absolute numbers of CD4$^+$ T cells are plotted at time of ACT (D7) and two weeks later (D21). Mice were either treated with the IgG control antibody (LTF-2) or the CD4-depletion antibody (GK1.5). Each dot represents one mouse (n=4-5/group) and data is plotted as mean ± SEM. ***p<0.001 (Student's t-test).

(C) Experimental scheme for (D-F).

(D) Peripheral blood of long-term surviving mice after CD8$^+$ T cell depletion (D15) was collected retroorbitally and absolute numbers of CD8$^+$ T cells are plotted. Mice were either treated with the IgG control antibody (LTF-2) or the CD8-depletion antibody (2.43). Each dot represents one mouse (n=9-10/group) and data is plotted as mean ± SEM. ***p<0.001 (Student's t-test).

(E) Tumor burden of mice injected with luciferase-expressing A20.CD19-KO cells was monitored using bioluminescence imaging. Average radiance per whole animal is plotted for the IgG treated mice (n=9) and the $CD8^+$ T cell depleted mice (n=10).
(F) Survival of mice treated in (C). Naïve age-matched BALB/c mice were used as controls. ***$p<0.001$ by a log-rank (Mantel-Cox) test. ns, non-significant.
(G) Surface CD19 expression on GFP^+ tumor cells at time-of-death (ToD) analyzed by flow cytometry and shown for one representative mouse in the $CD8^+$ T cell depleted cohort. All mice had tumors that were CD19-negative at ToD.

Discussion

This chapter described the recruitment of tumor-specific endogenous $CD8^+$ T cells after m1928z-CD40L CAR T cell treatment. Their mobilization was dependent on the presence of cross-presenting cDC1s and their elimination via anti-CD8 antibody-mediated cell depletion made mice susceptible to CAR-antigen-negative tumor cell outgrowth. These findings highlight the induction of a sustained host antitumor response by m1928z-CD40L CAR T cells.

Increased lymphocyte activation at the tumor site was evidenced by elevated IFNγ and TNFα production in TILs of $CD40L^+$ CAR T cell-treated mice. In addition, in vivo CD40/CD40L interactions did mobilize endogenous T cells to recognize the tumor in ex vivo ELISpot assays. The recruitment of endogenous T cells to aid in the antitumor response is especially valuable in the context of CAR-antigen-negative tumor outgrowth as seen in the clinic and as a consequence of tumor heterogeneity (Dupage et al., 2012; Park et al., 2018). Tumor neoantigens – mutated self proteins – are the source of de novo tumor recognition by T cells via their TCR (van der Bruggen et al., 1991). In immunotherapy, it has been appreciated that an increased mutational burden in the tumor correlates with an improved response to checkpoint blockade mAb therapy and that recognition of tumor-specific mutant proteins by T cells can mediate a protective effect (Gubin et al., 2014; Yadav et al., 2014). Using CAR antigen-negative tumor cell lines, we observed that m1928z-CD40L CAR T cell treatment protected mice from antigen-negative tumor outgrowth in two different tumor models.

This effect was mediated by non-CAR $CD8^+$ T cells present in the host, which were mobilized at early time points after ACT to recognize tumor cells through their TCR. This effect is presumably mediated by the recognition of neoantigens presented on MHC-I by the cancer cells to the cytotoxic $CD8^+$ T cells, as described in mice and human cancer patients (Matsushita et al., 2012; McGranahan et al., 2016). This early $CD8^+$ T cell priming seemed to generate a long-lived memory response that protected mice from CAR-antigen-negative

tumor outgrowth. More careful analysis of neoantigen presentation on A20 tumor cells is required to assess the extent of immunodominant epitope recognition by the $CD8^+$ T cell population. Exome sequencing of tumor cells in combination with in silico prediction of epitope presentation could identify such immunodominant epitopes and potential $CD8^+$ T cell clones recognizing them (Gubin et al., 2014). This would inform the extent of $CD8^+$ T cell tumor recognition and allow differentiation between a dominant clonal response and a possible oligoclonal T cell antitumor response.

Since A20 tumor cells are derived from transformed B cells, they express high levels of MHC-II. Unsurprisingly, $CD4^+$ T cells also responded to A20 cell co-culture with IFNγ release and this effect was elevated when mice had been treated with m1928z-CD40L CAR T cells. However, the $CD4^+$ T cell-specific antitumor response did not seem to be relevant, as prior depletion of $CD4^+$ T cells did not lessen the m1928z-CD40L CAR T cell-mediated antitumor response. $CD4^+$ T cells are important in helping to initiate a cytotoxic $CD8^+$ T cell response through CD40 signaling on APCs via surface CD40L expression (Behrens et al., 2004). Overexpression of CD40L on CAR T cells – both on $CD4^+$ and $CD8^+$ CAR T cells – obviates the need for $CD4^+$ T cell help, similar to earlier studies demonstrating efficient $CD8^+$ T cell priming with agonistic anti-CD40 antibodies independently of $CD4^+$ T cell help (Bennett et al., 1998; Schoenberger et al., 1998). Thus, $CD4^+$ T cells are dispensable in mounting an efficient antitumor response, as long as CD40 signaling on APCs in provided by an alternative source, such as $CD40L^+$ CAR T cells.

Why the cDC1-to-cDC2 ratio increases in tumors of m1928z-CD40L CAR T cell treated mice is unclear and warrants further investigation. The accumulation of cDC1s in the tumor tissue has been attributed to several NK cell-derived cytokines such as CCL5, FLT3L, and XCL1 (Barry et al., 2018; Böttcher et al., 2018). Thus, NK cell activation in m1928z-CD40L CAR T cell treated mice needs to be considered and presents an attractive target for additional analysis.

The priming of $CD8^+$ T cells by cDC1s has been described to happen in the tdLN after $CD103^+$ cDC1s take up the tumor antigen, upregulate CCR7 on their

surface to home to the lymph node, where they then cross-present antigen to LN-resident $CD8^+$ T cells (Roberts et al., 2016). We noticed efficient priming of splenic $CD8^+$ T cells, indicating a more systemic, rather than local, $CD8^+$ T cell activation by m1928z-CD40L CAR T cell treatment. This could potentially be explained by the accumulation of CAR T cells in the spleen, a site of high anti-CD19 CAR-antigen concentration. There, they induce licensing of APCs and provide a permissive environment for T cell priming. Use of a different tumor model, not targeting a ubiquitous antigen such as CD19 on B cells, could help to delineate if CD40L-modifed CAR T cells can prime $CD8^+$ T cells via APC licensing at a local level. However, m1928z-CD40L CAR T cell treatment did specifically lead to an increase in the tumor-resident $CD103^+$ cDC1 population, whereas lymphoid $CD8\alpha^+$ cDC1s were not elevated. This suggests priming of $CD8^+$ T cells in the tumor microenvironment, which is possible and has been described for TILs in a previous study (Thompson et al., 2010). More detailed analysis of tumor-infiltrating versus tdLN-resident $CD8^+$ T cells after m1928z-CD40L CAR T cell treatment could help to delineate the logistics of cDC1-$CD8^+$ T cell interactions. Additionally, it could inform us in which tissue environment the priming happens. This would help to design alternative strategies improving this priming process, which is crucial for mounting a sustained, endogenous antitumor response.

CHAPTER 6

Discussion

Concluding Remarks

In the present study we demonstrate that CAR T cells can be further modified to mobilize endogenous immune cells to aid in the antitumor response. Using an immunecompetent lymphoma mouse model, we observed DC activation by $CD40L^+$ CAR T cells in vivo, priming and recruitment of tumor-recognizing non-CAR T cells, culminating in a more potent antitumor response, and sustained protective immunity provided by $CD8^+$ T cells. All these effects were dependent on the CD40/CD40L interaction between the adoptively transferred CAR T cell and host cells expressing CD40, as demonstrated by the lack of antitumor efficacy in *Cd40*$^{-/-}$ mice. Furthermore, the importance of Batf3-expressing cross-presenting cDC1s in immune cell-mediated antitumor responses has been documented in recent years. Their necessary role in supporting the full antitumor immune response in $CD40L^+$ CAR T cell treatment was also shown here, wherein tumor-bearing *Batf3*$^{-/-}$ mice lacking the cDC1 population did not benefit from $CD40L^+$ CAR T cell injection. Endogenous $CD8^+$ T cells were only primed to recognize tumor cells via their TCR in the presence of cDC1s. This finding also provided a cellular link between $CD40L^+$ CAR T cells and activation of T cells in the host.

From an immunotherapeutic perspective, the goal is to engage as many immune effectors as possible in the antitumor response. The presented results demonstrate the ability of $CD40L^+$ CAR T cells to orchestrate a sustained endogenous antitumor response by mobilizing innate and adaptive members of the immune system. By combining the highly cytotoxic effect of CAR T cells – which has been so valuable in treating cancer malignancies – with the recruitment of non-CAR immune effectors, $CD40L^+$ CAR T cell treatment provides a multipronged immune attack on cancer cells. Future clinical studies will be able to assess if these processes can be translated into humans.

Clinical Implications

New therapeutic strategies are always associated with a certain level of uncertainty, especially in the translational phase of going from animal models to human subjects. The use of transgenic and non-transgenic inbred mice has been extremely valuable in elucidating biological processes in the laboratory setting, due to the highly controllable and reproducible nature of mouse models. However, with 65 million years of separate evolutionary paths, it is well appreciated that humans and mice differ significantly in immunological and other physiological processes (Mestas and Hughes, 2004). In the arena of CAR T cell immunotherapy, this difference is exemplified by the lack of CRS symptoms observed in the early mouse models. About 25% of human subjects suffer from severe CRS, which can even lead to death (Park et al., 2018). This clinical experience has prompted the classification of CRS into different grades depending on its severity and led to the implementation of intervention strategies that safely manage this adverse event (Lee et al., 2014). These toxicities were not anticipated based on the preclinical results, but recent efforts have gone from the bench-to-bedside-to-bench again to model CRS in mice in order to better understand the etiology (Giavridis et al., 2018; Norelli et al., 2018). One study identified CD40L-mediated macrophage activation as a factor exacerbating CRS-causing cytokine release (Giavridis et al., 2018). Again, mouse models can only partially predict immune responses in humans, but we did not detect elevated systemic cytokine levels after $CD40L^+$ CAR T cell treatment, except for IFNγ and TNFα. Differences in the study design, such as mouse strains (immunecompromised versus immunecompetent), CAR T cell dose and application (i.p. versus i.v.), and location of tumor cell growth (peritoneum versus liver), could potentially explain the differences in observations.

Still, a strong therapeutically induced immune response warrants heightened clinical precautions. Starting at low cell doses and close patient monitoring would be imperative when administering $CD40L^+$ CAR T cells to patients. Systemic administration of several different cytokines, such as GM-CSF, IL-2, IL-12, IFNα, IFNγ, and TNFα, in the clinic has been met with dose-limiting toxicities, including

lymphopenias and even fatal tissue damage (Dougan et al., 2018). This emphasizes the small therapeutic window of directly administered cytokines – soluble immune regulators that usually act in an autocrine or paracrine fashion over short distances. The use of cellular drugs, such as $CD40L^+$ CAR T cells, potentially only triggers CD40L-mediated cytokine production at sites of APC interaction. This would lead to local cytokine release and limited systemic elevation of cytokines.

Early studies of ACT in humans have shown that drug-induced lymphodepletion is necessary for successful in vivo expansion of adoptively transferred T cells (Rosenberg and Restifo, 2015). The same is true for ACT experiments in immunecompetent mice, where animals are pretreated with lymphoablative chemotherapeutic drugs or whole body irradiation to ensure successful cell transfer. In our immunecompetent mouse model, $CD40L^+$ CAR T cells did not require prior lymphodepletion. This could have positive clinical implications, as the intensity of preconditioning in $CD19^+$ hematological malignancies has been correlated with the CAR T cell induced severity of CRS symptoms (Hay et al., 2017). Additionally, due to the dependence of effective $CD40L^+$ CAR T cell therapy on endogenous immune cells, maintaining the pool of these cells by limiting or eliminating prior lymphodepletion would be beneficial in generating a curative antitumor response. However, lymphodepletion might still be necessary to guarantee cell persistence and function after CAR T cell administration due to the detection of antibodies against the scFv-portion of the CAR in the serum in a subset of solid tumor patients (Lamers et al., 2011; Maus et al., 2013). These humoral immunogenic reactions of human anti-mouse antibodies (HAMA) against the CAR T cell product were predominantly observed when murine-derived scFvs were used for CAR design. This prompted the generation of humanized scFvs with lower immunogenicity. In patients with B cell malignancies, the combination of preconditioning with B cell-targeted CAR T cells leads to profound B cell aplasia and subsequent absence of immunoglobulins, which probably explains the lack of anti-CAR antibodies. In solid tumor patients, profound B cell aplasia is not induced by the CAR T cells, but lymphodepletion

could potentially lower the probability of host immune reactions against the synthetic CAR fusion protein.

Future Perspectives

The success of CAR T cell therapy in certain hematological malignancies has not translated to solid cancer malignancies as yet. Antitumor T cells have to contend with several immunesuppressive factors in the tumor microenvironment of solid tumors: from T cell inhibitory receptors such as PD-L1 expressed on cancer and stromal cells (Joyce and Fearon, 2015), to vasculature and stromal effects excluding T cell trafficking to tumor sites by CXCL12/CXCR4-mediatedd T cell trapping in the tumor periphery (Feig et al., 2013), presence of immuneinhibitory cells in the tumor microenvironment such as tumor-associated macrophages, Tregs, or MDSCs (Joyce and Fearon, 2015), persistent tumor antigen presence causing chronic T cell stimulation and subsequent T cell dysfunction (Schietinger et al., 2016; Thommen and Schumacher, 2018), to metabolic competition for nutrients and biomass between proliferating tumor and immune cells (Sugiura and Rathmell, 2018). With all these factors at play, analyzing the antitumor effect of $CD40L^+$ CAR T cells in a solid tumor model could help elucidate if CD40/CD40L interactions induced by CAR T cells can relieve some immunesuppressive effects similar to agonistic anti-CD40 mAbs by reprogramming macrophages to infiltrate the tumor and aid in the antitumor response (Beatty et al., 2011). The use of a tumor model not targeting B cells or other lymphoid cells would also facilitate a better understanding of delineating lymphoid versus non-lymphoid effects of $CD40L^+$ CAR T cells. The use of CD19-targeted $CD40L^+$ CAR T cells additionally harbors the caveat of the target cell expressing high levels CD40 (both B cells and some $CD19^+$ tumor cells), making it difficult to assess the contribution of CD40/CD40L interactions between B cells and CAR T cells in the antitumor response.

Finally, the presented data analysis was focused on specific immune cell subsets (DCs, macrophages, T cells) and the expression of specific immune markers. This allowed detailed hypothesis testing based on known CD40/CD40L biology. The overexpression of CD40L in combination with a synthetic CAR

fusion protein in T cells via genetic engineering provides a new situation with potentially unanticipated biological consequences. Utilization of more unbiased analysis methods could provide a more global map of immune cell changes. Mass cytometry has been demonstrated to be especially valuable to ascertain changes in immune cell compositions after immunotherapy as it allows detection of more than 40 different parameters simultaneously (Bandura et al., 2009; Bendall et al., 2011). This enables the construction of immune cell maps that can guide the investigator's focus on important treatment induced immune cell alterations (Spitzer et al., 2017). Once significant changes in a particular cell population are identified, a more granular, high-resolution picture of transcriptional changes and cell identity can be drawn from single cell RNA-sequencing (scRNAseq) data. scRNAseq combines fluid, droplet-based single cell separation with RNAseq technology to identify the heterogeneity of an isolated cell population (Lavin et al., 2017; Tirosh et al., 2016; Zheng et al., 2017). These more unbiased analysis approaches could potentially identify the emergence of new or unanticipated cell populations after $CD40L^+$ CAR T cell treatment. Another benefit of this approach is that both technologies are amenable to the analysis of patient blood and tissue biopsies. Thus, blood and tumor tissue samples from $CD40L^+$ CAR T cell responders and non-responders could be compared to agnostically discover differences in their immune cell phenotype. With the combination of known immunotherapies targeting different cell subsets, altered cell populations in non-responders could be targeted to improve treatment outcome and survival in the overall patient cohort.

BIBLIOGRAPHY

Apperley, J.F., Jones, L., Hale, G., Waldmann, H., Hows, J., Rombos, Y., Tsatalas, C., Marcus, R.E., Goolden, A.W., Gordon-Smith, E.C., et al. (1986). Bone marrow transplantation for patients with chronic myeloid leukaemia: T-cell depletion with Campath-1 reduces the incidence of graft-versus-host disease but may increase the risk of leukaemic relapse. Bone Marrow Transpl.

Avanzi, M.P., Yeku, O., Li, X., Wijewarnasuriya, D.P., van Leeuwen, D.G., Cheung, K., Park, H., Purdon, T.J., Daniyan, A.F., Spitzer, M.H., et al. (2018). Engineered Tumor-Targeted T Cells Mediate Enhanced Anti-Tumor Efficacy Both Directly and through Activation of the Endogenous Immune System. Cell Rep.

Banchereau, J., and Steinman, R.M. (1998). Dendritic cells and the control of immunity. Nature *392*, 245–252.

Bandura, D.R., Baranov, V.I., Ornatsky, O.I., Antonov, A., Kinach, R., Lou, X., Pavlov, S., Vorobiev, S., Dick, J.E., and Tanner, S.D. (2009). Mass cytometry: Technique for real time single cell multitarget immunoassay based on inductively coupled plasma time-of-flight mass spectrometry. Anal. Chem.

Barbier, L., Tay, S.S., McGuffog, C., Triccas, J.A., McCaughan, G.W., Bowen, D.G., and Bertolino, P. (2012). Two lymph nodes draining the mouse liver are the preferential site of DC migration and T cell activation. J. Hepatol.

Barry, K.C., Hsu, J., Broz, M.L., Cueto, F.J., Binnewies, M., Combes, A.J., Nelson, A.E., Loo, K., Kumar, R., Rosenblum, M.D., et al. (2018). A natural killer–dendritic cell axis defines checkpoint therapy–responsive tumor microenvironments. Nat. Med.

Baxendale, A.J., Dawson, C.W., Stewart, S.E., Mudaliar, V., Reynolds, G., Gordon, J., Murray, P.G., Young, L.S., and Eliopoulos, A.G. (2005). Constitutive activation of the CD40 pathway promotes cell transformation and neoplastic growth. Oncogene.

Beatty, G.L., Chiorean, E.G., Fishman, M.P., Saboury, B., Teitelbaum, U.R., Sun, W., Huhn, R.D., Song, W., Li, D., Sharp, L.L., et al. (2011). CD40 agonists alter tumor stroma and show efficacy against pancreatic carcinoma in mice and humans. Science (80-.). *331*, 1612–1616.

Beatty, G.L., Torigian, D.A., Chiorean, E.G., Saboury, B., Brothers, A., Alavi, A., Troxel, A.B., Sun, W., Teitelbaum, U.R., Vonderheide, R.H., et al. (2013). A phase I study of an agonist CD40 monoclonal antibody (CP-870,893) in combination with gemcitabine in patients with advanced pancreatic ductal adenocarcinoma. Clin. Cancer Res. *19*, 6286–6295.

Behrens, G., Li, M., Smith, C.M., Belz, G.T., Mintern, J., Carbone, F.R., and Heath, W.R. (2004). Helper T cells, dendritic cells and CTL Immunity. Immunol. Cell Biol.

Bendall, S.C., Simonds, E.F., Qiu, P., Amir, E.A.D., Krutzik, P.O., Finck, R., Bruggner, R. V., Melamed, R., Trejo, A., Ornatsky, O.I., et al. (2011). Single-cell mass cytometry of differential immune and drug responses across a

human hematopoietic continuum. Science (80-.).
Bennett, S.R.M., Carbone, F.R., Karamalis, F., Flavell, R.A., Miller, J.F.A.P., and Heath, W.R. (1998). Help for cytotoxic-T-cell responses is mediated by CD40 signalling. Nature *393*, 478–480.
Binnewies, M., Mujal, A.M., Pollack, J.L., Combes, A.J., Hardison, E.A., Barry, K.C., Tsui, J., Ruhland, M.K., Kersten, K., Abushawish, M.A., et al. (2019). Unleashing Type-2 Dendritic Cells to Drive Protective Antitumor CD4 + T Cell Immunity. Cell *177*, 556-571.e16.
Bonifant, C.L., Jackson, H.J., Brentjens, R.J., and Curran, K.J. (2016). Toxicity and management in CAR T-cell therapy. Mol. Ther. - Oncolytics *3*.
Böttcher, J.P., Bonavita, E., Chakravarty, P., Blees, H., Cabeza-Cabrerizo, M., Sammicheli, S., Rogers, N.C., Sahai, E., Zelenay, S., and Reis e Sousa, C. (2018). NK Cells Stimulate Recruitment of cDC1 into the Tumor Microenvironment Promoting Cancer Immune Control. Cell.
Bourgeois, C., Rocha, B., and Tanchot, C. (2002). A role for CD40 expression on CD8+ T cells in the generation of CD8+ T cell memory. Science *297*, 2060–2063.
Brentjens, R.J., Latouche, J.B., Santos, E., Marti, F., Gong, M.C., Lyddane, C., King, P.D., Larson, S., Weiss, M., Rivière, I., et al. (2003). Eradication of systemic B-cell tumors by genetically targeted human T lymphocytes co-stimulated by CD80 and interleukin-15. Nat. Med. *9*, 279–286.
Brentjens, R.J., Santos, E., Nikhamin, Y., Yeh, R., Matsushita, M., La Perle, K., Quintás-Cardama, A., Larson, S.M., and Sadelain, M. (2007). Genetically targeted T cells eradicate systemic acute lymphoblastic leukemia xenografts. Clin. Cancer Res.
Brentjens, R.J., Rivière, I., Park, J.H., Davila, M.L., Wang, X., Stefanski, J., Taylor, C., Yeh, R., Bartido, S., Borquez-Ojeda, O., et al. (2011). Safety and persistence of adoptively transferred autologous CD19-targeted T cells in patients with relapsed or chemotherapy refractory B-cell leukemias. Blood.
Brentjens, R.J., Davila, M.L., Riviere, I., Park, J., Wang, X., Cowell, L.G., Bartido, S., Stefanski, J., Taylor, C., Olszewska, M., et al. (2013). CD19-targeted T cells rapidly induce molecular remissions in adults with chemotherapy-refractory acute lymphoblastic leukemia. Sci. Transl. Med. *5*.
Brocker, T., and Karjalainen, K. (1995). Signals through T cell receptor-zeta chain alone are insufficient to prime resting T lymphocytes. J. Exp. Med.
Brocker, T., Peter, A., Traunecker, A., and Karjalainen, K. (1993). New simplified molecular design for functional T cell receptor. Eur. J. Immunol.
Brown, M.P., Topham, D.J., Sangster, M.Y., Zhao, J., Flynn, K.J., Surman, S.L., Woodland, D.L., Doherty, P.C., Farr, A.G., Pattengale, P.K., et al. (1998). Thymic lymphoproliferative disease after successful correction of CD40 ligand deficiency by gene transfer in mice. Nat. Med. *4*, 1253–1260.
Broz, M.L., Binnewies, M., Boldajipour, B., Nelson, A.E., Pollack, J.L., Erle, D.J., Barczak, A., Rosenblum, M.D., Daud, A., Barber, D.L., et al. (2014). Dissecting the Tumor Myeloid Compartment Reveals Rare Activating Antigen-Presenting Cells Critical for T Cell Immunity. Cancer Cell.
Brudno, J.N., and Kochenderfer, J.N. (2016). Toxicities of chimeric antigen

receptor T cells: Recognition and management. Blood.
van der Bruggen, P., Traversari, C., Chomez, P., Lurquin, C., De Plaen, E., Van den Eynde, B., Knuth, A., and Boon, T. (1991). A gene encoding an antigen recognized by cytolytic T lymphocytes on a human melanoma. Science (80-.). *254*, 1643–1647.
Bunnell, B.A., Muul, L.M., Donahue, R.E., Blaese, R.M., and Morgan, R.A. (1995). High-efficiency retroviral-mediated gene transfer into human and nonhuman primate peripheral blood lymphocytes. Proc. Natl. Acad. Sci.
Byrne, K.T., and Vonderheide, R.H. (2016). CD40 Stimulation Obviates Innate Sensors and Drives T Cell Immunity in Cancer. Cell Rep. *15*, 2719–2732.
Byrne, K.T., Leisenring, N.H., Bajor, D.L., and Vonderheide, R.H. (2016). CSF-1R–Dependent Lethal Hepatotoxicity When Agonistic CD40 Antibody Is Given before but Not after Chemotherapy. J. Immunol.
Cameron, B.J., Gerry, A.B., Dukes, J., Harper, J. V., Kannan, V., Bianchi, F.C., Grand, F., Brewer, J.E., Gupta, M., Plesa, G., et al. (2013). Identification of a titin-derived HLA-A1-presented peptide as a cross-reactive target for engineered MAGE A3-directed T cells. Sci. Transl. Med.
Carswell, E.A., Old, L.J., Kassel, R.L., Green, S., Fiore, N., and Williamson, B. (1975). An endotoxin-induced serum factor that causes necrosis of tumors. Proc. Natl. Acad. Sci. U. S. A.
Casamayor-Palleja, M., Khan, M., and MacLennan, I.C. (1995). A subset of CD4+ memory T cells contains preformed CD40 ligand that is rapidly but transiently expressed on their surface after activation through the T cell receptor complex. J. Exp. Med. *181*, 1293–1301.
Castle, B.E., Kishimoto, K., Stearns, C., Brown, M.L., and Kehry, M.R. (1993). Regulation of expression of the ligand for CD40 on T helper lymphocytes. J. Immunol. *151*, 1777–1788.
Caux, C., Massacrier, C., Vanbervliet, B., Dubois, B., Van Kooten, C., Durand, I., and Banchereau, J. (1994). Activation of human dendritic cells through CD40 cross-linking. J. Exp. Med. *180*, 1263–1272.
Cella, M., Scheidegger, D., Palmer-Lehmann, K., Lane, P., Lanzavecchia, A., and Alber, G. (1996). Brief Definitive Report Ligation of CD40 on Dendritic Cells Triggers Production of High Levels of Interleukin-12 and Enhances T Cell Stimulatory Capacity: T-T Help via APC Activation. J Exp Med. *184*, 747–752.
Cheadle, E.J., Hawkins, R.E., Batha, H., O'Neill, A.L., Dovedi, S.J., and Gilham, D.E. (2010). Natural Expression of the CD19 Antigen Impacts the Long-Term Engraftment but Not Antitumor Activity of CD19-Specific Engineered T Cells. J. Immunol. *184*, 1885–1896.
Chen, L., and Flies, D.B. (2013). Molecular mechanisms of T cell co-stimulation and co-inhibition. Nat. Rev. Immunol.
Cherkassky, L., Morello, A., Villena-Vargas, J., Feng, Y., Dimitrov, D.S., Jones, D.R., Sadelain, M., and Adusumilli, P.S. (2016). Human CAR T cells with cell-intrinsic PD-1 checkpoint blockade resist tumor-mediated inhibition. J. Clin. Invest.
Chmielewski, M., Kopecky, C., Hombach, A., and Abken, H. (2011). IL-12 release by engineered T cells expressing chimeric antigen receptors can

effectively Muster an antigen-independent macrophage response on tumor cells that have shut down tumor antigen expression. Cancer Res. *71*, 5697–5706.

Choi, M.S.K., Boise, L.H., Gottschalk, A.R., Quintans, J., Thompson, C.B., and Klaus, G.G.B. (1995). The role of bcl-xL in CD40-mediated rescue from anti-μ-induced apoptosis in WEHI-231 B lymphoma cells. Eur. J. Immunol.

Coley, W.B. (1891). II. Contribution to the Knowledge of Sarcoma. Ann. Surg.

Coley, W.B. (1893). The treatment of malignant tumors by repeated inoculations of erysipelas. Am. J. Med. Sci.

Collins, R.H., Shpilberg, O., Drobyski, W.R., Porter, D.L., Giralt, S., Champlin, R., Goodman, S.A., Wolff, S.N., Hu, W., Verfaillie, C., et al. (1997). Donor leukocyte infusions in 140 patients with relapsed malignancy after allogeneic bone marrow transplantation. J. Clin. Oncol.

Curran, K.J., Seinstra, B.A., Nikhamin, Y., Yeh, R., Usachenko, Y., Van Leeuwen, D.G., Purdon, T., Pegram, H.J., and Brentjens, R.J. (2015). Enhancing antitumor efficacy of chimeric antigen receptor T cells through constitutive CD40L expression. Mol. Ther. *23*, 769–778.

Daud, A.I., DeConti, R.C., Andrews, S., Urbas, P., Riker, A.I., Sondak, V.K., Munster, P.N., Sullivan, D.M., Ugen, K.E., Messina, J.L., et al. (2008). Phase I trial of interleukin-12 plasmid electroporation in patients with metastatic melanoma. J. Clin. Oncol.

Davila, M.L., Kloss, C.C., Gunset, G., and Sadelain, M. (2013). CD19 CAR-Targeted T Cells Induce Long-Term Remission and B Cell Aplasia in an Immunocompetent Mouse Model of B Cell Acute Lymphoblastic Leukemia. PLoS One *8*.

Davila, M.L., Riviere, I., Wang, X., Bartido, S., Park, J., Curran, K., Chung, S.S., Stefanski, J., Borquez-Ojeda, O., Olszewska, M., et al. (2014). Efficacy and toxicity management of 19-28z CAR T cell therapy in B cell acute lymphoblastic leukemia. Sci. Transl. Med. *6*.

Dicker, F., Kater, A.P., Fukuda, T., and Kipps, T.J. (2005). Fas-ligand (CD178) and TRAIL synergistically induce apoptosis of CD40-activated chronic lymphocytic leukemia B cells. Blood *105*, 3193–3198.

Dimopoulos, M., Spencer, A., Attal, M., Prince, H.M., Harousseau, J.-L., Dmoszynska, A., Miguel, J.S., Hellmann, A., Facon, T., Foà, R., et al. (2007). Lenalidomide plus dexamethasone for relapsed or refractory multiple myeloma. N Engl J Med.

Dougan, M., Dranoff, G., and Dougan, S.K. (2018). Cancer Immunotherapy: Beyond Checkpoint Blockade. Annu. Rev. Cancer Biol.

Dupage, M., Mazumdar, C., Schmidt, L.M., Cheung, A.F., and Jacks, T. (2012). Expression of tumour-specific antigens underlies cancer immunoediting. Nature *482*, 405–409.

Eberlein, T.J., Rosenstein, M., and Rosenberg, S.A. (1982). Regression of a disseminated syngeneic solid tumor by systemic transfer of lymphoid cells expanded in interleukin 2. J. Exp. Med.

Elgueta, R., Benson, M.J., De Vries, V.C., Wasiuk, A., Guo, Y., and Noelle, R.J. (2009). Molecular mechanism and function of CD40/CD40L engagement in the

immune system. Immunol. Rev. *229*, 152–172.
Engel, P., Zhou, L.J., Ord, D.C., Sato, S., Koller, B., and Tedder, T.F. (1995). Abnormal B lymphocyte delevopment, activation, and differentiation in mice that lack or overexpress the CD19 signal transduction molecule. Immunity.
Engelhardt, J.J., Boldajipour, B., Beemiller, P., Pandurangi, P., Sorensen, C., Werb, Z., Egeblad, M., and Krummel, M.F. (2012). Marginating Dendritic Cells of the Tumor Microenvironment Cross-Present Tumor Antigens and Stably Engage Tumor-Specific T Cells. Cancer Cell.
Eshhar, Z., Waks, T., Gross, G., and Schindler, D.G. (1993). Specific activation and targeting of cytotoxic lymphocytes through chimeric single chains consisting of antibody-binding domains and the gamma or zeta subunits of the immunoglobulin and T-cell receptors. Proc. Natl. Acad. Sci. *90*, 720–724.
Eyquem, J., Mansilla-Soto, J., Giavridis, T., Van Der Stegen, S.J.C., Hamieh, M., Cunanan, K.M., Odak, A., Gönen, M., and Sadelain, M. (2017). Targeting a CAR to the TRAC locus with CRISPR/Cas9 enhances tumour rejection. Nature *543*, 113–117.
Fedorov, V.D., Themeli, M., and Sadelain, M. (2013). PD-1- and CTLA-4-based inhibitory chimeric antigen receptors (iCARs) divert off-target immunotherapy responses. Sci. Transl. Med.
Feig, C., Jones, J.O., Kraman, M., Wells, R.J.B., Deonarine, A., Chan, D.S., Connell, C.M., Roberts, E.W., Zhao, Q., Caballero, O.L., et al. (2013). Targeting CXCL12 from FAP-expressing carcinoma-associated fibroblasts synergizes with anti-PD-L1 immunotherapy in pancreatic cancer. Proc. Natl. Acad. Sci.
Feucht, J., Sun, J., Eyquem, J., Ho, Y.J., Zhao, Z., Leibold, J., Dobrin, A., Cabriolu, A., Hamieh, M., and Sadelain, M. (2019). Calibration of CAR activation potential directs alternative T cell fates and therapeutic potency. Nat. Med.
Finney, H.M., Lawson, A.D., Bebbington, C.R., and Weir, A.N. (1998). Chimeric receptors providing both primary and costimulatory signaling in T cells from a single gene product. J. Immunol.
Fry, T.J., Shah, N.N., Orentas, R.J., Stetler-Stevenson, M., Yuan, C.M., Ramakrishna, S., Wolters, P., Martin, S., Delbrook, C., Yates, B., et al. (2018). CD22-targeted CAR T cells induce remission in B-ALL that is naive or resistant to CD19-targeted CAR immunotherapy. Nat. Med.
Funakoshi, S., Longo, D.L., Beckwith, M., Conley, D.K., Tsarfaty, G., Tsarfaty, I., Armitage, R.J., Fanslow, W.C., Spriggs, M.K., and Murphy, W.J. (1994). Inhibition of human B-cell lymphoma growth by CD40 stimulation. Blood.
Gabrilovich, D. (2004). Mechanisms and functional significance of tumour-induced dendritic-cell defects. Nat. Rev. Immunol.
Gallardo, H.F., Tan, C., Ory, D., and Sadelain, M. (1997). Recombinant retroviruses pseudotyped with the vesicular stomatitis virus G glycoprotein mediate both stable gene transfer and pseudotransduction in human peripheral blood lymphocytes. Blood.
Galluzzi, L., Vacchelli, E., Bravo-San Pedro, J.-M., Buqué, A., Senovilla, L., Baracco, E.E., Bloy, N., Castoldi, F., Abastado, J.-P., Agostinis, P., et al.

(2014). Classification of current anticancer immunotherapies. Oncotarget.
Galluzzi, L., Chan, T.A., Kroemer, G., Wolchok, J.D., and López-Soto, A. (2018). The hallmarks of successful anticancer immunotherapy. Sci. Transl. Med.
Gao, Y., Nish, S.A., Jiang, R., Hou, L., Licona-Limón, P., Weinstein, J.S., Zhao, H., and Medzhitov, R. (2013). Control of T helper 2 responses by transcription factor IRF4-dependent dendritic cells. Immunity.
Garris, C.S., Arlauckas, S.P., Kohler, R.H., Trefny, M.P., Garren, S., Piot, C., Engblom, C., Pfirschke, C., Siwicki, M., Gungabeesoon, J., et al. (2018). Successful Anti-PD-1 Cancer Immunotherapy Requires T Cell-Dendritic Cell Crosstalk Involving the Cytokines IFN-γ and IL-12. Immunity.
Garrone, P., Neidhardt, E.M., Garcia, E., Galibert, L., van Kooten, C., and Banchereau, J. (1995). Fas ligation induces apoptosis of CD40-activated human B lymphocytes. J. Exp. Med. *182*, 1265–1273.
Giavridis, T., Van Der Stegen, S.J.C., Eyquem, J., Hamieh, M., Piersigilli, A., and Sadelain, M. (2018). CAR T cell-induced cytokine release syndrome is mediated by macrophages and abated by IL-1 blockade letter. Nat. Med.
Gong, M.C., Latouche, J.-B., Krause, A., Heston, W.D.W., Bander, N.H., and Sadelain, M. (1999). Cancer Patient T Cells Genetically Targeted to Prostate-Specific Membrane Antigen Specifically Lyse Prostate Cancer Cells and Release Cytokines in Response to Prostate-Specific Membrane Antigen. Neoplasia.
Gresser, I., Bourali, C., Levy, J.P., Fontaine-Brouty-Boye, D., and Thomas, M.T. (1969). Increased survival in mice inoculated with tumor cells and treated with interferon preparations. Proc. Natl. Acad. Sci. *63*, 51–57.
Griffith, J.W., Sokol, C.L., and Luster, A.D. (2014). Chemokines and Chemokine Receptors: Positioning Cells for Host Defense and Immunity. Annu. Rev. Immunol.
Gross, G., Waks, T., and Eshhar, Z. (1989). Expression of immunoglobulin-T-cell receptor chimeric molecules as functional receptors with antibody-type specificity. Proc. Natl. Acad. Sci. *86*, 10024–10028.
Grupp, S.A., Kalos, M., Barrett, D., Aplenc, R., Porter, D.L., Rheingold, S.R., Teachey, D.T., Chew, A., Hauck, B., Wright, J.F., et al. (2013). Chimeric Antigen Receptor–Modified T Cells for Acute Lymphoid Leukemia. N. Engl. J. Med.
Gubin, M.M., Zhang, X., Schuster, H., Caron, E., Ward, J.P., Noguchi, T., Ivanova, Y., Hundal, J., Arthur, C.D., Krebber, W.J., et al. (2014). Checkpoint blockade cancer immunotherapy targets tumour-specific mutant antigens. Nature *515*, 577–581.
Guedan, S., Posey, A.D., Shaw, C., Wing, A., Da, T., Patel, P.R., McGettigan, S.E., Casado-Medrano, V., Kawalekar, O.U., Uribe-Herranz, M., et al. (2018). Enhancing CAR T cell persistence through ICOS and 4-1BB costimulation. JCI Insight *3*.
Gust, J., Hay, K.A., Hanafi, L.A., Li, D., Myerson, D., Gonzalez-Cuyar, L.F., Yeung, C., Liles, W.C., Wurfel, M., Lopez, J.A., et al. (2017). Endothelial activation and blood–brain barrier disruption in neurotoxicity after adoptive immunotherapy with CD19 CAR-T cells. Cancer Discov.

Hacein-Bey-Abina, S., Von Kalle, C., Schmidt, M., McCormack, M.P., Wulffraat, N., Leboulch, P., Lim, A., Osborne, C.S., Pawliuk, R., Morillon, E., et al. (2003). LMO2-Associated Clonal T Cell Proliferation in Two Patients after Gene Therapy for SCID-X1. Science (80-.).

Hanahan, D., and Weinberg, R.A. (2011). Hallmarks of cancer: the next generation. Cell.

Hay, K.A., Hanafi, L.A., Li, D., Gust, J., Liles, W.C., Wurfel, M.M., López, J.A., Chen, J., Chung, D., Harju-Baker, S., et al. (2017). Kinetics and biomarkers of severe cytokine release syndrome after CD19 chimeric antigen receptor–modified T-cell therapy. Blood.

Helft, J., Böttcher, J., Chakravarty, P., Zelenay, S., Huotari, J., Schraml, B.U., Goubau, D., and Reis e Sousa, C. (2015). GM-CSF Mouse Bone Marrow Cultures Comprise a Heterogeneous Population of CD11c+MHCII+ Macrophages and Dendritic Cells. Immunity *42*, 1197–1211.

Hess, S., and Engelmann, H. (1996). A novel function of CD40: Induction of cell death in transformed cells. J. Exp. Med.

Heufler, C., Koch, F., Stanzl, U., Topar, G., Wysocka, M., Trinchieri, G., Enk, A., Steinman, R.M., Romani, N., and Schuler, G. (1996). Interleukin-12 is produced by dendritic cells and mediates T helper 1 development as well as interferon-gamma production by T helper 1 cells. Eur J Immunol *26*, 659–668.

Hildner, K., Edelson, B.T., Purtha, W.E., Diamond, M., Matsushita, H., Kohyama, M., Calderon, B., Schraml, B.U., Unanue, E.R., Diamond, M.S., et al. (2008). Batf3 deficiency reveals a critical role for CD8α + dendritic cells in cytotoxic T cell immunity. Science (80-.).

Hirano, a, Longo, D.L., Taub, D.D., Ferris, D.K., Young, L.S., Eliopoulos, a G., Agathanggelou, A., Cullen, N., Macartney, J., Fanslow, W.C., et al. (1999). Inhibition of human breast carcinoma growth by a soluble recombinant human CD40 ligand. Blood *93*, 2999–3007.

Hoffman, E.S., Smith, R.E.T., and Renaud, R.C. (2005). From the analyst's couch: TLR-targeted therapeutics. Nat. Rev. Drug Discov.

Hollmann, C.A., Owens, T., Nalbantoglu, J., Hudson, T.J., and Sladek, R. (2006). Constitutive activation of extracellular signal-regulated kinase predisposes diffuse large B-cell lymphoma cell lines to CD40-mediated cell death. Cancer Res.

Hombach, A., Wieczarkowiecz, A., Marquardt, T., Heuser, C., Usai, L., Pohl, C., Seliger, B., and Abken, H. (2001). Tumor-specific T cell activation by recombinant immunoreceptors: CD3 zeta signaling and CD28 costimulation are simultaneously required for efficient IL-2 secretion and can be integrated into one combined CD28/CD3 zeta signaling receptor molecule. J. Immunol. *167*, 6123–6131.

Hoyos, V., Savoldo, B., Quintarelli, C., Mahendravada, A., Zhang, M., Vera, J., Heslop, H.E., Rooney, C.M., Brenner, M.K., and Dotti, G. (2010). Engineering CD19-specific T lymphocytes with interleukin-15 and a suicide gene to enhance their anti-lymphoma/leukemia effects and safety. Leukemia.

Hu, B., Ren, J., Luo, Y., Keith, B., Young, R.M., Scholler, J., Zhao, Y., and June, C.H. (2017). Augmentation of Antitumor Immunity by Human and Mouse CAR

T Cells Secreting IL-18. Cell Rep. *20*, 3025–3033.
Hurton, L. V., Singh, H., Najjar, A.M., Switzer, K.C., Mi, T., Maiti, S., Olivares, S., Rabinovich, B., Huls, H., Forget, M.-A., et al. (2016). Tethered IL-15 augments antitumor activity and promotes a stem-cell memory subset in tumor-specific T cells. Proc. Natl. Acad. Sci.
Imai, C., Mihara, K., Andreansky, M., Nicholson, I.C., Pui, C.H., Geiger, T.L., and Campana, D. (2004). Chimeric receptors with 4-1BB signaling capacity provoke potent cytotoxicity against acute lymphoblastic leukemia. Leukemia.
Irving, B.A., and Weiss, A. (1991). The cytoplasmic domain of the T cell receptor ζ chain is sufficient to couple to receptor-associated signal transduction pathways. Cell.
Jaiswal, a I., Dubey, C., Swain, S.L., and Croft, M. (1996). Regulation of CD40 ligand expression on naive CD4 T cells: a role for TCR but not co-stimulatory signals. Int. Immunol. *8*, 275–285.
Jongbloed, S.L., Kassianos, A.J., McDonald, K.J., Clark, G.J., Ju, X., Angel, C.E., Chen, C.-J.J., Dunbar, P.R., Wadley, R.B., Jeet, V., et al. (2010). Human CD141 + (BDCA-3) + dendritic cells (DCs) represent a unique myeloid DC subset that cross-presents necrotic cell antigens . J. Exp. Med.
Joyce, J.A., and Fearon, D.T. (2015). T cell exclusion, immune privilege, and the tumor microenvironment. Science (80-.).
June, C.H., and Sadelain, M. (2018). Chimeric Antigen Receptor Therapy. N. Engl. J. Med.
June, C.H., Ledbetter, J.A., Gillespie, M.M., Lindsten, T., and Thompson, C.B. (1987). T-cell proliferation involving the CD28 pathway is associated with cyclosporine-resistant interleukin 2 gene expression. Mol. Cell. Biol.
Kagoya, Y., Tanaka, S., Guo, T., Anczurowski, M., Wang, C.H., Saso, K., Butler, M.O., Minden, M.D., and Hirano, N. (2018). A novel chimeric antigen receptor containing a JAK-STAT signaling domain mediates superior antitumor effects. Nat. Med. *24*, 352–359.
Kalos, M., Levine, B.L., Porter, D.L., Katz, S., Grupp, S.A., Bagg, A., and June, C.H. (2011). T cells with chimeric antigen receptors have potent antitumor effects and can establish memory in patients with advanced leukemia. Sci. Transl. Med. *3*.
Kantoff, P.W., Higano, C.S., Shore, N.D., Berger, E.R., Small, E.J., Penson, D.F., Redfern, C.H., Ferrari, A.C., Dreicer, R., Sims, R.B., et al. (2010). Sipuleucel-T Immunotherapy for Castration-Resistant Prostate Cancer. N. Engl. J. Med.
Kastenmüller, W., Brandes, M., Wang, Z., Herz, J., Egen, J.G., and Germain, R.N. (2013). Peripheral Prepositioning and Local CXCL9 Chemokine-Mediated Guidance Orchestrate Rapid Memory CD8 + T Cell Responses in the Lymph Node. Immunity.
Kebriaei, P., Singh, H., Huls, M.H., Figliola, M.J., Bassett, R., Olivares, S., Jena, B., Dawson, M.J., Kumaresan, P.R., Su, S., et al. (2016). Phase i trials using sleeping beauty to generate CD19-specific CAR T cells. J. Clin. Invest.
Kerkar, S.P., Goldszmid, R.S., Muranski, P., Chinnasamy, D., Yu, Z., Reger, R.N., Leonardi, A.J., Morgan, R.A., Wang, E., Marincola, F.M., et al. (2011). IL-12 triggers a programmatic change in dysfunctional myeloid-derived cells

within mouse tumors. J. Clin. Invest. *121*, 4746–4757.
Kim, K.J., Kanellopoulos-langevin, C., Merwin, R.M., Sachs, D.H., and Asofsky, R. (1979). Establishment and Characterization of BALB / c Lymphoma Lines with B Cell Properties. J. Immunol. *122*, 549–554.
Klebanoff, C.A., Rosenberg, S.A., and Restifo, N.P. (2016). Prospects for gene-engineered T cell immunotherapy for solid cancers. Nat. Med. *22*, 26–36.
Klinger, M., Brandl, C., Zugmaier, G., Hijazi, Y., Bargou, R.C., Topp, M.S., Gökbuget, N., Neumann, S., Goebeler, M., Viardot, A., et al. (2012). Immunopharmacologic response of patients with B-lineage acute lymphoblastic leukemia to continuous infusion of T cell-engaging CD19/CD3-bispecific BiTE antibody blinatumomab. Blood.
Kloss, C.C., Condomines, M., Cartellieri, M., Bachmann, M., and Sadelain, M. (2013). Combinatorial antigen recognition with balanced signaling promotes selective tumor eradication by engineered T cells. Nat. Biotechnol.
Kloss, C.C., Lee, J., Zhang, A., Chen, F., Melenhorst, J.J., Lacey, S.F., Maus, M. V., Fraietta, J.A., Zhao, Y., and June, C.H. (2018). Dominant-Negative TGF-β Receptor Enhances PSMA-Targeted Human CAR T Cell Proliferation And Augments Prostate Cancer Eradication. Mol. Ther.
Knochelmann, H.M., Smith, A.S., Dwyer, C.J., Wyatt, M.M., Mehrotra, S., and Paulos, C.M. (2018). CAR T Cells in Solid Tumors: Blueprints for Building Effective Therapies. Front. Immunol.
Knorr, D.A., Dahan, R., and Ravetch, J. V. (2018). Toxicity of an Fc-engineered anti-CD40 antibody is abrogated by intratumoral injection and results in durable antitumor immunity. Proc. Natl. Acad. Sci.
Koch, F., Stanzl, U., Jennewein, P., Janke, K., Heufler, C., Kämpgen, E., Romani, N., and Schuler, G. (1996). High level IL-12 production by murine dendritic cells: upregulation via MHC class II and CD40 molecules and downregulation by IL-4 and IL-10. J. Exp. Med.
Kochenderfer, J.N., Wilson, W.H., Janik, J.E., Dudley, M.E., Stetler-Stevenson, M., Feldman, S.A., Maric, I., Raffeld, M., Nathan, D.A.N., Lanier, B.J., et al. (2010). Eradication of B-lineage cells and regression of lymphoma in a patient treated with autologous T cells genetically engineered to recognize CD19. Blood *116*, 4099–4102.
Kolb, H.J., Schattenberg, A., Goldman, J.M., Hertenstein, B., Jacobsen, N., Arcese, W., Ljungman, P., Ferrant, A., Verdonck, L., Niederwieser, D., et al. (1995). Graft-versus-leukemia effect of donor lymphocyte transfusions in marrow grafted patients. Blood.
Koneru, M., O'Cearbhaill, R., Pendharkar, S., Spriggs, D.R., and Brentjens, R.J. (2015). A phase I clinical trial of adoptive T cell therapy using IL-12 secreting MUC-16ecto directed chimeric antigen receptors for recurrent ovarian cancer. J. Transl. Med.
Van Kooten, G., and Banchereau, J. (2000). CD40-CD40 ligand. J. Leukoc. Biol.
Kowolik, C.M., Topp, M.S., Gonzalez, S., Pfeiffer, T., Olivares, S., Gonzalez, N., Smith, D.D., Forman, S.J., Jensen, M.C., and Cooper, L.J.N. (2006). CD28 costimulation provided through a CD19-specific chimeric antigen receptor enhances in vivo persistence and antitumor efficacy of adoptively transferred T

cells. Cancer Res.
Krall, W.J., Skelton, D.C., Yu, X.J., Riviere, I., Lehn, P., Mulligan, R.C., and Kohn, D.B. (1996). Increased levels of spliced rna account for augmented expression from the mfg retroviral vector in hematopoietic cells. Gene Ther.
Krause, A., Guo, H.-F., Latouche, J.-B., Tan, C., Cheung, N.-K. V., and Sadelain, M. (1998). Antigen-dependent CD28 Signaling Selectively Enhances Survival and Proliferation in Genetically Modified Activated Human Primary T Lymphocytes. J. Exp. Med.
Krishnaswamy, J.K., Gowthaman, U., Zhang, B., Mattsson, J., Szeponik, L., Liu, D., Wu, R., White, T., Calabro, S., Xu, L., et al. (2017). Migratory CD11b + conventional dendritic cells induce T follicular helper cell–dependent antibody responses. Sci. Immunol.
Kuhn, N.F., Purdon, T.J., van Leeuwen, D.G., Lopez, A. V., Curran, K.J., Daniyan, A.F., and Brentjens, R.J. (2019). CD40 Ligand-Modified Chimeric Antigen Receptor T Cells Enhance Antitumor Function by Eliciting an Endogenous Antitumor Response. Cancer Cell.
Kuwana, Y., Asakura, Y., Utsunomiya, N., Nakanishi, M., Arata, Y., Itoh, S., Nagase, F., and Kurosawa, Y. (1987). Expression of chimeric receptor composed of immunoglobulin-derived V resions and T-cell receptor-derived C regions. Biochem. Biophys. Res. Commun. *149*, 960–968.
Lamers, C.H.J., Sleijfer, S., Vulto, A.G., Kruit, W.H.J., Kliffen, M., Debets, R., Gratama, J.W., Stoter, G., and Oosterwijk, E. (2006). Treatment of metastatic renal cell carcinoma with autologous T-lymphocytes genetically retargeted against carbonic anhydrase IX: first clinical experience. J. Clin. Oncol.
Lamers, C.H.J., Willemsen, R., Van Elzakker, P., Van Steenbergen-Langeveld, S., Broertjes, M., Oosterwijk-Wakka, J., Oosterwijk, E., Sleijfer, S., Debets, R., and Gratama, J.W. (2011). Immune responses to transgene and retroviral vector in patients treated with ex vivo-engineered T cells. Blood.
Lasek, W., Zagożdżon, R., and Jakobisiak, M. (2014). Interleukin 12: still a promising candidate for tumor immunotherapy? Cancer Immunol. Immunother. *63*, 419–435.
Lavin, Y., Kobayashi, S., Leader, A., Amir, E. ad D., Elefant, N., Bigenwald, C., Remark, R., Sweeney, R., Becker, C.D., Levine, J.H., et al. (2017). Innate Immune Landscape in Early Lung Adenocarcinoma by Paired Single-Cell Analyses. Cell.
Lee, B.O., Hartson, L., and Randall, T.D. (2003). CD40-deficient, Influenza-specific CD8 Memory T Cells Develop and Function Normally in a CD40-sufficient Environment. J. Exp. Med. *198*, 1759–1764.
Lee, D.W., Gardner, R., Porter, D.L., Louis, C.U., Ahmed, N., Jensen, M., Grupp, S.A., and Mackall, C.L. (2014). Current concepts in the diagnosis and management of cytokine release syndrome. Blood.
Lee, D.W., Kochenderfer, J.N., Stetler-Stevenson, M., Cui, Y.K., Delbrook, C., Feldman, S.A., Fry, T.J., Orentas, R., Sabatino, M., Shah, N.N., et al. (2015). T cells expressing CD19 chimeric antigen receptors for acute lymphoblastic leukaemia in children and young adults: A phase 1 dose-escalation trial. Lancet *385*, 517–528.

Lee, J., Sadelain, M., and Brentjens, R. (2009). Genetic Modification of Hematopoietic Stem Cells. *506*, 83–96.
Leen, A.M., Sukumaran, S., Watanabe, N., Mohammed, S., Keirnan, J., Yanagisawa, R., Anurathapan, U., Rendon, D., Heslop, H.E., Rooney, C.M., et al. (2014). Reversal of Tumor Immune Inhibition Using a Chimeric Cytokine Receptor. Mol. Ther.
Letourneur, F., and Klausner, R.D. (1991). T-cell and basophil activation through the cytoplasmic tail of T-cell-receptor zeta family proteins. Proc. Natl. Acad. Sci.
Lim, W.A., and June, C.H. (2017). The Principles of Engineering Immune Cells to Treat Cancer. Cell.
Liu, Z., Chen, O., Wall, J.B.J., Zheng, M., Zhou, Y., Wang, L., Ruth Vaseghi, H., Qian, L., and Liu, J. (2017). Systematic comparison of 2A peptides for cloning multi-genes in a polycistronic vector. Sci. Rep.
Macatonia, S.E., Hosken, N.A., Litton, M., Vieira, P., Hsieh, C.S., Culpepper, J.A., Wysocka, M., Trinchieri, G., Murphy, K.M., and O'Garra, A. (1995). Dendritic cells produce IL-12 and direct the development of Th1 cells from naive CD4+ T cells. J. Immunol. *154*, 5071–5079.
Maher, J., Brentjens, R.J., Gunset, G., Rivière, I., and Sadelain, M. (2002). Human T-lymphocyte cytotoxicity and proliferation directed by a single chimeric TCRζ/CD28 receptor. Nat. Biotechnol.
Marin-Acevedo, J.A., Dholaria, B., Soyano, A.E., Knutson, K.L., Chumsri, S., and Lou, Y. (2018). Next generation of immune checkpoint therapy in cancer: New developments and challenges. J. Hematol. Oncol.
Masuta, Y., Kato, K., Tomihara, K., Nakamura, K., Sasaki, K., Takahashi, S., and Hamada, H. (2007). Gene transfer of noncleavable cell surface mutants of human CD154 induces the immune response and diminishes systemic inflammatory reactions. J. Immunother.
Mathé, G., Amiel, J.L., Schwarzenberg, L., Cattan, A., and Schneider, M. (1965). Adoptive Immunotherapy of Acute Leukemia: Experimental and Clinical Results. Cancer Res.
Matsushita, H., Vesely, M.D., Koboldt, D.C., Rickert, C.G., Uppaluri, R., Magrini, V.J., Arthur, C.D., White, J.M., Chen, Y.S., Shea, L.K., et al. (2012). Cancer exome analysis reveals a T-cell-dependent mechanism of cancer immunoediting. Nature.
Maude, S.L., Frey, N., Shaw, P.A., Aplenc, R., Barrett, D.M., Bunin, N.J., Chew, A., Gonzalez, V.E., Zheng, Z., Lacey, S.F., et al. (2014). Chimeric Antigen Receptor T Cells for Sustained Remissions in Leukemia. N. Engl. J. Med. *371*, 1507–1517.
Maude, S.L., Laetsch, T.W., Buechner, J., Rives, S., Boyer, M., Bittencourt, H., Bader, P., Verneris, M.R., Stefanski, H.E., Myers, G.D., et al. (2018). Tisagenlecleucel in Children and Young Adults with B-Cell Lymphoblastic Leukemia. N. Engl. J. Med. *378*, 439–448.
Maus, M. V, Haas, A.R., Beatty, G.L., Albelda, S.M., Levine, B.L., Liu, X., Zhao, Y., Kalos, M., and June, C.H. (2013). T cells expressing chimeric antigen receptors can cause anaphylaxis in humans. Cancer Immunol. Res.

Mavilio, F., Ferrari, G., Rossini, S., Nobili, N., Bonini, C., Casorati, G., Traversari, C., and Bordignon, C. (1994). Peripheral blood lymphocytes as target cells of retroviral vector-mediated gene transfer. Blood.

McGranahan, N., Furness, A.J.S., Rosenthal, R., Ramskov, S., Lyngaa, R., Saini, S.K., Jamal-Hanjani, M., Wilson, G.A., Birkbak, N.J., Hiley, C.T., et al. (2016). Clonal neoantigens elicit T cell immunoreactivity and sensitivity to immune checkpoint blockade. Science (80-.).

Melero, I., Hirschhorn-Cymerman, D., Morales-Kastresana, A., Sanmamed, M.F., and Wolchok, J.D. (2013). Agonist antibodies to TNFR molecules that costimulate T and NK cells. Clin. Cancer Res.

Merad, M., Sathe, P., Helft, J., Miller, J., and Mortha, A. (2013). The Dendritic Cell Lineage: Ontogeny and Function of Dendritic Cells and Their Subsets in the Steady State and the Inflamed Setting. Annu. Rev. Immunol. *31*, 563–604.

Mestas, J., and Hughes, C.C.W. (2004). Of mice and not men: differences between mouse and human immunology. J. Immunol.

van Mierlo, G.J.D., den Boer, A.T., Medema, J.P., van der Voort, E.I.H., Fransen, M.F., Offringa, R., Melief, C.J.M., and Toes, R.E.M. (2002). CD40 stimulation leads to effective therapy of CD40- tumors through induction of strong systemic cytotoxic T lymphocyte immunity. Proc. Natl. Acad. Sci. *99*, 5561–5566.

Miller, J.F.A.P. (1961). Immunological function of the thymus. Lancet.

Miller, J.F.A.P. (1962). Effect of Neonatal Thymectomy on the Immunological Responsiveness of the Mouse. Proc. R. Soc. B Biol. Sci.

Milone, M.C., Fish, J.D., Carpenito, C., Carroll, R.G., Binder, G.K., Teachey, D., Samanta, M., Lakhal, M., Gloss, B., Danet-Desnoyers, G., et al. (2009). Chimeric receptors containing CD137 signal transduction domains mediate enhanced survival of T cells and increased antileukemic efficacy in vivo. Mol. Ther.

de Mingo Pulido, Á., Gardner, A., Hiebler, S., Soliman, H., Rugo, H.S., Krummel, M.F., Coussens, L.M., and Ruffell, B. (2018). TIM-3 Regulates CD103 + Dendritic Cell Function and Response to Chemotherapy in Breast Cancer. Cancer Cell *33*, 60-74.e6.

Mitchell, R.S., Beitzel, B.F., Schroder, A.R.W., Shinn, P., Chen, H., Berry, C.C., Ecker, J.R., and Bushman, F.D. (2004). Retroviral DNA integration: ASLV, HIV, and MLV show distinct target site preferences. PLoS Biol.

Morales, A., Eidinger, D., and Bruce, A.W. (1976). Intracavitary Bacillus Calmette-Guerin in the Treatment of Superficial Bladder Tumors. J. Urol.

Morgan, R.A., Yang, J.C., Kitano, M., Dudley, M.E., Laurencot, C.M., and Rosenberg, S.A. (2010). Case report of a serious adverse event following the administration of t cells transduced with a chimeric antigen receptor recognizing ERBB2. Mol. Ther.

Morgan, R.A., Chinnasamy, N., Abate-Daga, D., Gros, A., Robbins, P.F., Zheng, Z., Dudley, M.E., Feldman, S.A., Yang, J.C., Sherry, R.M., et al. (2013). Cancer regression and neurological toxicity following anti-MAGE-A3 TCR gene therapy. J. Immunother.

Morsut, L., Roybal, K.T., Xiong, X., Gordley, R.M., Coyle, S.M., Thomson, M.,

and Lim, W.A. (2016). Engineering Customized Cell Sensing and Response Behaviors Using Synthetic Notch Receptors. Cell.
Mueller, D.L., Jenkins, M.K., and Schwartz, R.H. (1989). Clonal Expansion Versus Functional Clonal Inactivation: A Costimulatory Signalling Pathway Determines the Outcome of T Cell Antigen Receptor Occupancy. Annu. Rev. Immunol.
Murphy, T.L., Grajales-Reyes, G.E., Wu, X., Tussiwand, R., Bris No, C.G., Iwata, A., Kretzer, N.M., Durai, V., Murphy, K.M., Briseño, C.G., et al. (2016). Transcriptional Control of Dendritic Cell Development. Annu. Rev. Immunol.
Nakanishi, Y., Lu, B., Gerard, C., and Iwasaki, A. (2009). CD8 + T lymphocyte mobilization to virus-infected tissue requires CD4 + T-cell help. Nature.
Neelapu, S.S., Locke, F.L., Bartlett, N.L., Lekakis, L.J., Miklos, D.B., Jacobson, C.A., Braunschweig, I., Oluwole, O.O., Siddiqi, T., Lin, Y., et al. (2017). Axicabtagene Ciloleucel CAR T-Cell Therapy in Refractory Large B-Cell Lymphoma. N. Engl. J. Med. NEJMoa1707447.
Newrzela, S., Cornils, K., Li, Z., Baum, C., Brugman, M.H., Hartmann, M., Meyer, J., Hartmann, S., Hansmann, M.L., Fehse, B., et al. (2008). Resistance of mature T cells to oncogene transformation. Blood.
Ng, K.W., Marshall, E.A., Bell, J.C., and Lam, W.L. (2018). cGAS–STING and Cancer: Dichotomous Roles in Tumor Immunity and Development. Trends Immunol.
Noone, A., Howlader, N., Krapcho, M., Miller, D., Brest, A., Yu, M., Ruhl, J., Tatalovich, Z., Mariotto, A., Lewis, D., et al. (2018). SEER Cancer Statistics Review, 1975-2015, National Cancer Institute. Bethesda, MD. SEER Cancer Stat. Rev. 1975-2015, Natl. Cancer Institute. Bethesda, MD.
Norelli, M., Camisa, B., Barbiera, G., Falcone, L., Purevdorj, A., Genua, M., Sanvito, F., Ponzoni, M., Doglioni, C., Cristofori, P., et al. (2018). Monocyte-derived IL-1 and IL-6 are differentially required for cytokine-release syndrome and neurotoxicity due to CAR T cells. Nat. Med.
Ochi, T., Fujiwara, H., Okamoto, S., An, J., Nagai, K., Shirakata, T., Mineno, J., Kuzushima, K., Shiku, H., and Yasukawa, M. (2011). Novel adoptive T-cell immunotherapy using a WT1-specific TCR vector encoding silencers for endogenous TCRs shows marked antileukemia reactivity and safety. Blood.
Old, L.J., Clarke, D.A., and Benacerraf, B. (1959). Effect of bacillus calmette-guérin infection on transplanted tumours in the mouse. Nature.
Ouaaz, F., Arron, J., Zheng, Y., Choi, Y., and Beg, A.A. (2002). Dendritic cell development and survival require distinct NF-κB subunits. Immunity.
Papadopoulos, E.B., Ladanyi, M., Emanuel, D., Mackinnon, S., Boulad, F., Carabasi, M.H., Castro-Malaspina, H., Childs, B.H., Gillio, A.P., Small, T.N., et al. (1994). Infusions of Donor Leukocytes to Treat Epstein-Barr Virus-Associated Lymphoproliferative Disorders after Allogeneic Bone Marrow Transplantation. N. Engl. J. Med.
Park, J.H., Rivière, I., Gonen, M., Wang, X., Sénéchal, B., Curran, K.J., Sauter, C., Wang, Y., Santomasso, B., Mead, E., et al. (2018). Long-Term Follow-up of CD19 CAR Therapy in Acute Lymphoblastic Leukemia. N. Engl. J. Med. *378*, 449–459.

Paszkiewicz, P.J., Fräßle, S.P., Srivastava, S., Sommermeyer, D., Hudecek, M., Drexler, I., Sadelain, M., Liu, L., Jensen, M.C., Riddell, S.R., et al. (2016). Targeted antibody-mediated depletion of murine CD19 CAR T cells permanently reverses B cell aplasia. J. Clin. Invest.

Pegram, H.J., Lee, J.C., Hayman, E.G., Imperato, G.H., Tedder, T.F., Sadelain, M., and Brentjens, R.J. (2012). Tumor-targeted T cells modified to secrete IL-12 eradicate systemic tumors without need for prior conditioning. Blood *119*, 4133–4141.

Pham, L. V., Tamayo, A.T., Yoshimura, L.C., Lo, P., Terry, N., Reid, P.S., and Ford, R.J. (2002). A CD40 Signalosome anchored in lipid rafts leads to constitutive activation of NF-κB and autonomous cell growth in B cell lymphomas. Immunity.

Postow, M.A., Sidlow, R., and Hellmann, M.D. (2018). Immune-Related Adverse Events Associated with Immune Checkpoint Blockade. N. Engl. J. Med. *378*, 158–168.

Prosser, M.E., Brown, C.E., Shami, A.F., Forman, S.J., and Jensen, M.C. (2012). Tumor PD-L1 co-stimulates primary human CD8+ cytotoxic T cells modified to express a PD1: CD28 chimeric receptor. Mol. Immunol.

Pulè, M.A., Straathof, K.C., Dotti, G., Heslop, H.E., Rooney, C.M., and Brenner, M.K. (2005). A chimeric T cell antigen receptor that augments cytokine release and supports clonal expansion of primary human T cells. Mol. Ther.

Qian, B.-Z., and Pollard, J.W. (2010). Macrophage diversity enhances tumor progression and metastasis. Cell.

Rafiq, S., Yeku, O.O., Jackson, H.J., Purdon, T.J., van Leeuwen, D.G., Drakes, D.J., Song, M., Miele, M.M., Li, Z., Wang, P., et al. (2018). Targeted delivery of a PD-1-blocking scFV by CAR-T cells enhances anti-tumor efficacy in vivo. Nat. Biotechnol.

Raje, N., Berdeja, J., Lin, Y., Siegel, D., Jagannath, S., Madduri, D., Liedtke, M., Rosenblatt, J., Maus, M. V., Turka, A., et al. (2019). Anti-BCMA CAR T-Cell Therapy bb2121 in Relapsed or Refractory Multiple Myeloma. N. Engl. J. Med. *380*, 1726–1737.

Ranheim, E. a, and Kipps, T.J. (1993). Activated T cells induce expression of B7/BB1 on normal or leukemic B cells through a CD40-dependent signal. J. Exp. Med. *177*, 925–935.

Ridge, J.P., Di Rosa, F., and Matzinger, P. (1998). A conditioned dendritic cell can be a temporal bridge between a CD4+ T-helper and a T-killer cell. Nature *393*, 474–478.

Riviere, I., Brose, K., and Mulligan, R.C. (1995). Effects of retroviral vector design on expression of human adenosine deaminase in murine bone marrow transplant recipients engrafted with genetically modified cells. Proc. Natl. Acad. Sci. *92*, 6733–6737.

Rizvi, N.A., Hellmann, M.D., Snyder, A., Kvistborg, P., Makarov, V., Havel, J.J., Lee, W., Yuan, J., Wong, P., Ho, T.S., et al. (2015). Mutational landscape determines sensitivity to PD-1 blockade in non-small cell lung cancer. Science (80-.). *348*, 124–128.

Roberts, E.W., Broz, M.L., Binnewies, M., Headley, M.B., Nelson, A.E., Wolf,

D.M., Kaisho, T., Bogunovic, D., Bhardwaj, N., and Krummel, M.F. (2016). Critical Role for CD103+/CD141+ Dendritic Cells Bearing CCR7 for Tumor Antigen Trafficking and Priming of T Cell Immunity in Melanoma. Cancer Cell.

Romeo, C., and Seed, B. (1991). Cellular immunity to HIV activated by CD4 fused to T cell or Fc receptor polypeptides. Cell.

Rosenberg, S.A., and Restifo, N.P. (2015). Adoptive cell transfer as personalized immunotherapy for human cancer. Science (80-.).

Rosenberg, S.A., Spiess, P., and Lafreniere, R. (1986). A new approach to the adoptive immunotherapy of cancer with tumor-infiltrating lymphocytes. Science (80-.).

Rosenberg, S.A., Packard, B.S., Aebersold, P.M., Solomon, D., Topalian, S.L., Toy, S.T., Simon, P., Lotze, M.T., Yang, J.C., and Seipp, C.A. (1988). Use of tumor-infiltrating lymphocytes and interleukin-2 in the immunotherapy of patients with metastatic melanoma: a preliminary report. N. Engl. J. Med. *319*, 1676–1680.

Rosenberg, S.A., Aebersold, P., Cornetta, K., Kasid, A., Morgan, R.A., Moen, R., Karson, E.M., Lotze, M.T., Yang, J.C., Topalian, S.L., et al. (1990). Gene Transfer into Humans — Immunotherapy of Patients with Advanced Melanoma, Using Tumor-Infiltrating Lymphocytes Modified by Retroviral Gene Transduction. N. Engl. J. Med.

Roybal, K.T., Williams, J.Z., Morsut, L., Rupp, L.J., Kolinko, I., Choe, J.H., Walker, W.J., McNally, K.A., and Lim, W.A. (2016). Engineering T Cells with Customized Therapeutic Response Programs Using Synthetic Notch Receptors. Cell.

Russell, S., Peng, K., and Bell, J. (2013). Oncolytic virotherapy. J. Vasc. Interv. Radiol. *24*, 1115–1122.

Sadelain, M., Brentjens, R., and Rivière, I. (2013). The basic principles of chimeric antigen receptor design. Cancer Discov.

Salmon, H., Idoyaga, J., Rahman, A., Leboeuf, M., Remark, R., Jordan, S., Casanova-Acebes, M., Khudoynazarova, M., Agudo, J., Tung, N., et al. (2016). Expansion and Activation of CD103+ Dendritic Cell Progenitors at the Tumor Site Enhances Tumor Responses to Therapeutic PD-L1 and BRAF Inhibition. Immunity *44*, 924–938.

Sandin, L.C., Orlova, A., Gustafsson, E., Ellmark, P., Tolmachev, V., Totterman, T.H., and Mangsbo, S.M. (2013). Locally Delivered CD40 Agonist Antibody Accumulates in Secondary Lymphoid Organs and Eradicates Experimental Disseminated Bladder Cancer. Cancer Immunol. Res.

Santomasso, B.D., Park, J.H., Salloum, D., Riviere, I., Flynn, J., Mead, E., Halton, E., Wang, X., Senechal, B., Purdon, T., et al. (2018). Clinical and Biological Correlates of Neurotoxicity Associated with CAR T-cell Therapy in Patients with B-cell Acute Lymphoblastic Leukemia. Cancer Discov.

Schietinger, A., Philip, M., Krisnawan, V.E., Chiu, E.Y., Delrow, J.J., Basom, R.S., Lauer, P., Brockstedt, D.G., Knoblaugh, S.E., Hämmerling, G.J., et al. (2016). Tumor-Specific T Cell Dysfunction Is a Dynamic Antigen-Driven Differentiation Program Initiated Early during Tumorigenesis. Immunity.

Schoenberger, S.P., Toes, R.E.M., Van der Voort, E.I.H., Offringa, R., and

Melief, C.J.M. (1998). T-cell help for cytotoxic T-lymphocytes is mediated by CD40-CD40L interactions. Nature *393*, 480–483.
Scholler, J., Brady, T.L., Binder-Scholl, G., Hwang, W.T., Plesa, G., Hege, K.M., Vogel, A.N., Kalos, M., Riley, J.L., Deeks, S.G., et al. (2012). Decade-long safety and function of retroviral-modified chimeric antigen receptor T cells. Sci. Transl. Med.
Schumacher, T.N.M. (2002). T-cell-receptor gene therapy. Nat. Rev. Immunol.
Schumacher, T.N., and Schreiber, R.D. (2015). Neoantigens in cancer immunotherapy. Science (80-.).
Schuster, S.J., Bishop, M.R., Tam, C.S., Waller, E.K., Borchmann, P., McGuirk, J.P., Jäger, U., Jaglowski, S., Andreadis, C., Westin, J.R., et al. (2018). Tisagenlecleucel in Adult Relapsed or Refractory Diffuse Large B-Cell Lymphoma. N. Engl. J. Med.
Scott, A.M., Wolchok, J.D., and Old, L.J. (2012). Antibody therapy of cancer. Nat. Rev. Cancer.
Singhal, S., Mehta, J., Desikan, R., Ayers, D., Roberson, P., Eddlemon, P., Munshi, N., Anaissie, E., Wilson, C., Dhodapkar, M., et al. (1999). Antitumor Activity of Thalidomide in Refractory Multiple Myeloma. N. Engl. J. Med.
Smith, E.L., Harrington, K., Staehr, M., Masakayan, R., Jones, J., Long, T.J., Ng, K.Y., Ghoddusi, M., Purdon, T.J., Wang, X., et al. (2019). GPRC5D is a target for the immunotherapy of multiple myeloma with rationally designed CAR T cells. Sci. Transl. Med.
Spitzer, M.H., Carmi, Y., Reticker-Flynn, N.E., Kwek, S.S., Madhireddy, D., Martins, M.M., Gherardini, P.F., Prestwood, T.R., Chabon, J., Bendall, S.C., et al. (2017). Systemic Immunity Is Required for Effective Cancer Immunotherapy. Cell.
Spranger, S., Dai, D., Horton, B., and Gajewski, T.F. (2017). Tumor-Residing Batf3 Dendritic Cells Are Required for Effector T Cell Trafficking and Adoptive T Cell Therapy. Cancer Cell.
Di Stasi, A., Tey, S.-K., Dotti, G., Fujita, Y., Kennedy-Nasser, A., Martinez, C., Straathof, K., Liu, E., Durett, A.G., Grilley, B., et al. (2011). Inducible Apoptosis as a Safety Switch for Adoptive Cell Therapy. N. Engl. J. Med. *365*, 1673–1683.
Van Der Stegen, S.J.C., Hamieh, M., and Sadelain, M. (2015). The pharmacology of second-generation chimeric antigen receptors. Nat. Rev. Drug Discov.
Stephan, M.T., Ponomarev, V., Brentjens, R.J., Chang, A.H., Dobrenkov, K. V., Heller, G., and Sadelain, M. (2007). T cell-encoded CD80 and 4-1BBL induce auto- and transcostimulation, resulting in potent tumor rejection. Nat. Med.
Suerth, J.D., Schambach, A., and Baum, C. (2012). Genetic modification of lymphocytes by retrovirus-based vectors. Curr. Opin. Immunol.
Sugiura, A., and Rathmell, J.C. (2018). Metabolic Barriers to T Cell Function in Tumors. J. Immunol.
Sung, J.H., Zhang, H., Ashley Moseman, E., Alvarez, D., Iannacone, M., Henrickson, S.E., De La Torre, J.C., Groom, J.R., Luster, A.D., and Von Andrian, U.H. (2012). Chemokine guidance of central memory T cells is critical

for antiviral recall responses in lymph nodes. Cell.
Tedder, T.F., Inaoki, M., and Sato, S. (1997). The CD19-CD21 complex regulates signal transduction thresholds governing humoral immunity and autoimmunity. Immunity.
Teng, M.W.L., Bowman, E.P., McElwee, J.J., Smyth, M.J., Casanova, J.L., Cooper, A.M., and Cua, D.J. (2015). IL-12 and IL-23 cytokines: From discovery to targeted therapies for immune-mediated inflammatory diseases. Nat. Med.
Thistlethwaite, F.C., Gilham, D.E., Guest, R.D., Rothwell, D.G., Pillai, M., Burt, D.J., Byatte, A.J., Kirillova, N., Valle, J.W., Sharma, S.K., et al. (2017). The clinical efficacy of first-generation carcinoembryonic antigen (CEACAM5)-specific CAR T cells is limited by poor persistence and transient pre-conditioning-dependent respiratory toxicity. Cancer Immunol. Immunother.
Thomas, E.D., Storb, R., Clift, R.A., Fefer, A., Johnson, F.L., Neiman, P.E., Lerner, K.G., Glucksberg, H., and Buckner, C.D. (1975). Medical Progress - Bone-Marrow Transplantation - part 2/2. N. Engl. J. Med.
Thommen, D.S., and Schumacher, T.N. (2018). T Cell Dysfunction in Cancer. Cancer Cell.
Thompson, E.D., Enriquez, H.L., Fu, Y.-X., and Engelhard, V.H. (2010). Tumor masses support naive T cell infiltration, activation, and differentiation into effectors. J. Exp. Med.
Till, B.G., Jensen, M.C., Wang, J., Qian, X., Gopal, A.K., Maloney, D.G., Lindgren, C.G., Lin, Y., Pagel, J.M., Budde, L.E., et al. (2012). CD20-specific adoptive immunotherapy for lymphoma using a chimeric antigen receptor with both CD28 and 4-1BB domains: Pilot clinical trial results. Blood.
Tirosh, I., Izar, B., Prakadan, S.M., Wadsworth, M.H., Treacy, D., Trombetta, J.J., Rotem, A., Rodman, C., Lian, C., Murphy, G., et al. (2016). Dissecting the multicellular ecosystem of metastatic melanoma by single-cell RNA-seq. Science (80-.).
Tong, A.W., and Stone, M.J. (2003). Prospects for CD40-directed experimental therapy of human cancer. Cancer Gene Ther. *10*, 1–13.
Tong, A.W., Papayoti, M.H., Armstrong, D.T., Ordonez, G., Lawson, J.M., Stone, M.J., and Netto, G. (2001). Growth-inhibitory effects of CD40 ligand (CD154) and its endogenous expression in human breast cancer. Clin. Cancer Res. *7*, 691–703.
Tran, E., Robbins, P.F., Lu, Y.-C., Prickett, T.D., Gartner, J.J., Jia, L., Pasetto, A., Zheng, Z., Ray, S., Groh, E.M., et al. (2016). T-Cell Transfer Therapy Targeting Mutant KRAS in Cancer. N. Engl. J. Med.
Trinchieri, G. (2003). Interleukin-12 and the regulation of innate resistance and adaptive immunity. Nat. Rev. Immunol.
Turtle, C.J., Hanafi, L., Berger, C., Gooley, T.A., Cherian, S., Hudecek, M., Sommermeyer, D., Melville, K., Pender, B., Budiarto, T.M., et al. (2016). CD19 CAR – T cells of defined CD4 + : CD8 + composition in adult B cell ALL patients. J Clin Invest *1*, 1–16.
Vogelstein, B., Papadopoulos, N., Velculescu, V.E., Zhou, S., Diaz, L.A., and Kinzler, K.W. (2013). Cancer genome landscapes. Science (80-.).

Vonderheide, R.H. (2018). The Immune Revolution: A Case for Priming, Not Checkpoint. Cancer Cell.
Vonderheide, R.H., and Glennie, M.J. (2013). Agonistic CD40 antibodies and cancer therapy. Clin. Cancer Res.
Voss, R., Willemsen, R., Kuball, J., Grabowski, M., Engel, R., Intan, R., Guillaume, P., Romero, P., Huber, C., and Theobald, M. (2008). Molecular design of the Calphabeta interface favors specific pairing of introduced TCRalphabeta in human T cells. J. Immunol. (Baltimore, Md 1950).
Walter, E.A., Greenberg, P.D., Gilbert, M.J., Finch, R.J., Watanabe, K.S., Thomas, E.D., and Riddell, S.R. (1995). Reconstitution of Cellular Immunity against Cytomegalovirus in Recipients of Allogeneic Bone Marrow by Transfer of T-Cell Clones from the Donor. N. Engl. J. Med.
Wang, X., and Rivière, I. (2015). Manufacture of tumor- and virus-specific T lymphocytes for adoptive cell therapies. Cancer Gene Ther.
Wang, J., Jensen, M., Lin, Y., Sui, X., Chen, E., Lindgren, C.G., Till, B., Raubitschek, A., Forman, S.J., Qian, X., et al. (2007). Optimizing Adoptive Polyclonal T Cell Immunotherapy of Lymphomas, Using a Chimeric T Cell Receptor Possessing CD28 and CD137 Costimulatory Domains. Hum. Gene Ther.
Wang, K., Wei, G., and Liu, D. (2012). CD19: a biomarker for B cell development, lymphoma diagnosis and therapy. Exp. Hematol. Oncol.
Wang, X., Chang, W.C., Wong, C.L.W., Colcher, D., Sherman, M., Ostberg, J.R., Forman, S.J., Riddell, S.R., and Jensen, M.C. (2011). A transgene-encoded cell surface polypeptide for selection, in vivo tracking, and ablation of engineered cells. Blood.
Weiden, P.L., Flournoy, N., Thomas, E.D., Prentice, R., Fefer, A., Buckner, C.D., and Storb, R. (1979). Antileukemic Effect of Graft-versus-Host Disease in Human Recipients of Allogeneic-Marrow Grafts. N. Engl. J. Med.
Wilkie, S., Van Schalkwyk, M.C.I., Hobbs, S., Davies, D.M., Van Der Stegen, S.J.C., Pereira, A.C.P., Burbridge, S.E., Box, C., Eccles, S.A., and Maher, J. (2012). Dual targeting of ErbB2 and MUC1 in breast cancer using chimeric antigen receptors engineered to provide complementary signaling. J. Clin. Immunol.
Wingett, D.G., Vestal, R.E., Forcier, K., Hadjokas, N., and Nielson, C.P. (1998). CD40 is functionally expressed on human breast carcinomas: Variable inducibility by cytokines and enhancement of Fas-mediated apoptosis. Breast Cancer Res. Treat.
Yacoub, D., Benslimane, N., Al-Zoobi, L., Hassan, G., Nadiri, A., and Mourad, W. (2013). CD154 is released from t-cells by a disintegrin and metalloproteinase domain-containing protein 10 (ADAM10) and ADAM17 in a CD40 protein-dependent manner. J. Biol. Chem. *288*, 36083–36093.
Yadav, M., Jhunjhunwala, S., Phung, Q.T., Lupardus, P., Tanguay, J., Bumbaca, S., Franci, C., Cheung, T.K., Fritsche, J., Weinschenk, T., et al. (2014). Predicting immunogenic tumour mutations by combining mass spectrometry and exome sequencing. Nature.
Yamamoto, T.N., Lee, P.-H., Vodnala, S.K., Gurusamy, D., Kishton, R.J., Yu, Z.,

Eidizadeh, A., Eil, R., Fioravanti, J., Gattinoni, L., et al. (2019). T cells genetically engineered to overcome death signaling enhance adoptive cancer immunotherapy. J. Clin. Invest.

Yeku, O.O., Purdon, T.J., Koneru, M., Spriggs, D., and Brentjens, R.J. (2017). Armored CAR T cells enhance antitumor efficacy and overcome the tumor microenvironment. Sci. Rep. *7*.

Zappasodi, R., Merghoub, T., and Wolchok, J.D. (2018). Emerging Concepts for Immune Checkpoint Blockade-Based Combination Therapies. Cancer Cell.

Zaretsky, J.M., Garcia-Diaz, A., Shin, D.S., Escuin-Ordinas, H., Hugo, W., Hu-Lieskovan, S., Torrejon, D.Y., Abril-Rodriguez, G., Sandoval, S., Barthly, L., et al. (2016). Mutations Associated with Acquired Resistance to PD-1 Blockade in Melanoma. N. Engl. J. Med.

Zhang, L., Morgan, R.A., Beane, J.D., Zheng, Z., Dudley, M.E., Kassim, S.H., Nahvi, A. V., Ngo, L.T., Sherry, R.M., Phan, G.Q., et al. (2015). Tumor-infiltrating lymphocytes genetically engineered with an inducible gene encoding interleukin-12 for the immunotherapy of metastatic melanoma. Clin. Cancer Res.

Zhang, W., Wang, Y., Guo, Y., Dai, H., Yang, Q., Zhang, Y., Zhang, Y., Chen, M., Wang, C., Feng, K., et al. (2016). Treatment of CD20-directed Chimeric Antigen Receptor-modified T cells in patients with relapsed or refractory B-cell non-Hodgkin lymphoma: an early phase IIa trial report. Signal Transduct. Target. Ther.

Zhao, Z., Condomines, M., van der Stegen, S.J.C., Perna, F., Kloss, C.C., Gunset, G., Plotkin, J., and Sadelain, M. (2015). Structural Design of Engineered Costimulation Determines Tumor Rejection Kinetics and Persistence of CAR T Cells. Cancer Cell *28*, 415–428.

Zheng, G.X.Y., Terry, J.M., Belgrader, P., Ryvkin, P., Bent, Z.W., Wilson, R., Ziraldo, S.B., Wheeler, T.D., McDermott, G.P., Zhu, J., et al. (2017). Massively parallel digital transcriptional profiling of single cells. Nat. Commun.